



3 1293 01020 5015

7/15/94

This is to certify that the

thesis entitled

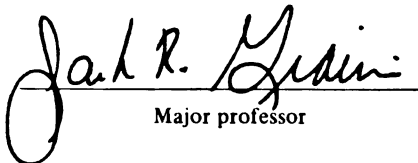
**The Effect of Surface Sulfonation on the Surface Free  
Energy, and Peel Adhesion Strength of Polymer Films**

presented by

**Insik Park**

has been accepted towards fulfillment  
of the requirements for

Master degree in Packaging

  
Major professor

Date June 30, 1994



**PLACE IN RETURN BOX to remove this checkout from your record.  
TO AVOID FINES return on or before date due.**

DATE DUE	DATE DUE	DATE DUE
_____	_____	_____
_____	_____	_____
_____	_____	_____
_____	_____	_____
_____	_____	_____
_____	_____	_____
_____	_____	_____

**THE EFFECT OF SURFACE SULFONATION ON THE SURFACE  
FREE ENERGY, AND PEEL ADHESION STRENGTH OF  
POLYMER FILMS**

By

**INSIK PARK**

**A THESIS**

Submitted to  
Michigan State University  
in partial fulfillment of the requirements  
for the degree of

**MASTER OF SCIENCE**

**School of Packaging**

**1994**



## **ABSTRACT**

### **The effect of Surface Sulfonation on the Surface Free Energy, and Peel Adhesion Strength of Polymer Films**

BY

**Insik Park**

Surface sulfonation of polypropylene (PP), polyethylene (PE), and polyethylene terephthalate (PET) film was carried out by reaction with gaseous  $\text{SO}_3$  in this study. The effect of surface sulfonation on the surface free energy of the these polymer films was determined by contact angle analysis. Electron Spectroscopy for Chemical Analysis (ESCA) of the polymer surfaces showed that the effectiveness of the sulfonation process was dependent upon the chemical structure of the polymer, with the sulfonation of the sulfonation of PP being very effective.

The adhesion strength of pressure sensitive adhesive (PSA) tape on PP, and PE films was determined by using the peel adhesion test. For PP film, the results showed that sulfonation increased the polar component of the surface free energy, and the peel adhesion strength of the treated film. Surface sulfonation of PP film is therefore a suitable method to modify its surface properties, improving surface free energy and peel adhesion strength.

**To my parents and family**

## ACKNOWLEDGEMENTS

I wish to express my sincere thanks and appreciation to Dr. Jack Giacin for his constant guidance, continuous encouragement, valuable suggestions, and financial support throughout this study.

Gratitude is also expressed to the members of my thesis committee, Dr. Susan Selke, Ruben J. Hernandez, and James P. Lucas for their comments and suggestions.

I am very grateful to Susan C. Jones, Brian Eriction, and Kitti Wangwiwatsilp for their impressive help and encouragement.

Above all, I especially wish to take opportunity to express gratitude to my parents and family for encouragement, patience, and understanding throughout the course of this study.

# TABLE OF CONTENTS

## List of Tables

## List of Figures

### Chapter 1. Introduction .....1

### Chapter 2. Background

2.1. The nature of interfacial forces in adhesion phenomena .....	5
2.2. Mechanisms of adhesion.....	7
2.2.1. Mechanical interlocking.....	7
2.2.2. Diffusion theory .....	8
2.2.3. Electronic theory .....	8
2.2.4. Adsorption theory.....	8
2.3. Work of Adhesion .....	9

### Chapter 3. Surface Energy of Polymer Solids

3.1. Relationships between contact angle, wetting and adhesion.....	12
3.2. Methods of estimating surface free energy of solid .....	16
3.2.1. The critical surface energy .....	16
3.2.2. Surface energy components to determine solid surface energy .....	17
3.2.3. The methods using the equations for the work of adhesion.....	21
3.3. Calculations of dispersion and polar force contributions to surface free energy of polymer .....	21

3.3.1. Determinant method .....	22
3.3.1(a) The least square method .....	23
3.3.1(b) Derivation of least squares method .....	23
3.3.1(c) Computer program "SFE" .....	28

## **Chapter 4. Surface Modification Technology**

4.1. Introduction .....	33
4.2. Chemical etching [2] techniques .....	34
4.3. Flame Treatment.....	36
4.4. Corona and Plasma treatments .....	36
4.5. Surface Sulfonation Technique.....	39

## **Chapter 5. Materials and Experimental Process**

5.1. Sulfonation Apparatus .....	42
5.1.1. The Unit of Sulfonation System .....	42
5.1.1(a) Sulfonating chamber .....	43
5.1.1(b) Sampling Port .....	43
5.2. Materials using for sulfonation.....	47
5.2.1. Polymer films.....	47
5.2.1(a) Oriented Polypropylene (OPP) film .....	47
5.2.1(b) Polyethylene (PE) .....	47
5.2.1(c) Polyethylene Terephthalate (PET) .....	47
5.2.2. Fuming Sulfuric Acid .....	47
5.2.3. Cleaning agent.....	48
5.2.4. Neutralization Agent.....	48
5.3. Sulfonation Procedure.....	48
5.4. Electron Spectroscopy for Chemical Analysis (ESCA) .....	49

## **Chapter 6. Physical tests**

6.1. Contact Angle Measurements of Polymers and Methods .....	50
6.1.1. Test Apparatus of Contact Angle Measurements.....	51
6.1.2. Sample Preparation and Contact Angle Measurements of Polymers .....	51
6.1.3. Calculation of surface energy of solid.....	54
6.2. Peel adhesion test.....	56
6.2.1. Test Apparatus and conditions .....	57
6.2.2. Pressure sensitive adhesive (PSA) test tape and backing tape .....	58
6.2.3. Test specimen preparation and scheme .....	58
6.2.4. Peel Adhesions Test Procedure .....	60
6.2.5. Analysis of peel adhesion test.....	61

## **Chapter 7. Sulfonation of Polypropylene**

7.1. Introduction .....	62
7.2. ESCA and Elemental Observations and Discussions .....	63
7.3. Results and discussions of contact angle measurements .....	69
7.3.1. Contact angles of probe liquids on OPP films tested.....	69
7.3.2. Determination of surface free energies of films .....	72
7.4. Results and discussions of peel adhesion test .....	77
7.5. Conclusions.....	81

## **Chapter 8. Sulfonation of Polyethylene**

8.1. Introduction .....	82
8.2. Sulfonation degree determined by the ESCA .....	83
8.3. Results and discussions of contact angle measurements .....	85
8.3.1. Contact angles of probe liquids on PE films tested.....	85

8.3.2. Determination of surface free energies of films.....	87
8.4. Results and discussions of the peel adhesion test.....	90
8.5. Conclusion .....	93

## **Chapter 9. Sulfonation of Polyethylene Terephthalate (PET) film**

9.1. Introduction .....	94
9.2. Results and Discussions .....	94

## **Chapter 10. Conclusions .....**

99

## **Chapter 11. Possible Future Studies.....**

101

## **Bibliography**

## List of Tables

<b>Table 1</b>	Types of physical attractive forces and typical bond energies .....6
<b>Table 2</b>	The characteristics of typical liquids used as probes for the contact angle measurements .....20
<b>Table 3</b>	A comparison of sulfuric acid and SO <sub>3</sub> gas as sulfonation agents. .....41
<b>Table 4</b>	The surface energy of liquids, and the corresponding polar and dispersive component, used for measuring contact angles on the respective polymer samples and pressure adhesive tape. .....50
<b>Table 5</b>	Result of Contact angles of probe liquids on the PSA tape .....58
<b>Table 6</b>	Atomic concentration for untreated and sulfonated OPP films determined by ESCA analysis.....65
<b>Table 7</b>	Relative Atomic Ratios of Sulfonated OPP films.....66
<b>Table 8</b>	The comparison of sulfur content, measured by ESCA and Elemental Analysis, in the film samples treated at various sulfonation time. ....66
<b>Table 9</b>	Contact angle obtained on tested polypropylene films using various liquids. ....69
<b>Table 10</b>	Surface Free Energy of PP films, Polarity, Atomic% of Sulfur by ESCA, and Total% of Sulfur per gram of film sample for OPP (untreated), SPP1 (Sulfonated for 1 minute), SPP1.5 (Sulfonated for 1.5 min.), SPP2 (Sulfonated for 2 min.), and SPP3 (Sulfonated 3 min.) .....73



<b>Table 11</b>	Peel adhesion strength for sulfonated film samples with the data of surface free energies .....	77
<b>Table 12</b>	Surface composition of HDPE film samples before and after sulfonation treatments at a various exposure time over SO <sub>3</sub> gas, determined by ESCA .....	84
<b>Table 13</b>	Contact angle obtained on sulfonated polypropylene using various liquids. ....	85
<b>Table 14</b>	Surface Free Energy of PE films, Polarity, and Atomic% of Sulfur by ESCA for PEU (untreated), PE1.5 (Sulfonated for 1.5 minute), PE3 (Sulfonated for 3 min.), PE5 (Sulfonated for 5 min.), and PEC (Corona treated) .....	87
<b>Table 15</b>	Peel adhesion strength for sulfonated film samples with the result of surface free energies in polar dispersion and polar components .....	90
<b>Table 16</b>	Surface composition of PET film samples before and after sulfonation treatments at a various exposure time over SO <sub>3</sub> gas, determined by ESCA .....	95
<b>Table 17</b>	Contact angle of liquids on the untreated PET film and sulfonated PET samples for 1 min. and 3 min. reaction time.....	96
<b>Table 18</b>	Surface Free Energy of PET films, Polarity, and Atomic% of Sulfur by ESCA for PETU (untreated), PET1 (Sulfonated for 1.5 minute), PET3 (Sulfonated for 3 min.) .....	98

## List of Figures

<b>Figure 1</b>	The surface tension balance at a point of three-phase contact at equilibrium for ideal surfaces. An <i>ideal</i> surface is a smooth surface without interfacial reactions with a liquid drop.....	13
<b>Figure 2</b>	A plot of cosine of angles vs. the surface energy of liquid, as proposed by Zisman.....	17
<b>Figure 3</b>	Presentation of typical individual relationships of $(\gamma_s^d)^{0.5}$ versus $(\gamma_s^p)^{0.5}$ deduced from one of equations [3.17] or [3.18]. Plot shows SPP1, sulfonated polypropylene for 1 min. The shaded part is in the boundary.....	24
<b>Figure 4(a)</b>	Program to calculate the average and standard deviation errors of measured contact of each liquid angles on a polymer sample. .....	29
<b>Figure 4(b)</b>	Figure shows the input data file for the program shown in <i>Figure 4(a)</i> . Columns in this data file present each liquid used for the contact angle measurement. Rows in this file are the duplicate of the measured contact angle of a liquid measured on different points of a film sample. ....	30
<b>Figure 4(c)</b>	This program provides a graphic like the one presented in <i>Figure 3</i> , which is plotted $(\gamma_s^d)^{0.5}$ versus $(\gamma_s^p)^{0.5}$ , deduced from one equations [3.17] or [3.18]. ....	31
<b>Figure 4(d)</b>	This program calculates surface free energy, corresponding dispersion component, and polar component, of solid by solving one of equations [3.27] or [3.28]. ....	32

<b>Figure 5</b>	A schematic representation of the interactions which are possible in a gas plasma impinging upon a substrate. ....	38
<b>Figure 6</b>	Sulfonation reaction mechanism of HDPE.....	39
<b>Figure 7</b>	The figure illustrates the formation of conjugated system of double bonds as a result of sulfonation .....	40
<b>Figure 8</b>	The figure illustrates the formation of alkene species during sulfonation .....	40
<b>Figure 9(a)</b>	Diagram for the gas-phase SO <sub>3</sub> generator unit(a) [Continued to Figure 9(b)] .....	44
<b>Figure 9(b)</b>	Schematic illustrates the SO <sub>3</sub> flow pattern in the sulfonating chamber [Continued from Figure 9(a)].....	45
<b>Figure 10</b>	View of Sulfonating Chamber, samples, sample holder.....	46
<b>Figure 11</b>	Diagram of contact angle specimen and sessile droplet form. .....	51
<b>Figure 12</b>	A schematic of Goniometer (Model 100-00 115, Rame-Hart, inc.). .....	52
<b>Figure 13</b>	Figure illustrates the procedure of the contact angle measurement with Goniometer.....	55
<b>Figure 14</b>	The schematic of the SFM machine, which is controlled by the computer.....	57
<b>Figure 15</b>	Schematic diagram of sample-tape composite for testing peel adhesion .....	59
<b>Figure 16</b>	Device to apply same force for laminating of the test film and PSA tape .....	60
<b>Figure 17</b>	The molecular structure of sulfonated polypropylene.....	64

<b>Figure 18</b>	Atomic ratio of O/C, and S/C determined by ESCA as a function of sulfonation time (at 1% SO <sub>3</sub> concentration).....	67
<b>Figure 19</b>	Sulfur content measured by ESCA, and Elemental Analysis, as a function of sulfonation time. ....	68
<b>Figure 20</b>	The changes in contact angle of 4 liquids on polypropylene with increasing time of sulfonation. ....	71
<b>Figure 21(a)</b>	Variation of solid surface energy, dispersive and polar energy components for untreated and sulfonated PP films .....	74
<b>Figure 21(b)</b>	Variation of surface free energies, corresponding to the dispersive and polar force components for untreated and sulfonated PP films as function of sulfonation time. Note the visible changes in polar force component of surface free energies of solid appeared within the one minute of sulfonation time. ....	75
<b>Figure 22</b>	Relationship between <i>Permeability Coefficient</i> of Ethyl Acetate in Polypropylene films and <i>Total Surface Free Energy</i> as a function of sulfonation time. Note the apparent changes occurred in the 90 sec., while the surface free energy changed within one minute of sulfonating time. ....	76
<b>Figure 23</b>	Peel adhesion strength of OPP films tested as a function of sulfonation time. In insert box, surface energies of the respective film samples vs. sulfonation time are presented for comparison with the increasing trend of the peel adhesion strength. ....	79
<b>Figure 24</b>	The relationship of peel adhesion strength vs. adhesion-interaction term. ....	80
<b>Figure 25</b>	Atomic% of sulfur measured by ESCA as a function of sulfonation time. ....	84

<b>Figure 26</b>	The changes in contact angle of 4 liquids on polyethylene with increasing time of sulfonation based on the untreated PE film as reference. ....	86
<b>Figure 27</b>	The effect of sulfonation time on the change in total surface free energy and the respective energy components for untreated, sulfonated HDPE films as a function of reaction time, and corona treated HDPE film. ....	89
<b>Figure 27(a)</b>	Peel adhesion strength of HDPE film samples as a function of sulfonation time. ....	91
<b>Figure 27(b)</b>	Histogram of peel adhesion strength of untreated, sulfonated HDPE film samples and corona treated HDPE film samples. ....	92
<b>Figure 28</b>	Contact angle change of liquids for sulfonated PET samples with increasing time of sulfonation. Based on the untreated PET film as reference. ....	96
<b>Figure 29</b>	Variation of solid surface energy corresponding dispersion and polar components for untreated and sulfonated PET samples. ....	98

## *Chapter 1. Introduction*

Polymer films, especially polyolefins, are widely used as a packaging material, as well as for industrial applications, due to their low specific weight, compatibility with other materials and relatively low cost. The low surface energy of polyolefins, and consequently their poor wetting and adhesion to other materials, requires enhancement of surface properties such as printability, wettability, and adhesion for new uses and technical applications. Several techniques have been developed to modify polymer surfaces in an attempt to improve adhesion, wettability, and other surface characteristics, with the aim of incorporating polar groups onto the polymer surfaces.<sup>[1]</sup> These techniques include plasma treatment,<sup>[2]-[9]</sup> flame treatment,<sup>[10]</sup> chromic acid etching,<sup>[11]</sup> and corona treatment.<sup>[12]-[14]</sup> Although the precise mechanism of enhanced adhesion on surface modified polymers is not completely understood, the experimental evidence points to changes in the chemical nature of the surface, such as the formation of polar groups<sup>[14]</sup>, elimination of weak boundaries.<sup>[15],[16]</sup>

Sulfonation, using gaseous  $\text{SO}_3$ , has been evaluated as an effective technique to improve the surface properties as well as the barrier properties of polymer films. Studies involving the sulfonation on polymer films have been performed to evaluate the effect of sulfonation on the physical and mechanical properties of polymer films to include: mechanical properties<sup>[18], [19]</sup>; electrical properties<sup>[11]</sup>; barrier properties<sup>[20]-[22]</sup>; and surface properties<sup>[23]</sup>.

Studies on the chemical changes of polyethylene during sulfonation, reported

by Ihata<sup>[24],[25]</sup>, indicated that introduction of polar sulfonic acid groups ( $\text{-SO}_3\text{H-}$ ), with unsaturated  $\text{C}=\text{C}$  bonds on the polyethylene surface is a result of chemical reactions taking place during surface treatment. Ihata<sup>[24]</sup> subsequently inferred that any polymer containing C-H or N-H bonds can be sulfonated. Erickson<sup>[19]</sup> also reported that the sulfonic acid group, neutralized with ammonium hydroxide ( $\text{NH}_4\text{OH}$ ), had penetrated into the bulk of the polymer, resulting in changes on the surface as well as within polymer bulk phase.

Wangwiwatsilp<sup>[21]</sup> has studied the effect of surface sulfonation on the barrier properties of polypropylene films, by using permeation and sorption measurements involving acetate and toluene. The author observed distinctively improved barrier properties by reduction in the diffusion and sorption coefficient of ethyl acetate following the surface sulfonation of oriented polypropylene (OPP) film. He also investigated the effect of surface sulfonation on the barrier properties of polyethylene terephthalate (PET) and Nylon 6.6 films, but found no significant improvement for either film, under the conditions employed.

The effects of surface treatments are usually evaluated by the surface nature changes through X-ray Photoelectron Spectroscopic (XPS) Analysis<sup>[27], [28]</sup>, Fourier-Transform Infra-red (FTIR) Analysis and Atomic Force Microscopy (AFM)<sup>[29]</sup>. Spectroscopic measurements are complementary, as they afford information related to chemical structure changes on the surface and bulk of polymers, but provide little information related directly to adhesion interactions. For example, Asthana<sup>[23]</sup> attempted to investigate the effect of sulfonation on the adhesion properties of polypropylene (PP) and polystyrene (PS)

films by observations of X-ray Photoelectron Spectroscopic (XPS) Analysis, Fourier-Transform Infra-red Analysis, and by Contact angle analysis with distilled water. Most of Asthana's work was directed to developing a better understanding of the surface chemical structural changes due to sulfonation of PP, and PS films, and a detailed analysis of the changes in polymer surface properties was not reported.

Knowledge of the surface energies and of the wetting characteristics of polymers, as well as information related to surface energy changes of polymers, is essential to evaluate the effect of surface treatment and the processibility of surface treated polymer film structures. Traditionally, contact angle measurements<sup>[30], [31]</sup> have been performed to obtain information on surface energies and on the wetting characteristics of solids. For example, the empirical method was described by Zisman<sup>[32]</sup>. Recently, Inverse Gas Chromatography<sup>([33]~[35])</sup> analysis has been proposed as an alternative method to determine polymer surface energy data.

In the present study, Contact Angle Measurements, and Electron Spectroscopy for Chemical Analysis (ESCA) techniques were employed to evaluate the effect of sulfonation on the surface free energy of polymer film and the associated relationship with the surface adhesion properties. Contact angle measurements were carried out with four liquids of known surface properties, on both the sulfonated and untreated polymer films. The level of sulfonation was determined by the ESCA analysis. The surface free energy of the surface modified polymer film, to include both dispersion and polar components, was determined from contact angle measurements by the method proposed by



Kinloch et al<sup>[36]</sup>.

A Peel Adhesion (PA) test, with pressure adhesive tape, was then carried out the respective film samples, which were sulfonated and untreated. Pressure Sensitive adhesive (PSA) tape was also characterized by the determination of the surface tension, prior to the PA test. The values of surface energy, determined for the respective polymer samples and the PSA tape, were then used to determine a correlation with the results of the PA tests.

In addition to surface energy characteristics, attempts were also made to investigate surface topographical changes due to sulfonation of polymers by using Atomic Force Microscopy (AFM). Unfortunately, due to the soft and flexible nature of the polymer surface, AFM was found to be an ineffective method to evaluate the rheology of the polymer films under the conditions employed.

The main objectives of this study are summarized;

1. To determine the effect of surface sulfonation of the oriented polypropylene (OPP), polyethylene (PE) and polyethylene terephthalate (PET) films on surface energies, as well as the corresponding to dispersion and polar components, by measuring contact angle of various liquids on the respective film samples.
2. To determine peel adhesion strength of PP and PE films, which were untreated, and sulfonated as a function of sulfonation time. The PA test followed the standard test method <sup>[37]</sup> with minor modification.
3. To evaluate and analyze the obtained data.

## ***Chapter 2. Background***

Adhesion is defined as the phenomenon in which two different surfaces (for example, solid-solid, and solid-liquid) are held together by interfacial forces. Polymer adhesion is fundamentally dependent on a variety of factors including interfacial forces which are related to morphology, rheology, barrier properties or mechanical properties of polymers. Brief descriptions of the nature of interfacial forces, mechanisms of adhesion, and work of adhesion related to surface free energies are included in this chapter.

### **2.1. The nature of interfacial forces in adhesion phenomena**

Interfacial forces are closely related to surface tensions, which occur as a result of the attraction of the bulk material to the surface layer. This attraction tends to reduce the number of molecules in the surface region, resulting in an increase in intermolecular distance.<sup>[17]</sup> The forces of establishing intrinsic molecular contact are decisive in determining adhesion strength. These forces of attraction include ionic forces, covalent bonds, hydrogen bonds and Van der Waals' forces of various types. These forces and their bonding energies are represented in *Table 1 (page 6)*<sup>[39]</sup>. From those forces of attraction, Van der Waals forces are the most common. Different effects are attributed to the overall Van der Waals attractions; they are (a) dispersion forces (or London forces), (b) induction forces (or Debye forces), and (c) Polar forces (or Keesom forces)

Dispersion forces are non-polar forces which arises from internal atom motions, whether atoms are charged or not. Dispersion forces exist between all

atoms<sup>[38]</sup>, because all atoms consist of positive nuclei around which negative electrons are moving. They are dependent on the total number of electrons and the positive charge to which these electrons are bound. Dispersion forces are short-range forces, and these forces display the important property wherein the energy of interaction due to such forces between unlike atoms is at most equal to the geometric mean of the energies between forces<sup>[39]</sup>.

**Table 1** Types of physical attractive forces and typical bond energies<sup>a</sup>

Types of Forces	Bond energy [kg/mol]
Primary bonds	
Ionic	600~1100
Covalent	60~700
Metallic	110~350
Donor-accepted bonds	
Bronsted acid-base interactions	Up to 1000
Lewis acid-base interactions	Up to 80
Secondary bonds: Hydrogen bonds	
Hydrogen bonds involving fluorine	Up to 40
Hydrogen bonds excluding fluorine	10~25
Van der Waals bonds	
Permanent dipole-dipole interactions	4~20
Dipole-induced dipole interactions	Less than 2
Dispersion(London) forces	0.08~40

a. From Ref., Kinloch, A.J., "Adhesion and Adhesives: Science and Technology"<sup>[39]</sup>, p. 79

Induction forces originates from an asymmetry of charge distribution. Induction forces are considered as polar forces but are very negligible compared to

dispersion forces<sup>[38]</sup>.

Polar forces (or Keesom forces) arises from the orientation of permanent electric dipoles and the induction effect of permanent dipoles on polarized material. Dispersion forces are usually weaker than the polar forces but dispersion forces are found in all materials<sup>[39]</sup>.

## **2.2. Mechanisms of adhesion**

Many adhesion models have been proposed to account for a wide range of related experimental observations, but there is no plausible single mechanism to cover all circumstances. There are four major mechanisms which are generally accepted as explaining adhesion phenomena including; mechanical interlocking, diffusion theory, electronic theory, and adsorption theory. Lately, the adsorption theory is the most widely accepted in understanding adhesion phenomena. Each of these theories has certain support in some cases, but also many weaknesses; at present, none of the above theories taken alone can adequately account for all of the experimental observations relating to improved adhesion properties<sup>[41]</sup>. More details are presented with examples in the reference of [39], and [41].

### **2.2.1. Mechanical interlocking**

The basic concept of this mechanism is that mechanical interlocking of adhesives with irregular substrate surfaces promotes intrinsic adhesion.<sup>[3]</sup> In certain instances mechanical interlocking may contribute to the intrinsic adhesion mechanisms. However, since strong adhesion also can be attained between smooth surfaces, the concept of interlocking is not adequate to explain adhe-

sion. Kinloch<sup>[39]</sup> stated that the increases in adhesion with increasing surface roughness might be related to other factors such as the removal of weak surface layers, or improved interfacial contact to make better wetting conditions.

### **2.2.2. Diffusion theory**

The diffusion theory, originated by Voyutskii<sup>[38]</sup>, supposes that the adhesion of polymers is caused by the mutual diffusion of polymer molecules across the interface, which conveys adhesive strength. Interdiffusion of polymer chains across the interface requires the polymers to be mutually soluble. This fact may limit this theory to the autohesion of elastomers or materials with similar solubility parameters. If the materials are not similar, diffusion across the interface will be very slow, and then interdiffusion will be an unlikely mechanism of adhesion.

### **2.2.3. Electronic theory**

Deryagin et al<sup>[44]</sup> suggested that electrostatic forces arising from such contact or junction potentials may contribute significantly to adhesion. In their work, an electric double layer was observed in the interface of pressure-sensitive tapes when the bond was broken. The concept of this theory is based on the adhesive/substrate system acting as a capacitor which can store electric energy charged due to the contact of two different substrates. From this theory, adhesion is postulated to occur due to the attraction of forces across the electrical double layer in the interface. The main argument made against this theory, however, is that any electrical double layer generated at the broken joint emerges from the failure of surface, rather than adhesion between the materi-

als.<sup>[39]</sup>

#### 2.2.4. Adsorption theory

The adsorption theory is the most widely applied in understanding adhesion phenomena with the base of attractive force. Attractive forces, arising from the interface in a joint between two materials, provide cohesive strength between the atoms and molecules. These attractive forces of interfaces are closely linked with chemical adsorption, and surface free energy. Since the nature of such forces was summarized in a previous chapter, the contributions of inter-molecular forces to the thermodynamic work of adhesion, to the surface free energies involved in adhesion will be detailed below.

#### 2.3. Work of Adhesion

The involvement in adhesion of surface and interfacial energies is explained by the equation for the thermodynamic work of adhesion.  $W_A$  is defined as a unit area of two phases from the interface across which forces are acting<sup>[48]</sup>. This yields the Duprè<sup>[43]</sup> equation:

$$W_A = \gamma_{sv} + \gamma_{lv} - \gamma_{sl} \quad [2.1]$$

where  $\gamma_s$ ,  $\gamma_l$ , and  $\gamma_{sl}$  are the surface free energy of the solid, liquid phase, and interface, respectively.

Good and Girifalco<sup>[46], [47]</sup> have evaluated this interfacial surface free energy by the ratio,  $R$ , of the free energy of adhesion to the geometric mean of the free energies of the solid and liquid phases:

$$(\gamma_s + \gamma_l - \gamma_{sl}) / 2 (\gamma_s \gamma_l)^{1/2} = R \quad [2.2]$$

where  $\gamma_s$ ,  $\gamma_l$ , and  $\gamma_{sl}$  are the surface free energy of the solid, liquid, and interface, respectively. By assuming  $R$  is approximately unity for the simplest cases, the equation [2.2] can be simplified as:

$$\gamma_{sl} = \gamma_s + \gamma_l - 2 (\gamma_s \gamma_l)^{1/2} \quad [2.3]$$

And then  $W_A$  is expressed [41];

$$W_A = 2 (\gamma_s \gamma_l)^{1/2} \quad [2.4]$$

Fokwes<sup>[48]</sup> proposed that this work of adhesion was due to the addition of contributions from many interfacial interactions such as dispersion forces, hydrogen bonds, dipole/dipole, dipole/induced forces, acid/base interactions, and so on, yielding:

$$W_A = W_A^d + (W_A^h + W_A^{dd} + W_A^{di}) + W_A^{ab} \quad [2.5]$$

where the superscripts represent  $d$ -(dispersion forces),  $h$ -(hydrogen bonds),  $dd$ -(dipole/dipole),  $di$ -(dipole/induced forces),  $ab$ -(acid/base) interactions, respectively. Recently, the work of adhesion has been recognized as effectively arising from two major components: the dispersion forces and the polar forces (or acid/base interactions). This can be expressed as follows:

$$W_A = W_A^d + W_A^p \quad [2.6]$$

where superscript  $d$ -dispersion force components, and p-polar forces components, respectively.



## ***Chapter 3. Surface energy of polymer solids***

The effects of surface modification are commonly characterized by the estimation of surface free energies of solid. The surface free energy of solid cannot be directly measured. The contact angle analysis is one of traditional method to estimate the surface free energy of solid.

### **3.1. Relationships between contact angle, wetting and adhesion**

Wetting is defined as the extent to which a liquid makes contact with a solid surface<sup>[39]</sup>. The wettability of liquids with respective surface can be characterized by measuring the peripheral contact angles between the surface of a small sessile drop of the liquid and the horizontal surface of the solid. Adhesion is the intimate sticking together of surfaces on which interfacial forces are acting. The work required to pull the interface apart to two faces can be estimated.<sup>[40]</sup>

Contact angle measurements provide a simple, inexpensive method to obtain direct information on wetting by the contact angle of a liquid, and can estimate the surface free energy terms of a solid as described in *Figure 1 (page 13)*. At equilibrium and in the absence of interfacial reactions, the extent of wetting on the surface by the liquid is determined by the force balance between the three phase contacts as illustrated in *Figure 1*. This balance of interfacial forces is generally described by Young's equation<sup>[49]</sup>:

$$\gamma_{sv} = \gamma_{sl} + \gamma_{lv} \cos \theta \quad [3.1]$$

where the terms  $\gamma_{lv}$  and  $\gamma_{sv}$  are the surface tension of the liquid and the

solid in equilibrium with the vapor, respectively, and  $\gamma_{sl}$  represents the interfacial tension between liquid and solid with the contact angle  $\theta$ .

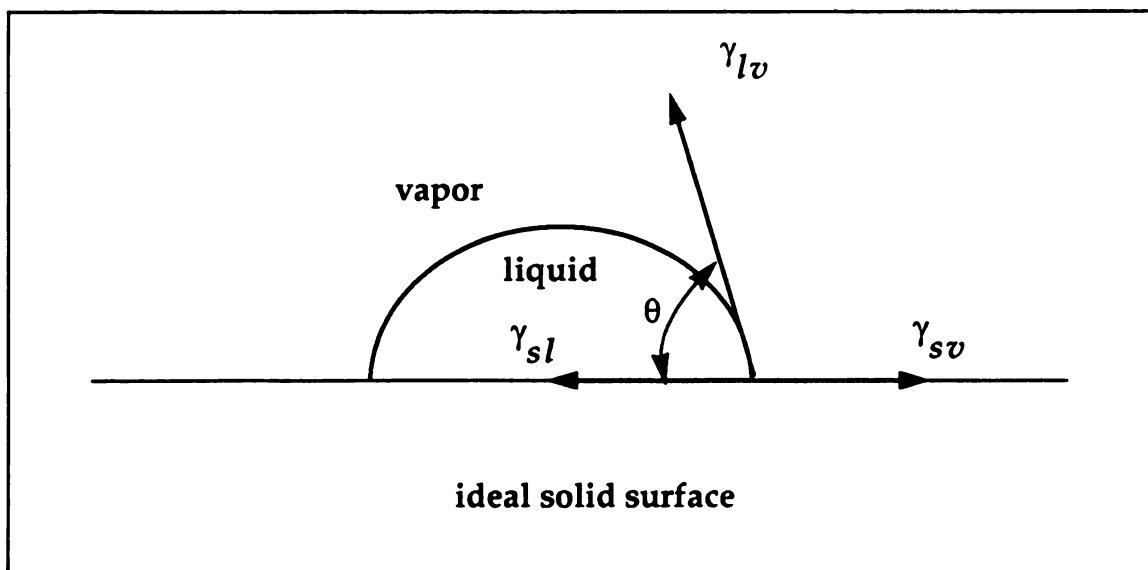


**Figure 1** The surface tension balance at a point of three-phase contact at equilibrium for ideal surfaces. An *ideal* surface is a smooth surface without interfacial reactions with a liquid drop.

The surface free energy(  $\gamma_s$  ) of a polymer can also be expressed by the equilibrium spreading pressure ( $\pi_e$ ) of a test vapor due to the adsorption of vapor molecules [39]:

$$\gamma_s = \gamma_{sl} + \pi_e \quad [3.2]$$

where  $\pi_e$  is defined as the reduction of  $\gamma_s$  due to the adsorption of vapor by the surface, when the vapor obeys the ideal gas laws as in equation [3.3]:

$$\pi_e = RT \int_0^{p_o} \Gamma d(\ln p) \quad [3.3]$$

where  $p$  is the vapor pressure,  $p_o$  is the saturation vapor pressure;  $R$  and  $T$  are the gas constant and temperature, respectively, and  $\Gamma$  is the surface concentration of absorbed vapor.<sup>[39]</sup> For a polymer with low surface energy,  $\pi_e$  can usually be neglected so that equation [3.1] is approximated:

$$\gamma_s \approx \gamma_{sl} + \gamma_{lv} \cos \theta \quad [3.4]$$

Equation [3.4] provides a way to indicate the spreadability (or wettability) of liquids on the solids. The criteria of the spreading of liquid on a solid can be expressed by defining a parameter of the equilibrium spreading coefficient,  $S_e$ :

$$S_e = \gamma_s - (\gamma_{sl} + \gamma_{lv}) = \gamma_{lv} (\cos \theta - 1) \quad [3.5]$$

When  $\theta$  is zero, i.e.  $\cos \theta = 1$ ,  $S_e = 0$ , the liquid spontaneously spreads over the surface because of the negative free energy association with the process. When  $\theta$  is not zero, i.e.  $\cos \theta < 1$ ,  $S_e < 0$ , then the liquid is non-spreading over the surface.

The work of adhesion separates two phases which are originally in intimate contact with each other. The work of adhesion,  $W_A$ , can be combined with equation [3.4] to give a direct relationship between  $W_A$  and wetting, yielding;

$$W_A = \gamma_{sv} + \gamma_{lv} - \gamma_{sl} = \gamma_{lv} (1 + \cos \theta) \quad [3.6]$$

Equation [3.6] indicates that  $W_A$  can be maximized when the liquid exhibits a

zero or near zero contact angle.

In addition to the concept of the wetting equilibria described by thermodynamic relationships with contact angles, the rate at which the contact angle equilibrium is approached depends on such factors as the driving force for wetting, the viscosity of the liquid, and roughness of the solid.<sup>[39]</sup>

### **3.2. Methods of estimating surface free energy of solid**

Surface energies of solids are usually estimated from the contact angle measurements using probe liquids of known surface characteristics. Most of the contact angle methods to estimate surface free energy of solid are based on the Young's equation (Equation [3.1]) by using a liquid drop on the smooth and undeformed surface of solid. Various methods are proposed to estimate the surface energy of solid. Since the surface energy of solid cannot be directly measured, the methods of estimating surface energy solids have been attempted by many authors. The methods which have been proposed are reviewed in the following.

#### **3.2.1. The critical surface energy, $\gamma_c$**

The critical surface tension, originated by Zisman<sup>[32]</sup>, was the first approach to characterize low-energy solids by measuring contact angles of a homologous series of liquids. He used a rectilinear relationship existing between the contact angle and the surface tension of the wetting liquid. As shown in *Figure 2 (page 17)*, which was obtained from contact angles of liquids for untreated polymer films, a straight line is obtained when  $\cos\theta$  is plotted against the liquid surface tension. The intercept of the line  $\cos\theta=1$  is defined as critical sur-

face energy,  $\gamma_{\text{crt}}$ , which just spreads over the solid. Kinloch<sup>[39]</sup> indicated that  $\gamma_{\text{crt}}$  is not identical with the surface energy of solid, but is only an empirical parameter with relative values which act as one would expect of the surface free energy. From Zisman's method,  $\gamma_{\text{crt}}$  can be expressed as an equation [3.7] by substitution of  $\cos\theta = 1$  into equation 2:

$$\gamma_{\text{crt}} = \gamma_s - \gamma_{\text{sl}} - \pi_e \quad [3.7]$$

This equation reveals that  $\gamma_{\text{crt}}$  can only be identical with  $\gamma_s$  when the interfacial tension between solid and liquid,  $\gamma_{\text{sl}}$ , and  $\pi_e$  are negligible for the polymer surface<sup>[39]</sup>. Hata et al<sup>[45]</sup> also stated that the critical surface energy,  $\gamma_{\text{crt}}$ , provides minimum surface energy, and that homologues and nonhomologous series of liquids should be selected to maximize  $\gamma_{\text{crt}}$  if  $\gamma_{\text{crt}}$  is to be used to as a measure of surface free energy,  $\gamma_s$ .

Later, Dann<sup>[50]</sup> observed the different values of  $\gamma_{\text{crt}}$  depending on the values of  $\gamma_{\text{sl}}$  by measuring the contact angles of various liquid series on the a number of polymers and explained this feature by employing the concepts of Good<sup>[46]</sup>, Girifalco<sup>[47]</sup> and Fokwes.<sup>[48]</sup> He also demonstrated the limitation of Zisman's approach, which was restricted to the range of surface tensions of a homologous series of liquids for  $\gamma_{\text{crt}}$  measurements because no polar force components were involved in the total surface tension contributions.

### 3.2.2. Surface free energy components to determine solid surface energy

This method starts from Fowkes' suggestion<sup>[48]</sup> that surface free energy components exist which are due to particular types of intermolecular forces,

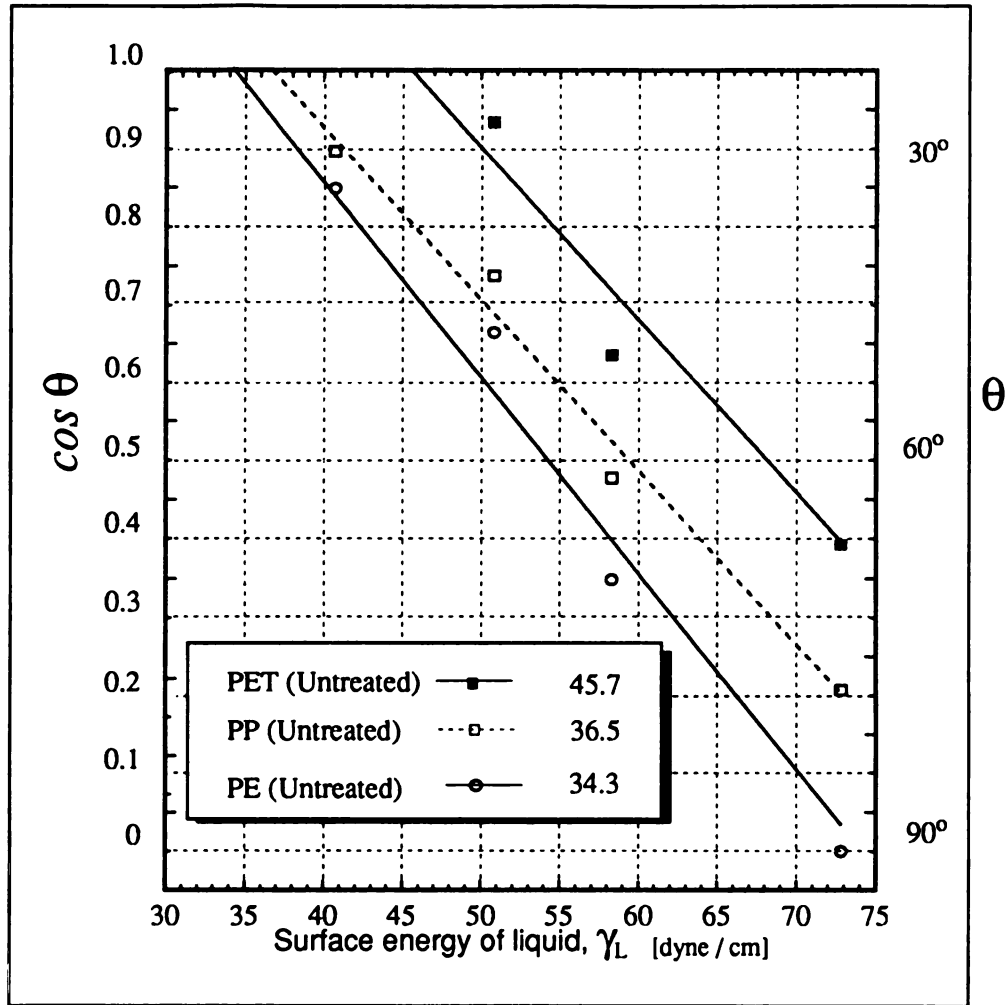


**Figure 2** A plot of cosine of angles vs. the surface energy of liquid, as proposed by Zisman.

including dispersion forces, dipole-dipole forces, or hydrogen-bonding interaction. It has been recognized as effectively caused by two major components; the dispersion forces (or London forces) and the polar forces, which are considered as acid/base interactions, are expressed as follows:

$$\gamma = \gamma^d + \gamma^p \quad [3.8]$$

where the superscripts  $d$  and  $p$ , respectively, are dispersion and polar force components of solid surface energy.

Fowkes<sup>[48]</sup> then applied the geometric mean to the dispersive force components for estimating the surface energies involving only dispersion forces:

$$\gamma_{ab} = \gamma_a + \gamma_b - 2\sqrt{\gamma_a^d \gamma_b^d} \quad [3.9]$$

where  $\gamma_a$  and  $\gamma_b$  are the surface energies of the two phases, and superscript  $d$  is dispersive component of the interfacial energy.

Owens et al<sup>[52]</sup> presented an equation to describe the interfacial energy between two surfaces by combining all interactions including dispersion forces into a single  $\gamma^p$  term. They assumed that the geometric mean expression could be extended to polar interactions and subsequently to equation [3.9] in the a solid/liquid system, as following;

$$\gamma_{sl} = \gamma_{sv} + \gamma_{lv} - 2\sqrt{\gamma_s^d \gamma_l^d} - 2\sqrt{\gamma_s^p \gamma_l^p} \quad [3.10]$$

where  $d$  and  $p$  denote dispersion and polar components of interfacial free energy, respectively.

Finally an equation to manipulate estimating the surface free energy of solid can be reached by combining equation [3.10] with equation[3.4] (on page 14) and [3.8] (on page 18), which eliminates the interfacial energy of solid and liquid:

$$\gamma_l (1 + \cos\theta) = 2\sqrt{\gamma_s^d \gamma_l^d} + 2\sqrt{\gamma_s^p \gamma_l^p} \quad [3.11]$$

where  $\gamma_l$  is the surface tension of the liquid, which is the sum of dispersion and polar force components.

$$\gamma_l = \gamma_l^d + \gamma_l^p . \quad [3.12]$$

By making contact angle measurements with two probe liquids of known characteristics [Table 2 (on page 20)]; two equations can be set up on the common solid surface and solved for the unknown  $\gamma_s^d$ , and  $\gamma_s^p$ . Then the surface energy of the solid,  $\gamma_s$ , is the sum of these two components.

$$\gamma_s = \gamma_s^d + \gamma_s^p \quad [3.13]$$

This method is described in greater detail in the *Chapter 3.3.1. (on page 22)*

Dann<sup>[50]</sup> evaluated the surface energy of many liquids used for contact-angle measurements from the previously reviewed equations. Basically, he determined only the dispersion-force components of the liquid surface tension,  $\gamma_l^d$ , by measuring contact angles against a solid that was intended to have only a dispersion-type surface energy. He measured contact angles of various liquids on paraffin, assuming  $\gamma_s^p$  as zero, and evaluated the dispersion component of the liquid using the equation [3.14]:

$$\gamma_l^d = \frac{4\gamma_p^d \cdot (\cos\theta)}{\gamma_l} \quad [3.14]$$



where  $\gamma_l^d$  is the dispersion force component of the liquid surface free energy;  $\gamma_l$  is the total surface free energy of the liquid which can be directly measured by using the Du Nouy ring method or Wilhemy plate technique; and  $\gamma_p^d$  is the paraffin surface energy of the dispersion-force component which was known as 25.5 [dynes/cm]. Then the  $\gamma_l^p$ , the polar (or non-dispersion) component of liquid surface tension was calculated by using Equation[3.8] (on page 18).

Some typical liquids used in the contact angle method to characterize the solid surface are given with  $\gamma_l^d$ ,  $\gamma_l^p$  and  $\gamma_l$  in Table 2.

**Table 2** The characteristics of typical liquids used as probes for the contact angle measurements<sup>a</sup>

Liquid	$\gamma_l^d$ [Dyne/cm]	$\gamma_l^p$ [Dyne/cm]	$\gamma_l$ [Dyne/cm]
Distilled Water	22.0	50.2	72.2
Glycerol	34.0	39.0	73
Formamide	32.3	26	58.3
Di-iodomethane	48.5	2.3	50.8
I-Bromonaphthalene <sup>b</sup>	44.6	0.0	44.6
Dimethylsulphoxide <sup>b</sup>	36.2	4.5	40.7
Tricresylphosphate <sup>b</sup>	36.2	4.5	40.7
Polyglycol E-200	28.2	15.3	43.5
Polyglycol 15-200	26.0	10.6	36.6
Hexadecane	27.6	0.0	27.6

a. Dann, unless otherwise noted

b. Fowkes

### 3.2.3. The methods using the equations for the work of adhesion

This method starts from the surface tension that can be divided into two components, the dispersion force and polar force components, and is represented by  $\gamma = \gamma^d + \gamma^p$  (equation [3.8] (on page 18)). The equation [2.4] (on page 10), which is  $W_A = 2 (\gamma_s \gamma_l)^{1/2}$  can be extended with the concept of Owens, et al<sup>[52]</sup>, following;

$$W_A = 2\sqrt{\gamma_s^d \gamma_l^d} + 2\sqrt{\gamma_s^p \gamma_l^p} \quad [3.15]$$

Combining this equation [3.15] with Young-Dupre equation [3.6] (on page 14) yields:

$$\gamma_l (1 + \cos \theta) = 2\sqrt{\gamma_s^d \gamma_l^d} + 2\sqrt{\gamma_s^p \gamma_l^p} \quad [3.16]$$

### 3.3. Calculations of dispersion and polar force contributions to surface free energy of polymer

Contact angle measurements have been widely used to calculate the values of the dispersion force,  $\gamma_s^d$ , and polar force,  $\gamma_s^p$ , components to the total surface free energy,  $\gamma_s$ , by using equation [3.11] (on page 19) or [3.15] (page 21). Kaelble and Cirlin<sup>[53]</sup> used two fluids to calculate the surface energy (Details in 3.3.1.). Carley et al<sup>[12]</sup> used four liquids rather than two liquids to characterize each test surface and Kinloch et al<sup>[36]</sup> have well developed the equation to reduce errors during calculation of surface energies on the solids by using four liquids (Details in 3.3.1(a)). The followings details the derivation of equations and methods.

### 3.3.1. Determinant method

Kaelble, et al<sup>[53]</sup> analyzed the experimental values in work of adhesion acquired by using the equation  $W_A = \gamma_l (1 + \cos\theta)$ . In his analysis a pair of simultaneous equations is derived for two liquids,  $m$  and  $n$ , on a common solid surface:

$$(W_A)_m = 2\left(\gamma_s^d\right)^{1/2}\left(\gamma_l^d\right)_m^{1/2} + 2\left(\gamma_s^p\right)^{1/2}\left(\gamma_l^p\right)_m^{1/2} \quad [3.17]$$

$$(W_A)_n = 2\left(\gamma_s^d\right)^{1/2}\left(\gamma_l^d\right)_n^{1/2} + 2\left(\gamma_s^p\right)^{1/2}\left(\gamma_l^p\right)_n^{1/2} \quad [3.18]$$

where  $\theta$  is the contact angle of the liquid on the solid surface. Thus, if the values of  $\theta$ ,  $\gamma_l^d$ ,  $\gamma_l^p$  for the two liquids are known, these equations may be solved to yield the dispersion and polar force components to the surface free energy of the solid surface. The total surface energy is then simply the sum of these components. But this has some limitation for using contact angle data for only two liquids, and suffers having errors when calculation of the surface energies is performed to other liquids.

The equation [3.17] or equation [3.18] has a linear relationship in the schematic representation of  $(\gamma_s^d)^{0.5}$  versus  $(\gamma_s^p)^{0.5}$  as shown in (Figure 3) where four linear relationships obtained from four liquids contact angles are illustrated. Previously reported work has solved for the two unknowns by solving for each individual pair of lines and then averaging the results, but this direct approach was found to lead to considerable errors in the values of  $\gamma_s^d$  and  $\gamma_s^p$ , which had

been calculated.

Kaelble<sup>[53]</sup> suggested that the pairs of lines have exceeding values of boundary condition should be excluded to minimize errors, where  $D_{\text{boundary}}$  is given by:

$$D_{\text{boundary}} = \left[ \left( \gamma_l^d \right)_m \left( \gamma_l^d \right)_n \right]^{1/2} - \left[ \left( \gamma_l^p \right)_m \left( \gamma_l^p \right)_n \right]^{1/2} \geq \pm 10 \quad [3.19]$$

Though this condition was shown to contribute somewhat to reducing the scattering, the condition of  $D_{\text{boundary}}$  remains unverified condition. According to this method, points A and B in (Figure 3) are disregarded in the calculation of the surface energy of solids, which may lead to some errors.

### 3.3.1(a) The least square method

Kinloch<sup>[36]</sup> provided this method to make possible not only to calculate the surface energy values by accepting all the contact angle data, but also to reduce errors in calculations. This technique is not depending on the individual intersections but on the slopes of the straight lines shown schematically in Figure 3. It is possible to use equation [3.16] (on page 21), [3.17] and [3.18] (on page 22) with method of least squares to obtain best values of the dispersion force,  $\gamma_s^d$ , and polar force,  $\gamma_s^p$ , components for each treated surface, based on the data from several liquids instead of just two. The derivation of this procedure and a computer program for solving equations are detailed below.

### 3.3.1(b) Derivation of least squares method

The equation [3.16] can be rewritten for each liquid used for the contact angle measurement on the common film surface as an equation:

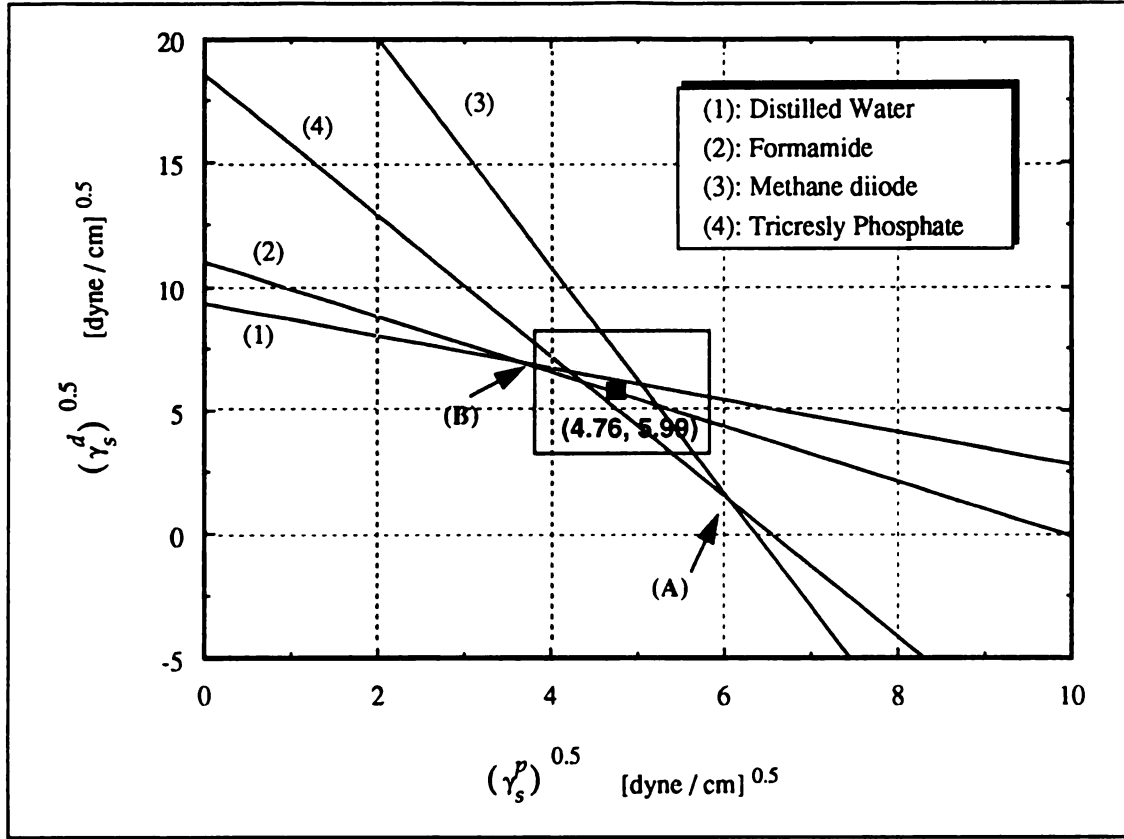


**Figure 3** Presentation of typical individual relationships of  $(\gamma_s^d)^{0.5}$  versus  $(\gamma_s^p)^{0.5}$  deduced from one of equations [3.17] or [3.18]. Plot shows SPP1, sulfonated polypropylene for 1 min. The shaded part is in the boundary

$$2 \left( \frac{\sqrt{\gamma_l^d}}{\gamma_l} \right) \sqrt{\gamma_s^d} + 2 \left( \frac{\sqrt{\gamma_l^p}}{\gamma_l} \right) \sqrt{\gamma_s^p} = 1 + \cos \theta \quad [3.20]$$

When  $k$  numbers of liquids are used for the contact angle measurement, equation [3.20] can be simplified as in the matrix form with two unknown compo-

nents of the surface free energy:

$$[A]_{k \times 2} [X]_{2 \times 1} = [B]_{k \times 1} + [e]_{k \times 1} \quad [3.21]$$

where matrix  $[A]$  represents the constant coefficients of the two unknowns,  $\sqrt{\gamma_s^d}$  and  $\sqrt{\gamma_s^p}$ , in Matrix  $[X]$ . Matrix  $[B]$  represents the constant values of right-hand side of equation [3.20], i.e.  $1 + \cos\theta$ . And matrix  $[e]$  is the error involved in balancing the individual equation.

When  $m$  numbers of contact angle of each liquid on a film are recorded, then equation [3.21] can be extended as:

$$[A]_{k \times 2} [X]_{2 \times m} = [B]_{k \times m} + [e]_{k \times m} \quad [3.22]$$

Matrix  $[B]$  is taken to the left-hand side of the equation [3.22], and multiplied by both sides of the equality with the transpose of the left-hand side:

$$\begin{aligned} \{ [A]_{k \times 2} [X]_{2 \times m} - [B]_{k \times m} \}^T \{ [A]_{k \times 2} [X]_{2 \times m} - [B]_{k \times m} \} \\ = \{ [A]_{k \times 2} [X]_{2 \times m} - [B]_{k \times m} \}^T \{ [e] \} \end{aligned} \quad [3.23]$$

where superscript  $T$  presents the transpose of the matrix concerned.

The equation can be expanded as giving,

$$\begin{aligned} \{ [X]^T [A]^T [A] [X] \}_{m \times m} - \{ [X]^T [A]^T [B] \}_{m \times m} \\ - \{ [B]^T [A] [X] \}_{m \times m} + \{ [B]^T [B] \}_{m \times m} = [E]_{m \times m} \end{aligned} \quad [3.24]$$

When the partial derivative of matrix  $[E]$  is employed for the two unknowns ( $X_1$  and  $X_2$ ) and made to zero to minimize the error then:

$$\partial [E] / \partial x_1 = [A]^T [A] [X] + [X]^T [A]^T [A] - [A]^T [B] - [B]^T [A] = 0 \quad [3.25]$$

$$\partial [E] / \partial x_2 = [A]^T [A] [X] + [X]^T [A]^T [A] - [A]^T [B] - [B]^T [A] = 0$$

Since the above two equations are the same, rearranging one of the equations gives:

$$\{ [A]^T [A] [X] - [A]^T [B] \}_{2 \times m} + \{ [X]^T [A]^T [A] - [B]^T [A] \}_{m \times 2} = 0 \quad [3.26]$$

The equation [3.26] is in the form of  $[Z] + [Z]^T = 0$ . In order to satisfy the equality to zero, then both matrixes should be individually equal to zero. Therefore:

$$\{ [A]^T [A] [X] \}_{2 \times m} = \{ [A]^T [B] \}_{2 \times m} \quad [3.27]$$

and

$$\{ [X]^T [A]^T [A] \}_{m \times 2} = \{ [B]^T [A] \}_{m \times 2} \quad [3.28]$$

Equation [3.27] is the transpose of equation [3.28]. Therefore one of these two equations is required for analysis for contact angle measurements. Matrix  $[X]$  in the above equations can be solved by one of equations below:

$$[X]_{2 \times m} = \{inverse \{ [A]^T [A] \} \} \{ [A]^T [B] \}_{2 \times m} \quad [3.29]$$

and

$$[X]_{m \times 2} = \{inverse \{ [A]^T [A] \} \} \{ [B]^T [A] \}_{m \times 2} \quad [3.30]$$

There are several advantages to using this method; this method yields the least errors, it accept all the data, and it is very simple to employ into a computer program. A computer program to solve this equation can be made by using fortran, basic, or any software which can calculate the matrix. In the present study, "Matlab" (The MathWorks, Inc.) software has been used to solve the matrix  $[X]$  in the equation [3.29].



### 3.3.1(c) Computer program "SFE"

A program to calculate surface free energy by solving matrix  $[X]$  in equation [3.29] has been presented from *Figure 4 (a)* to *Figure 4 (d)*. A program 'SFE' was written using MATLAB software (The MathWorks, Inc., Natick, MA) which is available for both the Personal Computer and the Unix Operating System computer.

```
!rm diary;
clear;
clg;
%input('datafile=')
load test;
test=B;
Ag=mean(B);
Std_angle=std(B);
G= [21.8 51; 32.3 26; 48.5 2.3; 36.2 4.5];
T= G(:,1) + G(:,2);
GL = [G T]
diary on
B
[Ag, Std_angle]
GL
diary off                                     % [continued]
```

**Figure 4 (a)** Program to calculate the average and standard deviation errors of measured contact of each liquid angles on a polymer sample.

The average value and standard deviation of contact angles for each liquid are expressed as in *Ag and Std-angle matrix*,  $[m \times k]$ , respectively, where  $k$  is the number of liquids used and  $m$  is a measured number on a common surface with each liquid.

Applying this data, measured contact angles for various liquids on a film surface should be in the *matrix "test"*,  $[m \times k]$ , where *column*,  $k$ , represents the liquid used for measurements, and *rows*,  $m$ , are duplicates of recorded contact angles.

#### Datafile "test"

C:\ type test

86.2	68	44.9	32.1
86	69	42.8	34.4
87	67	43.7	31.7
88.8	67.4	42.1	32.1
85.3	68.2	43	31.8
86.7	64.7	42.7	34.3
94.3	66.2	41.8	32.9
87.2	68.9	46.2	33.8
89.2	67.2	43.6	32.7
87.2	70.2	44.5	33.2

**Figure 4 (b)** Figure shows the input data file for the program shown in Figure 4 (a). Columns in this data file present each liquid used for the contact angle measurement. Rows in this file are the duplicate of the measured contact angle of a liquid measured on different points of a film sample.

The surface energies of liquids used in contact angle measurement are presented in the *matrix*  $GL$ ,  $[3 \times 4]$  from the *matrix*  $G$ ,  $[2 \times 4]$ , where the first column is the dispersive component, the second column is polar component of liquid surface energy, and the third column is total surface energy of the liquid expressed in the *matrix*  $T$ ,  $[4 \times 1]$ , as the sum of the first and second columns of *matrix*  $G$ .

```

Ca=cos(B*pi/180);
Aa=cos(Ag*pi/180)
C=1+Ca;
[A]=[2.*(GL(:,1).^0.5)./GL(:,3)
      2.*(GL(:,2).^0.5)./GL(:,3)];

x=(-4:.5:15)';
y1=-A(1,1)./A(1,2).*x+C(1,1)./A(1,2);
y2=-A(2,1)./A(2,2).*x+C(1,2)./A(2,2);
y3=-A(3,1)./A(3,2).*x+C(1,3)./A(3,2);
y4=-A(4,1)./A(4,2).*x+C(1,4)./A(4,2);

plot(x,y1,'y-',x,y2,'-.',x,y3,'--',x,y4)
axis([-5 15 -40 50])
axis('square=')
grid
%gtext('PET film (Untreated)')
title =('Surface Free Energy(sfe) of solid
        by the plot')
xlabel ('dispersive component,(dyne/cm)^0.5')
ylabel ('polar component,(dyne/cm)^0.5')
print result
clg;
pause;
%
```

%[continued]

**Figure 4 (c)** This program provides a graphic like the one presented in *Figure 3* (on page 24), which is plotted  $(\gamma_s^d)^{0.5}$  versus  $(\gamma_s^p)^{0.5}$ , deduced from one equations [3.17] or [3.18] (page 22).

A solution for either equation of [3.29] or [3.28] (page 26) can be obtained by the following program;

```

E = [inv([A]'*[A])*([A]'*[C]')];

AA = E';

XY_point=mean(AA);

Ans=E.^2;

s=Ans';

n =size(s,1);

s_avg=sum(s)./n;

Sur_dp = [s_avg];

Total_se = s_avg(:,1)+s_avg(:,2)

end

```

**Figure 4 (d)** This program calculates surface free energy, corresponding dispersion component, ( $\gamma_s^d$ ) and polar component, ( $\gamma_s^p$ ) of solid by solving one of equations [3.27] or [3.28].

## ***Chapter 4. Surface modification technology***

### **4.1. Introduction**

Over the years, several methods have been developed to modify polymer surfaces for improved adhesion, wettability, and printability. These include mechanical treatments, wet-chemical treatments, exposure to flames, corona discharge and glow discharge plasmas. The most commonly using modification methods on the polymer surface are<sup>[1]</sup>;

- Chemical etching
- Flame Treatment
- Corona and Plasma treatments

The basic objective of such treatments is to remove weakly bonded surface contamination and to provide intimate contact between the two interacting materials on a molecular scale, for molecular energies across an interface decrease with increasing intermolecular distance.<sup>[4]</sup> Kinloch<sup>[39]</sup> summarized that the purpose of any particular surface treatment might be various but the main aims are usually increasing adhesion properties of the polymer by one or more mechanisms as follows:

1. The removal of any weak boundary layer, such as may occur from low molecular weight contamination, antioxidants, processing aids or the tail of the polymer's molecular weight distribution.

2. The introduction of specific groups on the surface to aid the formation of the interfacial polar interactions, hydrogen bonds, acid-base interactions to increase the extent of interfacial contact and the degree of intrinsic adhesion. This is usually reflected in higher values for the surface energy, thermodynamic work of adhesion.
3. The creation of a surface topography suitable for mechanical interlocking to occur, thereby increasing the intrinsic adhesion.

In the following sections the various types of surface treatment techniques and the effect of different treatments will be briefly described. The sulfonation technique is considered separately since the principles involved are quite new and are conveniently reviewed in a separate chapter.

## **4.2. Chemical etching techniques**

Chemical etching is the treatment of polymer surfaces by exposure to solutions of reactive chemical compounds, which may cause a chemical change on the surface and also may introduce micro roughness by removing some material.<sup>[40]</sup> Thereby surface bondability and wettability are improved. This technique, however, has some limitations: it requires immersion for some time period; the polymer surface must be rinsed and dried. Therefore, chemical etching is used only when simpler and less expensive methods are not available. For example fluorocarbon polymers are often etched chemically because other treatments do not produce sufficiently good bondability.<sup>[41]</sup>

Etching with sulfuric and chromic acids are suitable for modifying the surface of polyethylene, polypropylene, ABS, polyether, and polystyrene.<sup>[1]</sup> Chromic acid etching removes amorphous areas, forming cavities which contribute to

the improved bondability. Some surface oxidation may also take place which improves surface wettability.

Chromic etching of polyethylene has showed a combined mechanism for enhanced bondability and thus adhesion. Blais et al observed fine surface roughness after an etching treatment, which led to the increased bondability. The calculated surface tension of a solid was 34.2 dynes/cm for untreated, and 52.3 dynes/cm for a treated polyethylene surface. However, Blais et al revealed extensive chemical changes with an increasing concentration of OH,  $>C=O$  groups in the surface layer. They also suggested the main mechanism for the increased adhesion to be due to the removal by the etchant of a weak boundary layer covering the polyolefin surface.

Briggs et al[9] investigated treated low-density PE, and PP with ESCA and showed that oxidation and sulfonation occurred in the outermost surface regions of both materials with evidence for  $-COH$ ,  $>C=O$ ,  $-COOH$ , and  $-S(=O)_2OH$  groups. These incorporated specific groups that are due to etching treatment may have a major role in increasing surface polarity and thus enhancing adhesion and bondability.

No single identifiable mechanism has yet been established for developing the etching technique. One of chemistry changes due to the introduced group at the surface of the polymer seems to be an essential mechanism for improving bondability and adhesion, but with some polyolefins the removal of a weak boundary layer may be a necessary step for modifying the make polymer surface.



### 4.3. Flame Treatment

Flame treatment is one of the most common surface treatments for improving the adhesion of such molded polyolefin products, as containers. While the corona discharge is used for sheeting below a thickness of 0.6 mm, flame treatment is applied to thicker sheeting.<sup>[39]</sup>

Flame treatment oxidizes the polymer surface and makes it more easily wettable. Because the flame treatment can readily induce to degradation of the polymer surface, optima in process is quite critical. Important parameters for optimum conditions are the position of the component relative to the flame; the air, gas; the air/gas flow rate; the nature of the gas; and the exposure time.<sup>[40]</sup>

Briggs et al extensively examined the effect of flame treatment and the mechanism of surface modification on low density polyethylene(LDPE) by employing ESCA. They showed that flame treatment caused oxidation with a range between 4 nm and 9 nm of the polymer surface. They assumed that a chain-reaction free radical process takes place due to the thermal oxidation, which may induce surface modification for the improved adhesion.

### 4.4. Corona and Plasma treatments

The plasma treatment has been recently introduced as an effective and economic route for polymer surface modification. Like corona treatment, plasma treating uses an electromagnetic energy to ionize gas molecules, which in turn react with the polymer surface. But plasma treatment takes place in a vacuum, unlike corona treatment, and plasma can use gases other than air to achieve a

wider variety of surface modification effects. (Plastics Technol., Feb. 1993)

Corona, also known as "atmospheric" or "nonvacuum" plasmas, are ionized gases which can react with a polymer surface to improve adhesion for printing, painting or laminating. Plasma treatment is a very effective method for modifying the polymer surfaces. Corona and Plasma treatment do not usually affect wettability but cross-linked the surface material, thereby improving bondability and adhesion. A schematic represented in *Figure 5 (page 38)* illustrates various interactions which are possible in a gas plasma contact on a polymer.<sup>[4]</sup>

In plasmas, four main effects are normally observed with singly or combined depending on the substrate and the gas chemistry, the reactor design, and the operating parameters.<sup>[4]</sup> They are:

1. Surface Cleaning, that is, removal of low molecular weight contamination, e.g. processing additives, which are present on the surface. Surface cleaning is a major effects for improved bonding to plasma-treated polymers because it does not leave any organic residual, the way most other cleaning procedures do, which interferes with adhesion processes.
2. Degradation and ablation of material from the surface, which can remove a weak boundary layer and increase the surface area. The ablation effect causes a change in surface morphology which provides mechanical interlocking and sites for chemical interaction. But some polymers, such as PET, are more prone to these effects, which give a porous surface due to overtreatment.
3. Cross-linking, which can cohesively strengthen the surface layer. The free radical can be created on the polymer surface exposed to the novel gas plasmas, and the free radicals resulting can react with other surface

radicals to form stable moieties. Cross-linking may have an advantage, e.g. hamper the development of a weak boundary layer at the joint interface. But lack of heat sealing due to Cross-linking is a disadvantage.

4. Modification of surface chemical structure, which can occur during plasma treatment. The plasmas often lead to the introduction of polar groups, such as carbonyl groups, into the surface regions of the substrate. Due to the polar groups, the polymer surface has an increased surface energy which leads to improved wetting and thus adhesion.

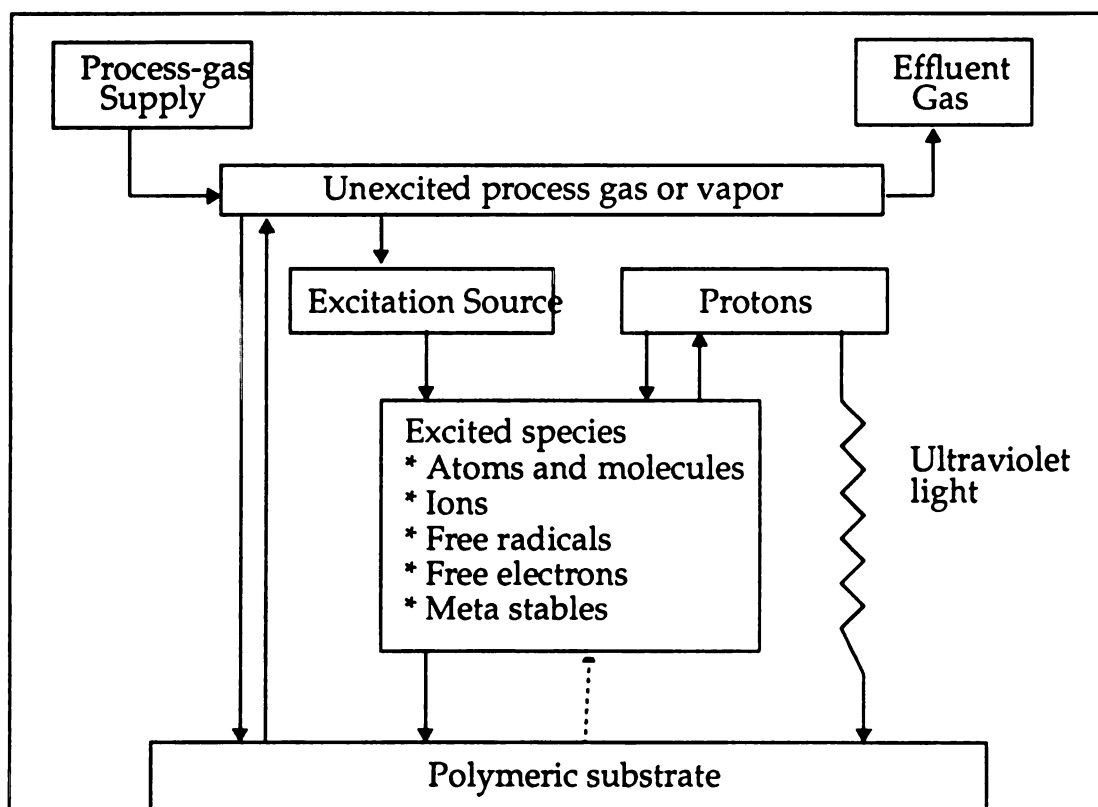


**Figure 5** A schematic representation of the interactions which are possible in a gas plasma impinging upon a substrate. <sup>[4]</sup>

#### 4.5. Surface Sulfonation Technique

The surface modification by a chemical technique requires a repeatable and controllable reaction through the modification process. The sulfonation process, exposing the polymer to gaseous  $\text{SO}_3$  or fuming sulfuric acid to form sulfonic acid groups, has this potential. Sulfonation has advantages which can control the depth of surface modification by regulating concentration of  $\text{SO}_3$  gas and reaction time.<sup>[23]</sup> These two factors, concentration and reaction time, can be offered as good alternatives to form acid groups in contribution of changing surface properties. The surface sulfonation of a polymer can result in changes of the physical and mechanical properties, such as adhesion<sup>[19], [23]</sup>, electrical conductivity<sup>[18]</sup>, and barrier properties.<sup>[21], [22]</sup>

A broad range of polymers, (except a fluorocarbon-based polymer), can be readily sulfonated.<sup>[24]</sup> It was found that a PE film and  $\text{SO}_3$  produced unsaturated sulfonic acid with the highly conjugated  $\text{C}=\text{C}$  unsaturated bonds.<sup>[20]</sup> Ihata<sup>[24]</sup> reported the reaction mechanism of sulfonation, that the reaction of PE film with  $\text{SO}_3$  was initiated by the abstraction of a hydrogen atom by  $\text{SO}_3$  to give a PE radical. This free radical could either react with  $\text{SO}_3$  to give a sulfonic acid group (Figure 6a) or eliminate a hydrogen atom to form an unsaturated bond (Figure 6 b).

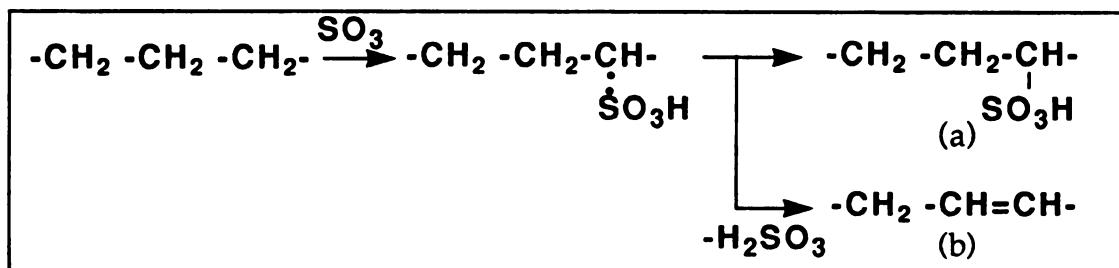


**Figure 6** Sulfonation reaction mechanism of HDPE [Ihata]

Similar results have been also observed by Asthana<sup>[23]</sup> who investigated adhesion properties in polypropylene and polystyrene films. He suggested, for polypropylene, that the tertiary carbons in the molecules are most probable to be attacked, and that reaction continues until conjugated  $-C=C-$  unsaturated bonds are formed due to desulfonation. For polystyrene, he confirmed that the para position of the aromatic rings are responsible for the active sites of reaction, and that the alkene species are formed during sulfonation. The reaction schemes for PP and PS are presented in *Figure 7* and *Figure 8*, respectively.

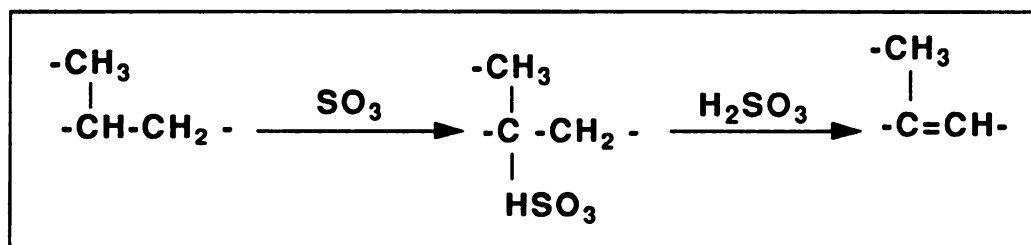


**Figure 7** The figure illustrates the formation of conjugated system of double bonds as a result of sulfonation<sup>[23]</sup>

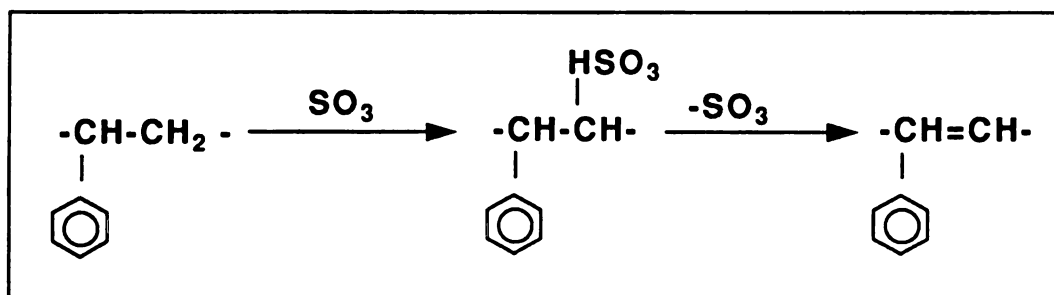


**Figure 8** The figure illustrates the formation of alkene species during sulfonation<sup>[23]</sup>

Since the  $\text{SO}_3$  group is not stable, the neutralization step is required to stabilize the  $\text{SO}_3$  group on the surface. Aqueous ammonium hydroxide ( $\text{NH}_4\text{OH}$ ) and ammonia gas ( $\text{NH}_3$ ) are usually used as neutralization agents, however various bases can be selected, (such as  $\text{Li}^+$ ,  $\text{Na}^+$ ,  $\text{Cu}^{++}$ ,  $\text{Mg}^{++}$ ), depending on the polymer properties.<sup>[22]</sup>

There are several sulfonating agents, including fluorosulfonic acid, chlorosulfonic acid and sulfur trioxide complexes, of organic compounds. Among them, sulfuric acid and fuming sulfuric (oleum)<sup>[20], [23]</sup>, are most popular in the form of  $\text{H}_2\text{SO}_4 \cdot x\text{H}_2\text{O}$ . They are extremely hygroscopic and react with water. Some important factors of those agents have been compared in Table1.<sup>[23]</sup>

**Table 3** A comparison of sulfuric acid and  $\text{SO}_3$  gas as sulfonation agents.<sup>[23]</sup>

Factor compared	Sulfuric Acid	Sulfuric trioxide
Reaction rate	Slow	Instantaneous
Heat Input	Heat requires for reaction	Strongly exothermic reaction
Side reaction	Minor	Extensive
Boiling point	290-317 °C	42-44 °C
Extent of reaction	Partial	Complete

## ***Chapter 5. Sulfonation of Polymer films***

The effect of surface sulfonation on the surface properties of three commodity films was studied by Electron Spectroscopy for Chemical Analysis (ESCA), Contact Angle Measurement Analysis (CAMA), and Peel Adhesion (PA) test. The type of polymers and exposure time for sulfonation were evaluated as experimental parameters.

### **5.1. Sulfonation Apparatus**

The surface treatment using sulfonation was performed at the Composite Materials and Structures Center (CMSC), at Michigan State University. The unit used was designed and manufactured by Coalition Technologies, Ltd., Midland, Mi.

#### **5.1.1. The Unit of Sulfonation System**

The sulfonation generator is a novel system that produces sulfur trioxide ( $\text{SO}_3$ ) gas from fuming sulfuric acid ( $\text{H}_2\text{S}_2\text{O}_7$ ), or oleum. Schematic diagrams of the sulfonation unit are presented in *Figure 9 (a)*, and *Figure 9 (b)*. The main unit is divided into two sections, the sulfur trioxide generator shown in *Figure 9 (a)*, and the unit with sulfonating chamber set-up as shown in *Figure 9 (b)*.

The gaseous  $\text{SO}_3$  concentration should be of constant composition and must be repeatable. There are two crucial external factors affecting the  $\text{SO}_3$  concentration: moisture and temperature. Since  $\text{SO}_3$  is a highly reactive chemical species with moisture, the system must be designed so as to avoid contact with

moisture. Also the temperature of the oleum reactor should be maintained at a constant level because the vapor pressure of gaseous  $\text{SO}_3$  is very sensitive to the temperature.

#### **5.1.1(a) Sulfonating chamber**

The sulfonating chamber is a stainless steel parallelepiped box with manifolds at two of its narrow sides. The dimensions of the box are 15x15x1.75 inches. Both the manifolds are welded to the narrow sides of the box and are made of stainless steel fittings. *Figure 10* shows a schematic of the sulfonating chamber, samples, and sample holder. This chamber is designed to mount four film sheets (6 x 13 in. each sheet) to be sulfonated with a sample holder, which assures that the sheets are not touching each other, nor the sides of the chamber.

#### **5.1.1(b) Sampling Port**

The sampling port, made up of stainless steel, is located in the main line which carries the  $\text{SO}_3$  gas into the sulfonating chamber, and functions to measure the  $\text{SO}_3$  concentration while sulfonating.



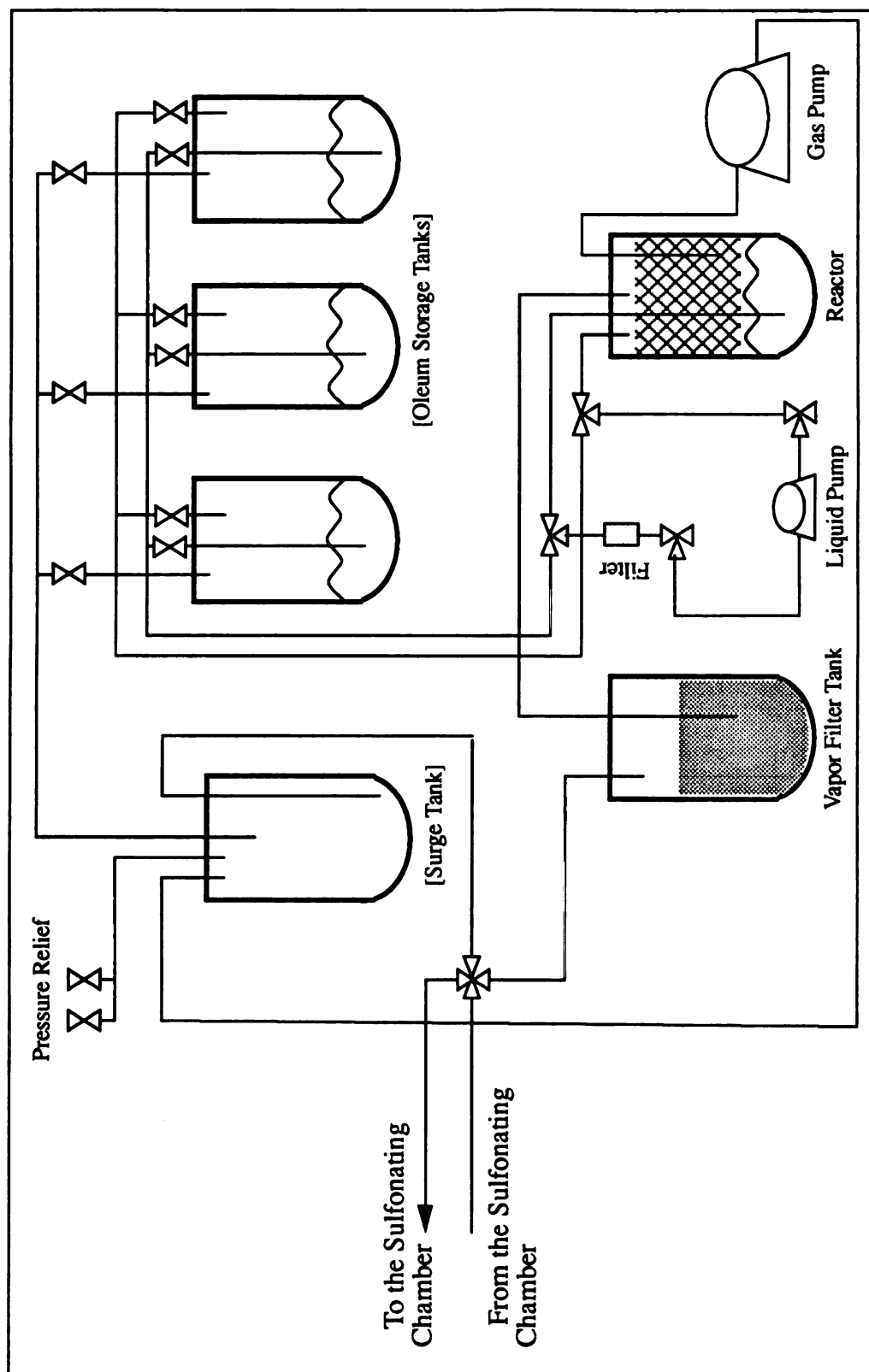


**Figure 9 (a)** Diagram for the gas-phase  $\text{SO}_3$  generator unit(a) [Continued to Figure 9(b)]

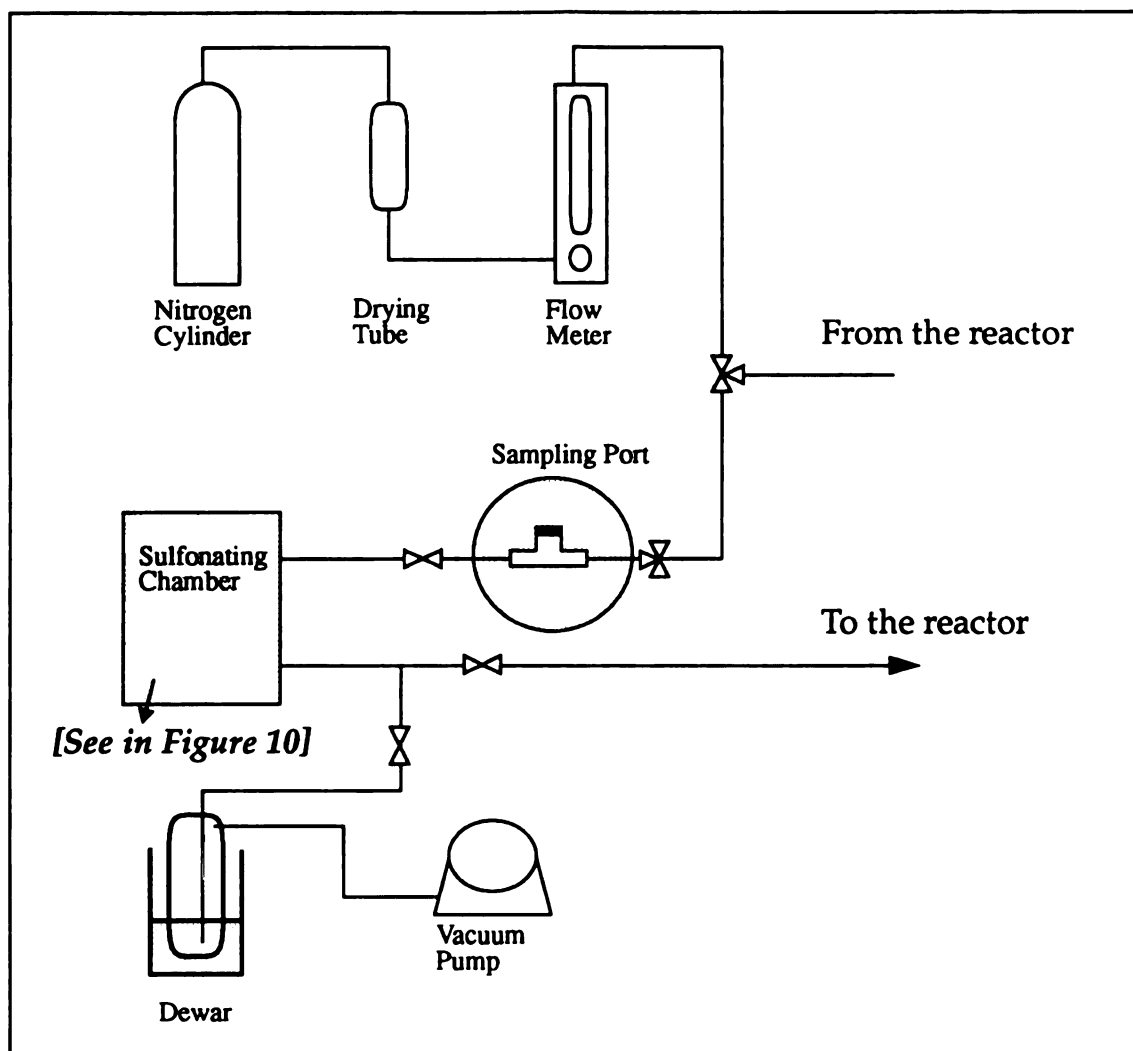


**Figure 9 (b)** Schematic illustrates the SO<sub>3</sub> flow pattern in the sulfonating chamber<sup>[23]</sup> [Continued from Figure 9(a)]

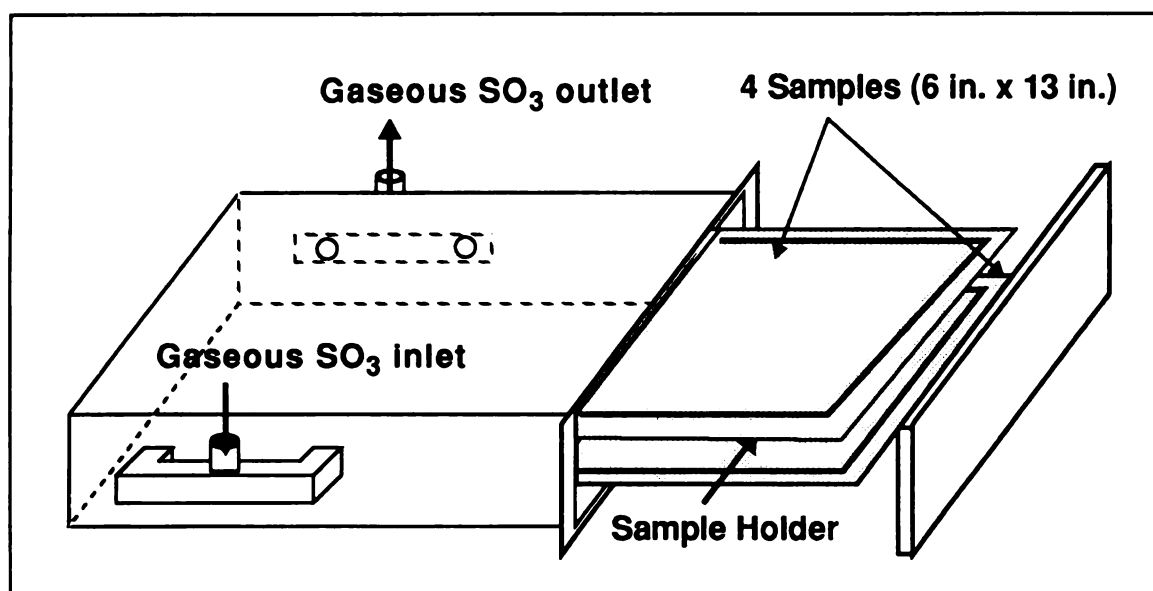


**Figure 10** View of Sulfonating Chamber, samples, sample holder<sup>[23]</sup>

## **5.2. Materials using for sulfonation**

### **5.2.1. Polymer films**

Films of oriented polypropylene (OPP, 2 mil thickness, 45.7% crystallinity, Mobile Company), polyethylene terephthalate (PET, 0.5 mil thickness, 31% crystallinity, DuPont), untreated polyethylene (UPE, 1 mil thickness, Tredgar<sub>TM</sub>) were surface sulfonated. Corona discharged polyethylene (CPE, 1 mil thickness, Tredgar<sub>TM</sub>) was also used in the present studies for the CAMA and PA test.

### **5.2.2. Fuming Sulfuric Acid**

Oleum ( $\text{H}_2\text{S}_2\text{O}_7$ ), otherwise known as 30% fuming sulfuric acid, was used to generate free  $\text{SO}_3$  gas during sulfonation. Oleum concentration was measured by weight percent of  $\text{SO}_3$  in the mixture, which consists of 70% (wt.) of sulfuric acid and 30% (wt.) of free  $\text{SO}_3$ .

### **5.2.3. Cleaning agent**

Deionized water with 2% Micro<sup>TM</sup> solution was used to remove any contaminations from manufacturing or handling of test samples prior to sulfonation. Micro<sup>TM</sup> was supplied by the Cole-Parmer Instrument Company (Niles, IL)

### **5.2.4. Neutralization Agent**

Ammonium hydroxide ( $\text{NH}_4\text{OH}$ ) solution (5% wt/v) was used to stabilize all sulfonated film samples. The sulfonated film samples were placed in  $\text{NH}_4\text{OH}$  solution for five minutes, and rinsed under running deionized water.

### 5.3. Sulfonation Procedure

All the reactions are carried out under ambient conditions. All the sheets were washed and rinsed in deionized water thoroughly and the samples were air-dried. In order to minimize the effect of moisture and to ensure the repeatability of the sulfonation on the polymer, the following procedure was followed in each run:

1. Film samples were carefully cut from each polymer film roll, the size of 6 inches by 13 inches. They were cleaned with Micro™ solution, and rinsed under running deionized water to eliminate contaminants from manufacturing and handling the films. Then they were completely dried at room temperature prior to further tests. Complete drying is a crucial process, as moisture is extremely reactive with  $\text{SO}_3$  to form sulfuric acid, consequently it is harmful to the concentration of  $\text{SO}_3$ .
2. A vacuum of about 300 microns was applied to the sulfonating chamber (*Figure 10 (page 46)*) with the samples for 10 minutes to remove the moisture. Also the sulfonating chamber was flushed with dry nitrogen gas at a rate of 32 liters per minute to avoid any reaction of active gases in the chamber with  $\text{SO}_3$  gases, which results in uniform sulfonation on the polymers.
3. The samples were sulfonated for the desired time. Sulfur trioxide gas, generated from the sulfonation unit (*Figure 9 (a) (page 44)*), was circulated through the external circulation lines. The  $\text{SO}_3$  generator temperature was adjusted to maintain a constant  $\text{SO}_3$  concentration of about 1% volume/volume. The gas was continuously circulated through the chamber for a predetermined time interval, to obtain various sulfonation levels, which were controlled by exposure time to sulfur trioxide gas.

4. Constant  $\text{SO}_3$  concentration during circulation, being one of the most important factors, must be controlled and monitored for each sulfonation run. A pH method was applied in order to monitor the concentration of  $\text{SO}_3$  (volume%) for each run. A 100 ml gas sample, during circulation, was taken with a gas-tight syringe through the septa which was placed in the external circulation sulfonation lines. The gas sample was then injected into a 125 ml Erlenmeyer flask containing 20 ml of deionized water. The flask was shaken to react the  $\text{SO}_3$  and water and then the pH of the acid solution was measured using a Corning model M-250 pH/ISE meter, with an accuracy of +0.001 pH. The  $\text{SO}_3$  concentration was calculated using the following equation.<sup>[19]</sup>

$$\text{SO}_3 [\%] = 209.94 \times (-2.065 \times [\text{pH}]) \quad [5.1]$$

5. The system was then flushed with dry nitrogen for 5 minutes before opening the sulfonating chamber. This ensures that all the residual  $\text{SO}_3/\text{H}_2\text{SO}_4$  is purged out of the system through the vent tube.
6. The films were neutralized with a 5% ammonium hydroxide solution ( $\text{NH}_4\text{OH}$ ) for five minutes and placed in a deionized water bath for another five minute. Before drying the films at room temperature, they were rinsed under running deionized water to remove the excess  $\text{NH}_4\text{OH}$ . After the films had dried, they were stored at ambient temperatures for further tests.

#### 5.4. Electron Spectroscopy for Chemical Analysis (ESCA)

All film samples were submitted to the CMSC, at Michigan State University, for determining the extent of sulfonation.

## Chapter 6. Physical tests

### 6.1. Contact Angle Measurements of Polymers and Methods

One of the goals of the present study was to calculate the surface energy of the polymer in order to compare the effectiveness of surface sulfonation. The surface energies of both untreated and sulfonated polymers were computed from contact angle analysis values, obtained with distilled water, formamide, di-iodomethane, and tricresyl phosphate, on the respective polymer sample surfaces. The surface energy characteristics of the four liquids are given in *Table 4*. The surface energy values of OPP, PET, PE films and corona treated PE films determined by contact angle analysis were used as a reference to determine the effects of sulfonation on the polymer films.

**Table 4** The surface energy of liquids, and the corresponding polar and dispersive component, used for measuring contact angles on the respective polymer samples and pressure adhesive tape.

Liquid	$\gamma_l^d$ [dyne/cm]	$\gamma_l^p$ [dyne/cm]	$\gamma_l$ [dyne/cm]
Distilled Water	22.0	50.2	72.2
Formamide	32.3	26	58.3
Di-iodomethane	48.5	2.3	50.8
Tricresyl phosphate	36.2	4.5	40.7

### 6.1.1. Test Apparatus for Contact Angle Measurements

Contact angles of liquids on test polymers were measured with a Goniometer (Model 100-00 115, Rame-Hart, Inc., Mountain Lakes, NJ), which was available at the Chemical Engineering Department, Michigan State University. A schematic of the Goniometer is shown in *Figure 12*.

### 6.1.2. Sample Preparation and Contact Angle Measurements of Polymers

Unmodified films were cleaned by the procedure outlined above for sulfonation, prior to measuring contact angles of test fluids. Clean and air dried films (2 in. x 1 in.) were mounted very evenly on a glass slide by using double adhesive tape as seen in *Figure 11*.

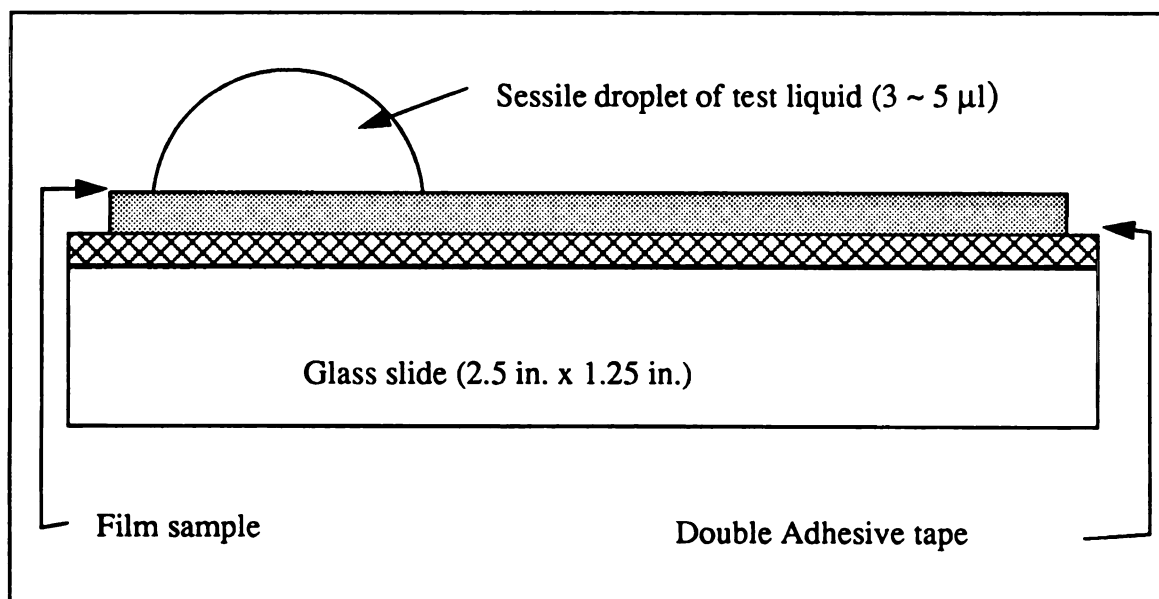


**Figure 11** Diagram of contact angle specimen and sessile droplet form.



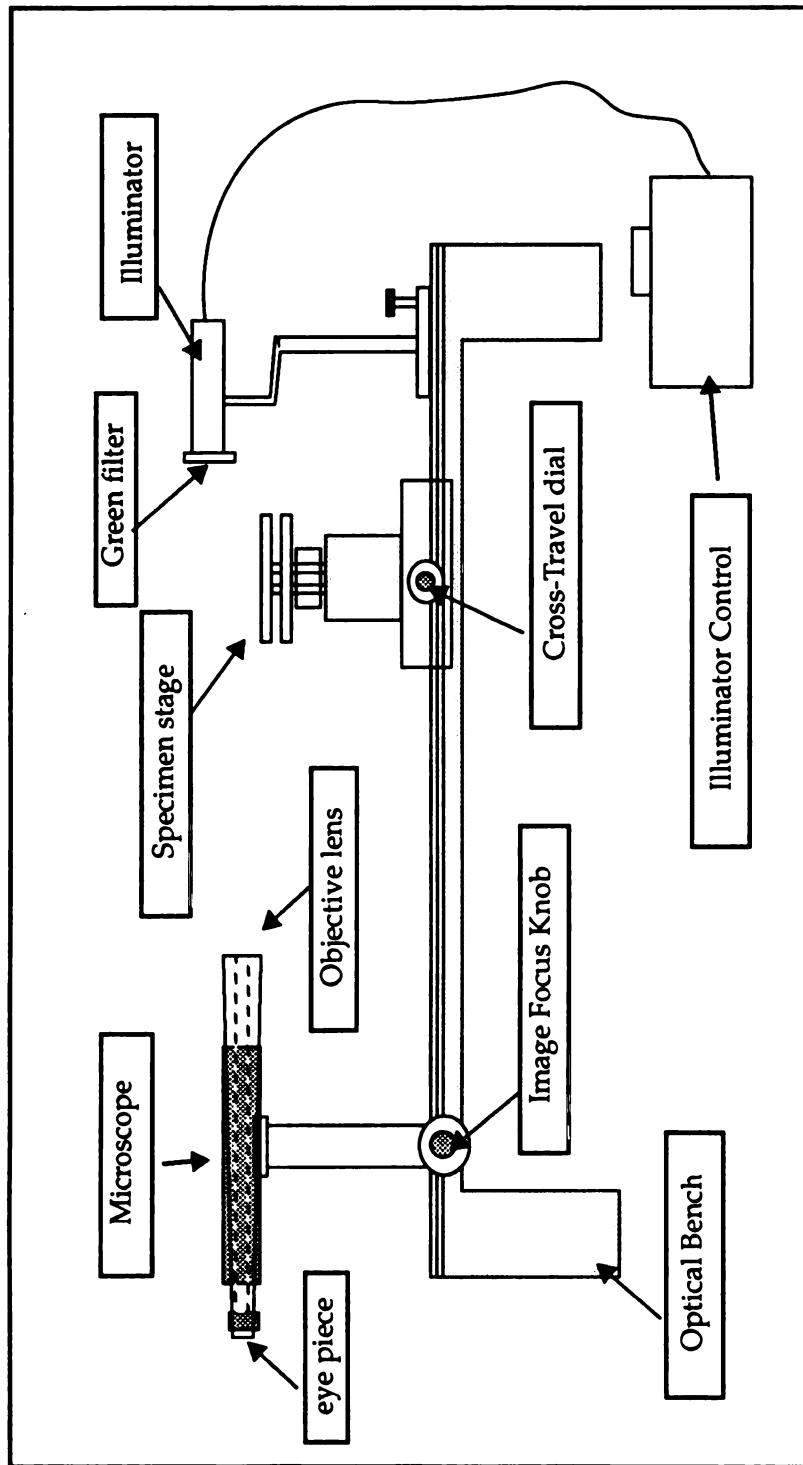


**Figure 12** A schematic of Goniometer (Model 100-00 115, Rame-Hart, inc.).

The sessile-drop method of measuring contact angles was used in this study, in ambient air and at room temperature. Droplets of 3 ~ 5  $\mu\text{l}$  size were formed on the polymer film surfaces delivered from a Pipetman pipet (0~200  $\mu\text{l}$ ) in such a way as to make the angles advance. A minimum of 10 contact angle measurements were made for each liquid, within the error of 3 degrees. All contact angles measured were used to calculate the surface energy of the test polymer film by the computer program 'SFE' (*Chapter 3.3.1(c) on page 28*). Angles were read to the nearest degree by using a 10X microscope with a protractor eyepiece. The procedure followed for each specimen to measure the contact angle<sup>[55]</sup> is as follows:

1. The polymer sample mounted on the glass slide was placed on the specimen stage of the Goniometer. The microscope was focused on the nearest edge of the film surface and adjusted the film surface and 'base-line' to achieve coincidence. This setting was not changed during the reading of the contact angle [*Figure 13(a)*].
2. A liquid droplet of 3 ~ 5  $\mu\text{l}$  volume, depending on the test liquids, was deposited onto the film to form a sessile drop of about 2.5 mm diameter with a 200  $\mu\text{l}$  pipet [*Figure 13(b)*].
3. The specimen stage was adjusted to view the extreme left side of the sessile drop, and the microscope was refocused for accurate drop profile, by shifting the line of sight [*Figure 13(c)*].
4. The measuring cross line was adjusted to tangency above the base of the drop to create a wedge of light bounded by the two cross lines and the drop profile [*Figure 13(d)*].

5. The cross line was slowly rotated in order to measure it while adjusting the cross travel of the specimen stage so that the wedge of light would be gradually extinguished and the cross-line would attain tangency with the drop profile at the base of the drop [Figure 13 (e)].
6. The contact angle value was then read directly from the measuring reticle at the bottom of the eyepiece.
7. This process from (b) to (e) was repeated for measuring other contact angles on the same sample. At least 10 droplets were used to measure contact angles in this study.

For water, and formamide (having high surface tension which results in forming relatively large contact angles on the film), the same contact angles were observed after more than 2 minutes of forming the droplet. Therefore, readings were generally taken within 20 ~ 30 seconds. But the liquids with low surface tension, such as di-iomethane and tricrysyl phosphate, were able to spread rapidly on the film so that contact angles were read as soon as the droplets formed. They were usually spread out within 20 seconds of forming the sessile drops. For tricrysyl phosphate on the PET films (untreated and sulfonated), the droplet spread too rapidly to allow a reading of the angles formed. Therefore, for PET films, three test liquids were used to measure contact angles, and surface energy of PET films was calculated with the data from then three contacting liquids.

### 6.1.3. Calculation of surface energy of solid

The measured contact angle values on the film surfaces from the four liquids were used to calculate surface free energies, and the corresponding dispersion and polar components, according to the method of solving the equation pro-

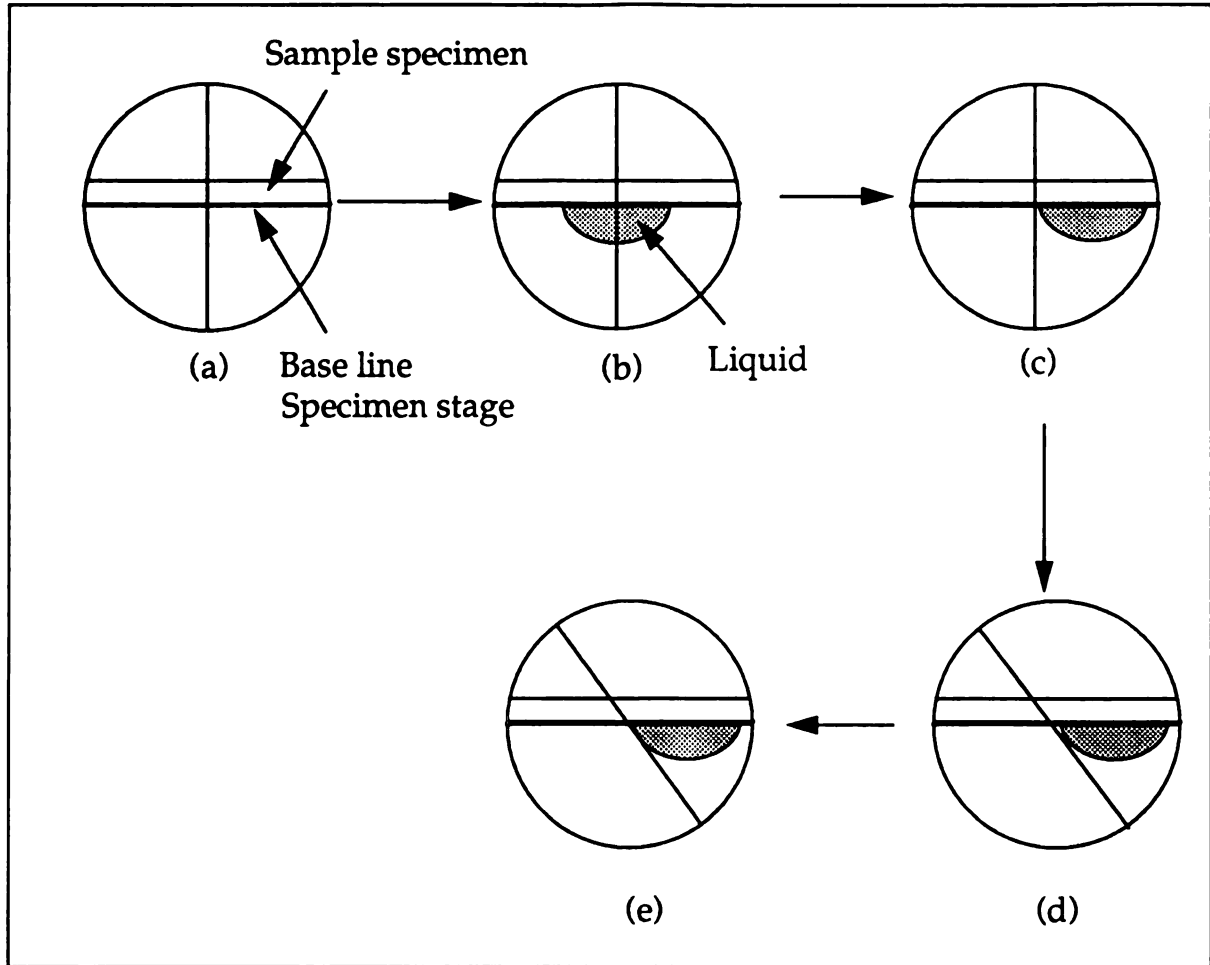


**Figure 13** Figure illustrates the procedure of the contact angle measurement with Goniometer.

posed by Kaelble<sup>[53]</sup>.

The equation [3.11] (on page 19) describing the interaction of liquids with a solid surface was based on the geometric means of the force interactions and the sum of the dispersive and polar terms.

$$\gamma_L (\cos \theta + 1) = 2 \left( \gamma_S^D \cdot \gamma_L^D \right)^{1/2} + 2 \left( \gamma_S^P \cdot \gamma_L^P \right)^{1/2} \quad [6.1]$$

$\gamma_S^D$ , and  $\gamma_S^P$  can be calculated by solving two equations which were set up by contact angle measurements with two liquids of known surface tension values. (See “*Determinant method*” on page 22 for more details) The least square method was used to obtain the best values of the surface energy of the test solid. (See “*The least square method*” on page 23)

Program ‘SFE’ (Chapter 3.3.1(c) on page 28) was developed to make possible not only calculating surface free energy of polymers with polar and dispersive components, but also for providing a graphic representation of  $(\gamma_S^D)^{1/2}$  versus  $(\gamma_S^P)^{1/2}$ , where the four linear relationships are plotted using one of the simultaneous equations given in Equation [6.1]. The procedures of Kaelble<sup>[53]</sup>, using the determinant method, and of Kinloch et al<sup>[36]</sup>, using the least square method, were fully detailed in the previous Chapter.

## 6.2. Peel adhesion test

Another purpose of the present study was to establish a correlation between changes in surface energies of film and adhesion strength, in order to examine the effects of surface sulfonation on polyethylene and polypropylene films. The peel test (180° peel-test, See “*Schematic diagram of sample-tape composite for testing peel adhesion*” on page 60) is usually carried out to determine the force required to peel a PSA tape from a film surface. The peel test for untreated film was used as a reference. The ASTM D2578-67<sup>[37]</sup>, *Adhesion Ratio of Polyethylene film*, test procedure was followed with some modification. However, the test conditions under which adhesion of the tape to, and separation of the tape from the surfaces were carried out, followed those specified in ASTM D2578-67 standard procedure.

### 6.2.1. Test Apparatus and conditions

A PSA tape peel test was performed on the respective film samples by using a computer controlled Tensile System (SFM, United calibration corporation) at the CMSC, at Michigan State University. Since the program for a peel-adhesion test was not set up in the computer, the program for tensile test of polymers has been modified prior to the test. *Figure 14 (on page 58)* shows the schematic of the test machine. A 500 gram load cell was used to maximize the sensitivity of the machine during the peel test, and thus make possible the measurement of the force with minimal fluctuations during the test.

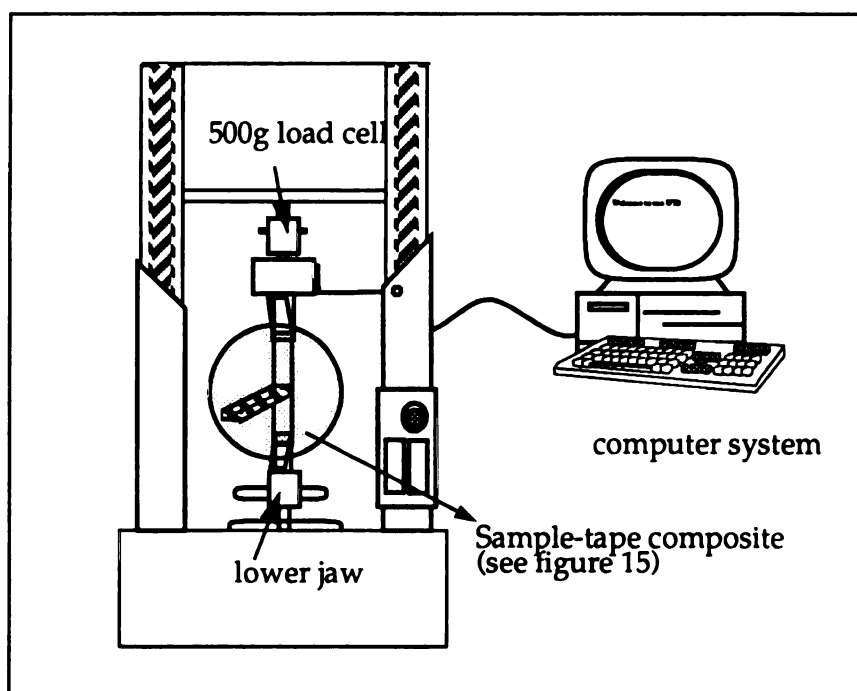


**Figure 14** The schematic of the SFM machine, which is controlled by the computer.

### 6.2.2. Pressure sensitive adhesive (PSA) test tape and backing tape

Three rolls of PSA tape (2 in. width), provided by Kochiom International Inc., (Seoul, Korea) were used as a test tape and backing tape. Contact angle determinations of the surface of the PSA tape were also carried out. The results are presented in the *Table 5*.

**Table 5** Result of Contact angles of probe liquids on the PSA tape

Liquid	Mean $\theta$ [degrees]
Distilled Water	$96.5 \pm 1.5$
Formamide	$85.0 \pm 1.9$
Di-iodomethane	$79.9 \pm 2.8$
Tricresly phosphate	$54.6 \pm 1.8$

The total surface free energy of the adhesive tape was then calculated, which are 21.46 dyne/cm. Polar and dispersion components contribution to the total surface energy was 2.8 dyne/cm, and 18.66 dyne/cm, respectively.

### 6.2.3. Test specimen preparation and scheme

The test specimens, shown in *Figure 15 (on page 60)*, consist of strips not less than 1.5 in. width and 6 inches in length, having their edges approximately parallel and free of tears or creases. The greater dimension of the test specimen was in the direction of extrusion (machine direction). The schematic diagram, presented at *Figure 15 (on page 60)*, illustrates the sample-tape composite with dimensions of film sample and PSA tape used for the peel adhesion test. A test specimen was prepared by laminating with constant force applied. A device which consisted of a rubber roller, and spring system was made in order to

obtain the same conditions. *Figure 16 (on page 61)* is a schematically presented diagram of this device.

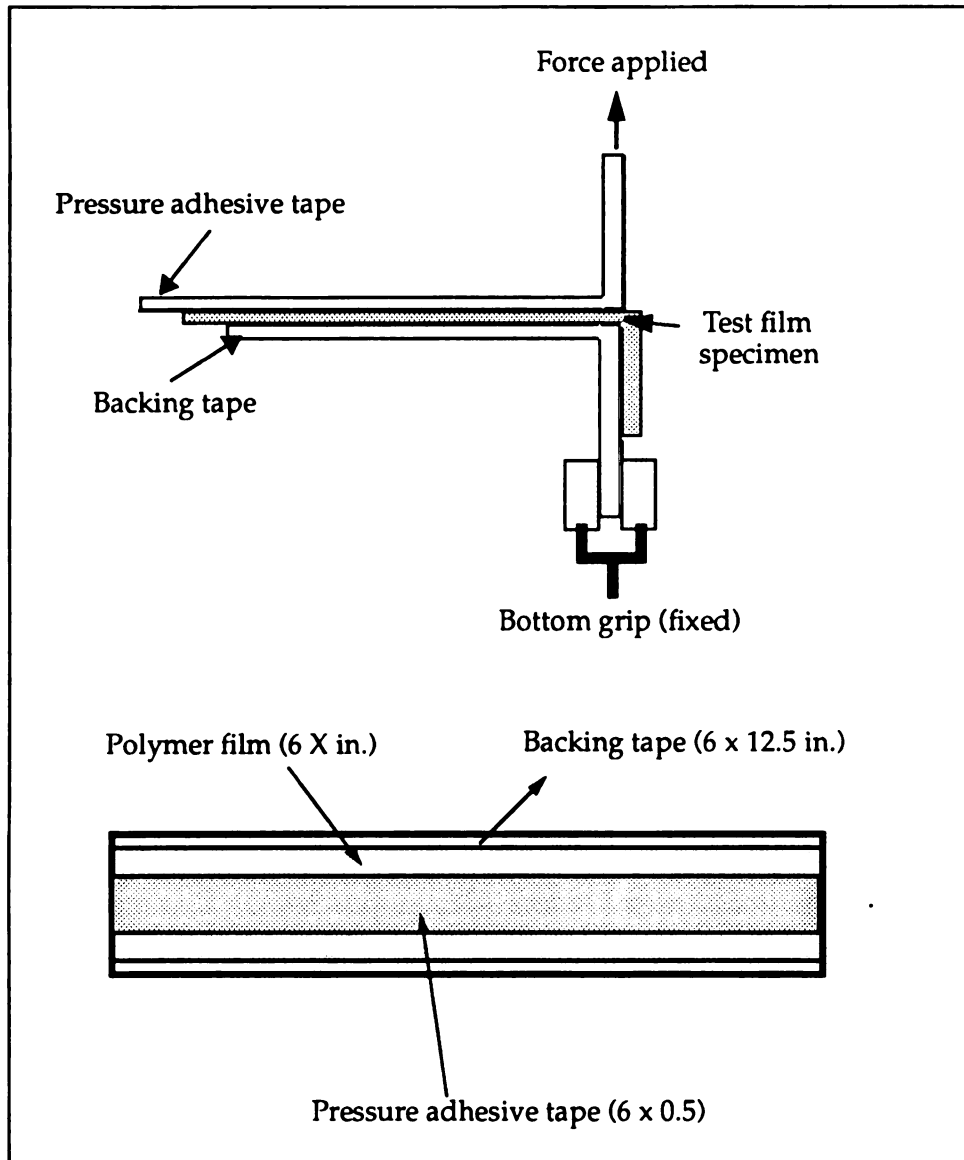


**Figure 15** Schematic diagram of sample-tape composite for testing peel adhesion



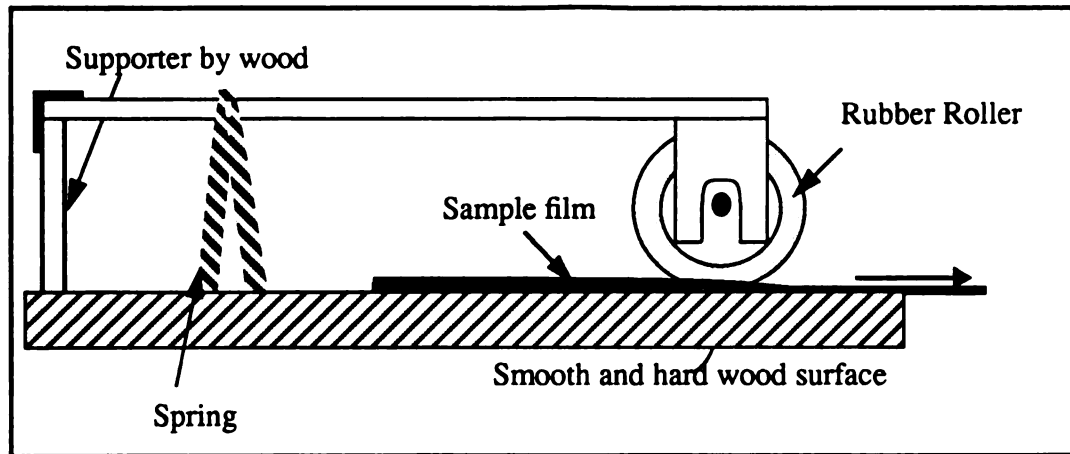


**Figure 16** Device to apply same force for laminating of the test film and PSA tape.

#### 6.2.4. Peel Adhesions Test Procedure

At least three specimens of the respective film samples were tested in the present study. Because the test requires control of the time between lamination and peel measurement, specimens were prepared just before the peel adhesion test. The following describes the test procedure;

1. The tape was peeled about 0.5 in. from the specimen at the doubled end to allow a total of 1 in. of the specimen to remain exposed, and this portion of the exposed specimen was clamped to the fixed lower jaw.
2. The other end of the tape was carefully clamped to the loose upper jaw so not to disturb the sample.

3. The machine was calibrated with a 500 gram load cell, and set at a rate of 20 inch/minute speed by using a computer program. Since the adhesion peel test requires the force to be applied to the peel tape over the sample, a specific program was not developed to carry out this test.
4. The tape was peeled from the specimen, and the data of distance versus the force was automatically recorded, to assess the average load required to peel the test tape from the sample specimen. The data in the first and last 1 inch of tape was not considered in calculating the average load to avoid unexpected results.

#### 6.2.5. Analysis of peel adhesion test

1. The average adhesion strength for each tested surface was calculated in grams per 0.5 inch of PSA tape width by dividing the average load in grams required to peel PSA tape (0.5 inch width) from the film surface. The average load was determined from the graphic data, which plotted values of force as a function of distance. An example of such a plot is shown in the appendix #. From the plot of distance vs. force, any sharp peaks or troughs were disregarded to calculate the average load.
2. An adhesion-interaction term,  $A_{pt}$ , was also determined for each tested sample on which tape adhesion was measured. This interaction term, proposed by Carley et. al.<sup>[12]</sup>, is the sum of the geometric mean of polar and dispersion forces across the tape-polymer film interface and is shown as follows;

$$A_{pt} = \sqrt{\left(\gamma_s^d \gamma_t^d\right)} + \sqrt{\left(\gamma_s^p \gamma_t^p\right)} \quad [6.2]$$

where subscripts  $s$  and  $t$  denote the test polymer and PSA tape, respectively.

## ***Chapter 7. Sulfonation of Polypropylene***

### **7.1. Introduction**

Polypropylene is an extremely versatile material in the packaging industry. The reason for its adaptability is the ease with which its polymer structure and additive packages can be tailored to meet diverse requirements. Many useful properties are inherent in polypropylene. It has low density (high yield), a relatively high melting point, and good strength at a modest cost. However, like most polymers, polypropylene has poor adhesion properties due to its low surface energy. In recent experiments, surface modification of polypropylene using sulfonation has been found to improve its adhesion properties<sup>[19],[23]</sup> as well as its barrier properties<sup>[21]</sup>.

In the present study, the PP film surface was sulfonated by using gaseous SO<sub>3</sub>. The level of sulfonation, as a function of reaction time, was characterized by ESCA and by Elemental analysis. Untreated OPP film was used as a control to evaluate the effect of sulfonation on the surface properties of OPP films as a function of reaction time. The effects of sulfonation on the OPP films were investigated by analyzing the surface properties of the film samples, while included changes of the surface free energy, and peel adhesion test as a result of sulfonation. Results and discussions are reported in the following chapters.

### **7.2. ESCA and Elemental Observations and Discussions**

Electron Spectroscopy for Chemical Analysis (ESCA) provides a global evaluation of the surface composition of the untreated OPP film sample as compared

to sulfonated OPP samples of a various sulfonation time (1minute to 3 minute). The results obtained are summarized in *Table 6*, and presented graphically in *Figure 18*.

Summarized in *Table 6* are the atomic concentration for carbon, oxygen, nitrogen and sulfur determined for the respective film samples. The oxygen detected in the non-sulfonated OPP film is assumed to be the result of corona treatment<sup>[21]</sup>, or oxidation of the outer layer during the film-making process. From *Table 6*, it can be seen that the respective atomic concentration values approach constant levels following one minute reaction time, under the reaction conditions employed. As shown in *Table 7*, the atomic ratios obtained for the respective sulfonated films were in agreement with the theoretical molecular structure of the sulfonate group. For the ammonium sulfonate group ( $-\text{SO}_3^- \text{NH}_4^+$ ), the atomic ratios for S/O and O/C reported were based on corrected values for the oxygen atomic concentration level, where the initial oxygen atomic concentration was subtracted from the total atomic concentration to yield a corrected value. The respective atomic ratio of O/C, and S/C, as a function of reaction time, are presented graphically in *Figure 18*. *Figure 18* shows good agreement with the stoichiometry of the ammonium sulfonate group ( $-\text{SO}_3^- \text{NH}_4^+$ ) on the surface of film samples; i.e. the ratio of O/C is almost three times as high as that of S/C, which is the same as the stoichiometry of the grafted sulfonated group.

Recently, Asthana<sup>[23]</sup> proposed that the surface of polymers, to include polypropylene, could not be sulfonated beyond a limit. The author also proposed that there was chain movement within the polymer at the molecular

level, that did not allow insertion of additional sulfonate groups after a sulfonation limit. For polypropylene, the sulfonation limit was reported by Asthana<sup>[23]</sup> to be one sulfonate group per three repeat monomer units, on average, which is in good agreement with the results obtained in the present studies. Asthana<sup>[23]</sup> confirmed that the site of reaction in polypropylene would be at the tertiary carbon, as described previously. From the present study, the average ratio of C/S is about 10, which means that 1 atom of sulfur is present for every 10 atoms of carbon. Each repeating unit of polypropylene contains 3 carbons; therefore, on average, one sulfonate group is present for at least 3 repeating monomer units. The proposed repeat structure is presented below (*Figure 17*).

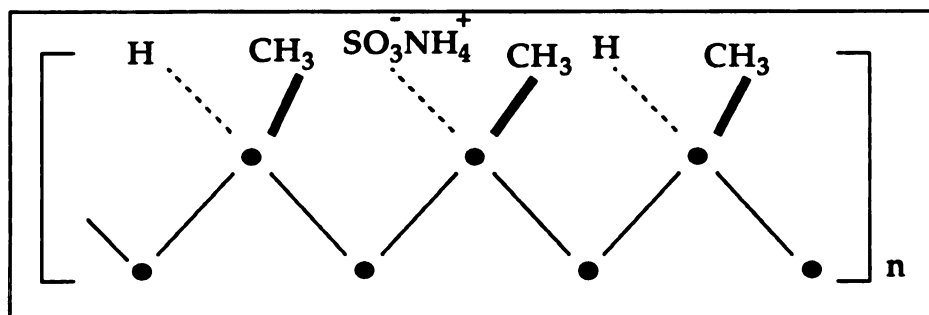


**Figure 17** The molecular structure of sulfonated polypropylene

In addition to ESCA, elemental analysis was also performed on the respective film samples to determine the total percent sulfur per gram of polymer. The comparison of sulfur content measured by ESCA analysis and elemental analysis, as a function of sulfonation time, are summarized in *Table 8* and *Figure 19*,

respectively. As shown by the results of ESCA analysis, the atomic percent sulfur approaches a constant value within the first minute of treatment. It should be noted that ESCA is a surface technique which can determine the composition on the material surface within 50~60 angstroms. As shown in *Figure 19*, while the atomic percent sulfur determined by ESCA seems to approach a constant value, the total weight percent sulfur, as determined by elemental analysis, increases in a linear fashion with sulfonation time. This is assumed to be the result of SO<sub>3</sub> diffusion and subsequent reaction beyond the surface and within the film bulk phase, with extended treatment times.

**Table 6** Atomic concentration for untreated and sulfonated OPP films determined by ESCA analysis <sup>a</sup>

Sample	Reaction time [sec]	C (%)	O (%)	N (%)	S (%)
OPP	0	93.1	6.9	0	0
OPP1	60	66.5	23.1	5.9	4.5
OPP1.5	90	65.5	24.3	5.2	5.1
OPP2	120	58	28.9	6.6	6.5
OPP3	180	60.4	27.9	5.4	6.3

a. Observed by Wangwiwatsilp<sup>[21]</sup>

**Table 7** Relative Atomic Ratios of Sulfonated OPP films<sup>a</sup>

Sample	Reaction time [sec]	C/S	O/S	N/S
OPP	0	-	-	-
OPP1	60	14.7	3.6	1.3
OPP1.5	90	12.8	3.4	1.02
OPP2	120	8.9	3.4	1.01
OPP3	180	9.5	3.4	0.86

a. Determined by Wangwiwatsilp<sup>[21]</sup>

**Table 8** The comparison of sulfur content, measured by ESCA and Elemental Analysis, in the film samples treated at various sulfonation time. <sup>a</sup>

Sample	Sulfonation time [sec.]	Atomic% of Sulfur	Total% Sulfur per gram of film sample
		ESCA Analysis	Elemental Analysis
OPP	0	0	0
SPP1	60	4.5	0.062
SPP1.5	90	5.1	0.11
SPP2	120	6.5	0.15
SPP3	180	6.4	0.24

a. Determined by Wangwiwatsilp<sup>[21]</sup>

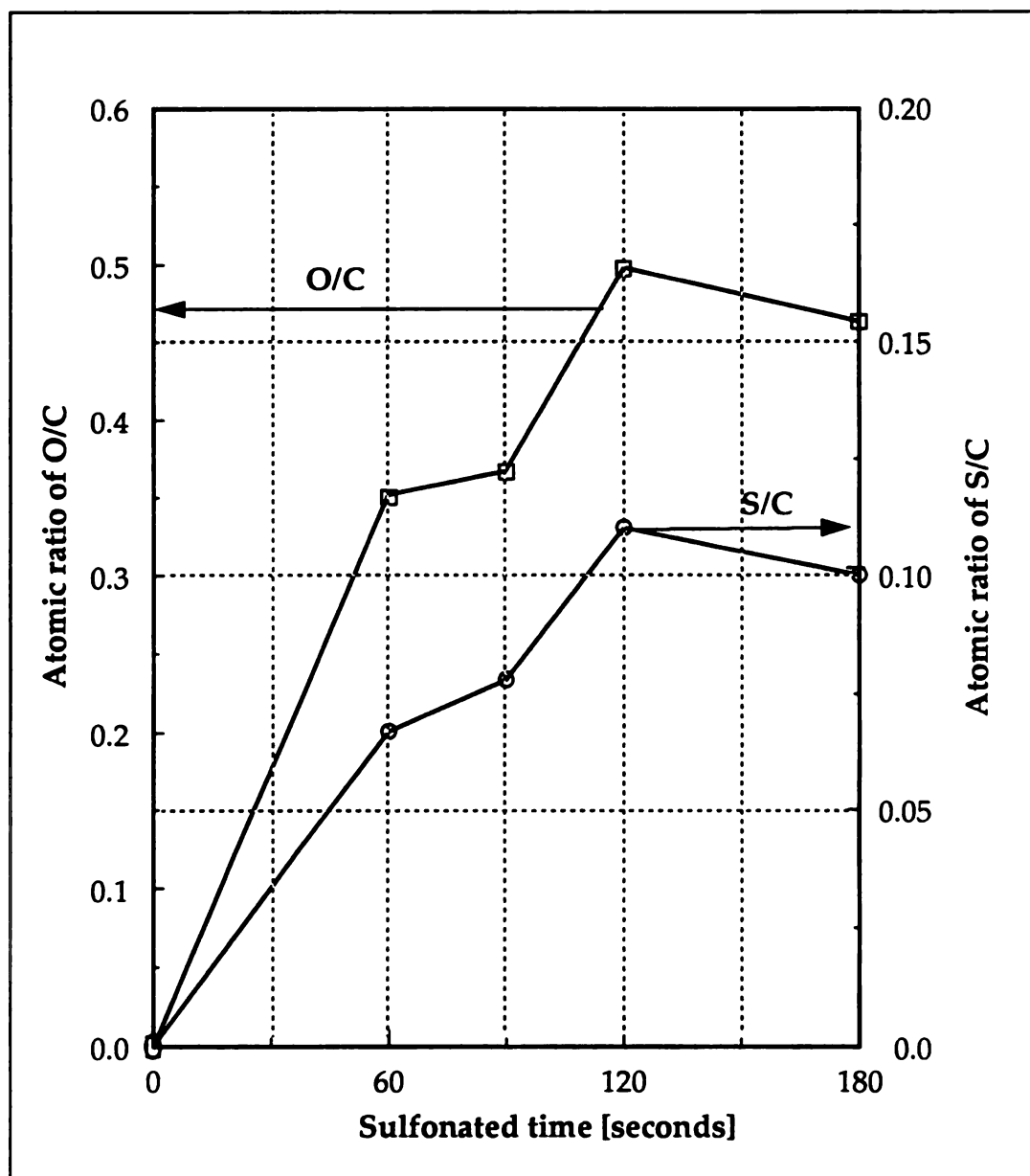


**Figure 18** Atomic ratio of O/C, and S/C determined by ESCA as a function of sulfonation time (at 1% SO<sub>3</sub> concentration)



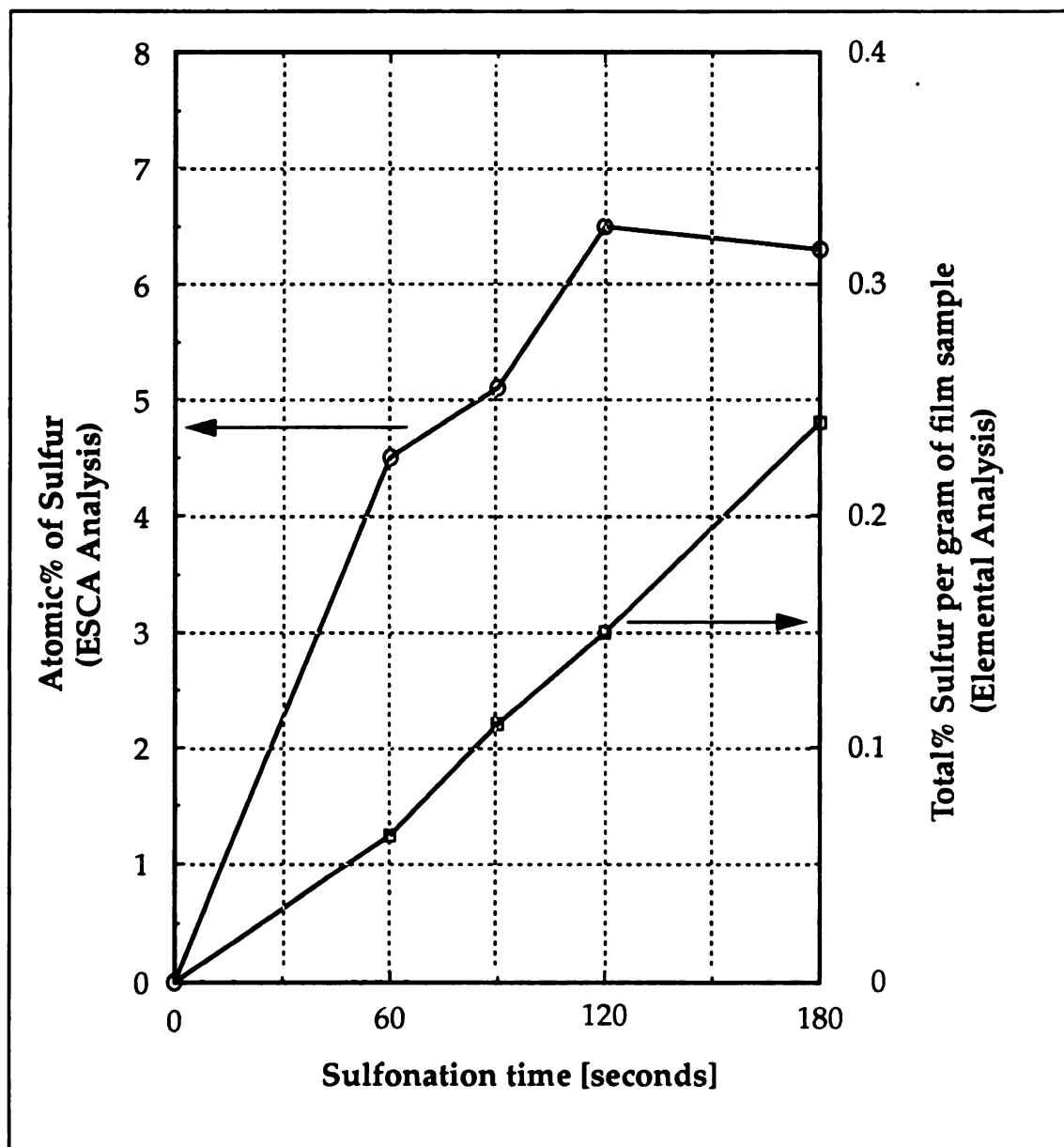


**Figure 19** Sulfur content measured by ESCA, and Elemental Analysis, as a function of sulfonation time.

### 7.3. Results and discussions of contact angle measurements

#### 7.3.1. Contact angles of probe liquids on OPP films tested

The contact angles were measured directly using a Rame-Hart Goniometer Model 100-00 115 with liquids having strong polar properties, such as distilled water and formamide, and with liquids having weak polar properties like di-iodomethane, and tricresylphosphate as the test liquids. The results of the contact angle measurements on the oriented polypropylene film and for film samples sulfonated for 1, 1.5, 2 and 3 minutes, respectively, are tabulated in *Table 9* and presented by histogram in *Figure 20*.

**Table 9** Contact angle obtained on tested polypropylene films using various liquids.

Sample	Contact Angle Measured, mean $\theta$ [degrees] <sup>a</sup>			
	Distilled Water	Formamide	Di-iodomethane	Tricresyl phosphate
OPP	$78.1 \pm 2.3$ (90.7) <sup>b</sup>	$61.5 \pm 2.2$	$42.4 \pm 2.4$	$26.3 \pm 1.8$
SPP1	$31.6 \pm 1.3$ (82.8) <sup>b</sup>	$22.5 \pm 2.4$	$39.5 \pm 3.2$	$20 \pm 1.8$
SPP1.5	$17.6 \pm 1.8$	$10.1 \pm 1.6$	$34.8 \pm 1.6$	$14.2 \pm 1.5$
SPP2	$16.2 \pm 2.4$ (14.5) <sup>b</sup>	$10.6 \pm 2.5$	$35.1 \pm 1.7$	$12.8 \pm 2.2$
SPP3	$12.5 \pm 1.5$	$8.5 \pm 1.5$	$33.9 \pm 3.1$	$10.4 \pm 1.5$

a. Averaged value over at least 10 different measurements, performed in different positions of the sample surface. The typical standard error was within  $\pm 3^\circ$ .

b. Asthana measured contact angle of distilled water on the PP film.

Seen from the data in *Table 9* and the histogram in *Figure 20* (page 71) that larg-

est apparent contact angle changes of probe liquids appeared with the water and formamide. This indicates that sulfonation resulted in an increase in surface polar properties. This has been confirmed by ESCA which shows that sulfur and oxygen concentrations are rapidly increased on the surface within the first minute of sulfonation time. These findings were not in agreement with observations of contact angles of distilled water on the polypropylene film measured by Asthana<sup>[23]</sup>. His results are presented in *Table 9 (page 69)* for comparison. The author has reported that the first minute of sulfonation did not change the surface properties of polypropylene appreciably. But as mentioned earlier, a cause for the discrepancy lies in the fact that the conclusions of Asthana have been based on studies carried out with a different source of polypropylene which was found to have a different content of oxygen in the untreated PP film (See "*ESCA and Elemental Observations and Discussions*" on page 62). From this fact, it may be concluded that initially present oxygen on the surface would be one factor in promoting sulfonation of polypropylene. It is of importance to note that the OPP film sulfonated for 2 minutes showed contact angle values with untreated, which agreed with those of Asthana<sup>[23]</sup>.

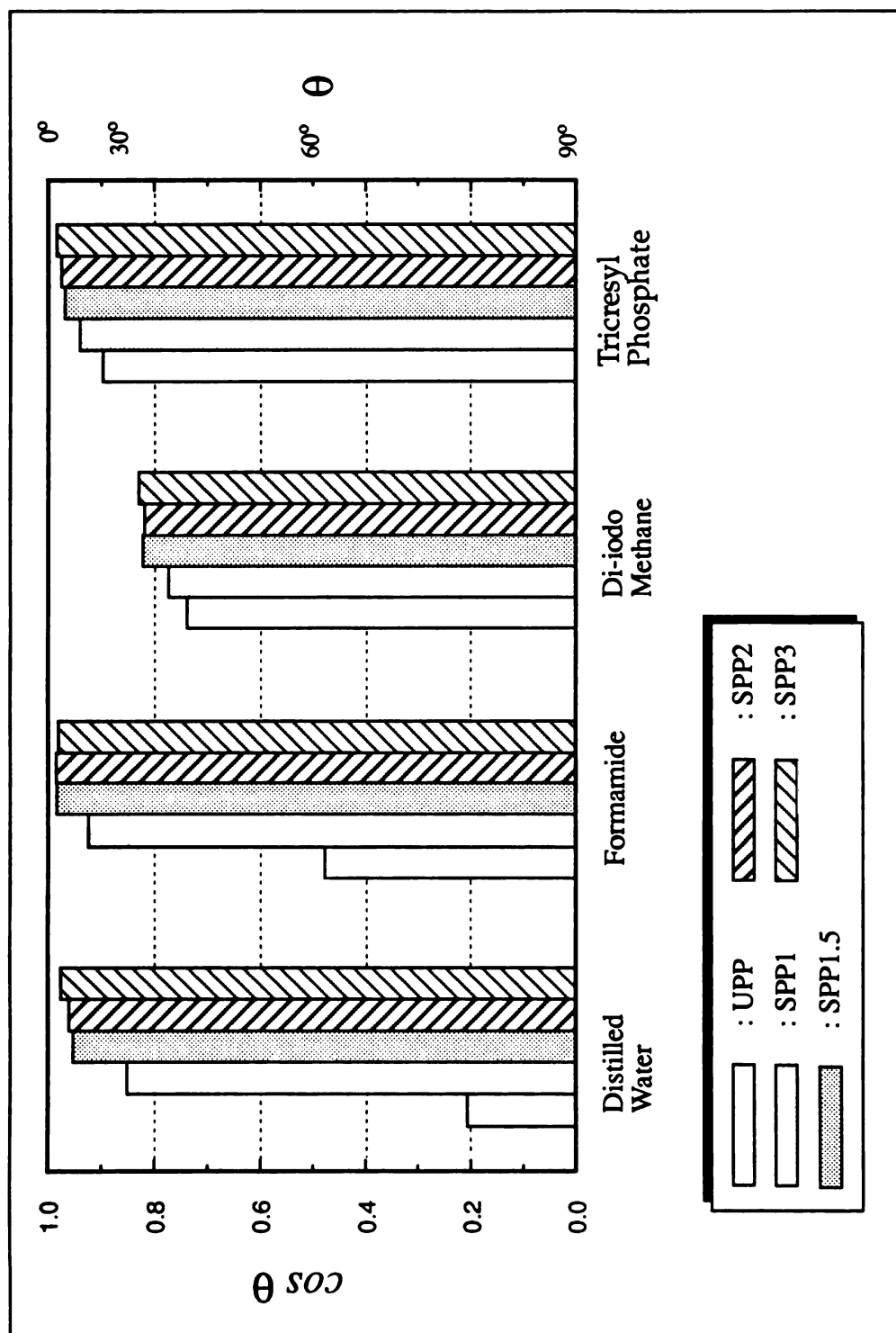


**Figure 20** The changes in contact angle of 4 liquids on polypropylene with increasing time of sulfonation.

### 7.3.2. Determination of surface free energies of films

Whereas ESCA and Elemental Analysis provide an evaluation of the surface concentration of sulfonate groups for sulfonated OPP films, the surface free energies of the sulfonated OPP films determined from contact angle measurements, consider only the outer accessible layer of the treated surface. Surface free energies, and their corresponding polar and dispersive components, were calculated using the computer program SFE, in accordance with the method described in *Chapter 3.3.1(a) "The least square method" on page 23*. The polarity, defined<sup>[1]</sup> as the ratio of the polar component to the total surface energy,  $\gamma_s^p / \gamma_s$ , was also determined. The results of contact angle analysis are presented with the results of ESCA analysis and Elemental analysis in *Table 10*. The atomic% of sulfur and total sulfur concentration of the respective films are also summarized in *Table 10* to allow comparison with the surface free energy values of the test films. The histogram of surface free energy is presented in *Figure 21 (b) (page 75)*. The effect of sulfonation time on the polar, dispersion and total surface free energy values is also shown graphically in *Figure 21 (b) (page 75)*, where the respective surface free energy values are plotted as a function of sulfonation time.

As shown, the increase in the values of the polar component of the surface free energies appears to have approached maximum levels within one minute's exposure time for the sulfonated OPP film. Also the observed changes in the total surface free energy can be attributed to the increased contribution of the polar component. Further sulfonation resulted in little or no changes in the polar and dispersion component of the film surface free energy.

Recently, Wangwiwatsilp<sup>[21]</sup> observed a significant decrease in the permeability coefficient for ethyl acetate in OPP film following sulfonation. This is illustrated in *Figure 22* (page 76), where the permeability coefficient for ethyl acetate in OPP film is plotted as a function of sulfonation time. Superimposed in *Figure 21 (b)* is a plot of the total surface free energy as a function of sulfonation time. As shown, as the total surface free energy approaches a constant value, the permeability coefficient also approaches minimum level.

**Table 10** Surface Free Energy of PP films, Polarity, Atomic% of Sulfur by ESCA, and Total% of Sulfur per gram of film sample for OPP (untreated), SPP1 (Sulfonated for 1 minute), SPP1.5 (Sulfonated for 1.5 min.), SPP2 (Sulfonated for 2 min.), and SPP3 (Sulfonated 3 min.)

Samples	Surface free energies of solid [dyne/cm]			Polarity	Atomic% of Sulfur <sup>(a)</sup>	Total% Sulfur per gram of film sample <sup>(a)</sup>
	Dispersive Component	Polar Component	Total			
OPP	32.61	5.11	37.72	0.14	0	0
SPP 1	22.69	35.94	58.63	0.61	4.5	0.062
SPP 1.5	22.75	41.22	63.96	0.64	5.1	0.11
SPP 2	22.66	41.67	64.33	0.65	6.5	0.15
SPP 3	22.86	42.22	65.08	0.65	6.4	0.24

a. Observed by K. Wangwiwatsilp<sup>[21]</sup>

Wittenbeck<sup>[6]</sup> observed, that for plasma treatments on PP surfaces, the functional group introduced on the surface of PP during treatments has considerable mobility. He proposed that mobility of the functional groups allowed them to rotate into the interior of the OPP. Occhillo<sup>[5]</sup> also proposed that

plasma treated surface of PP possessed the tendency to minimize its interfacial energy by macromolecular movement into the polymer bulk phase.

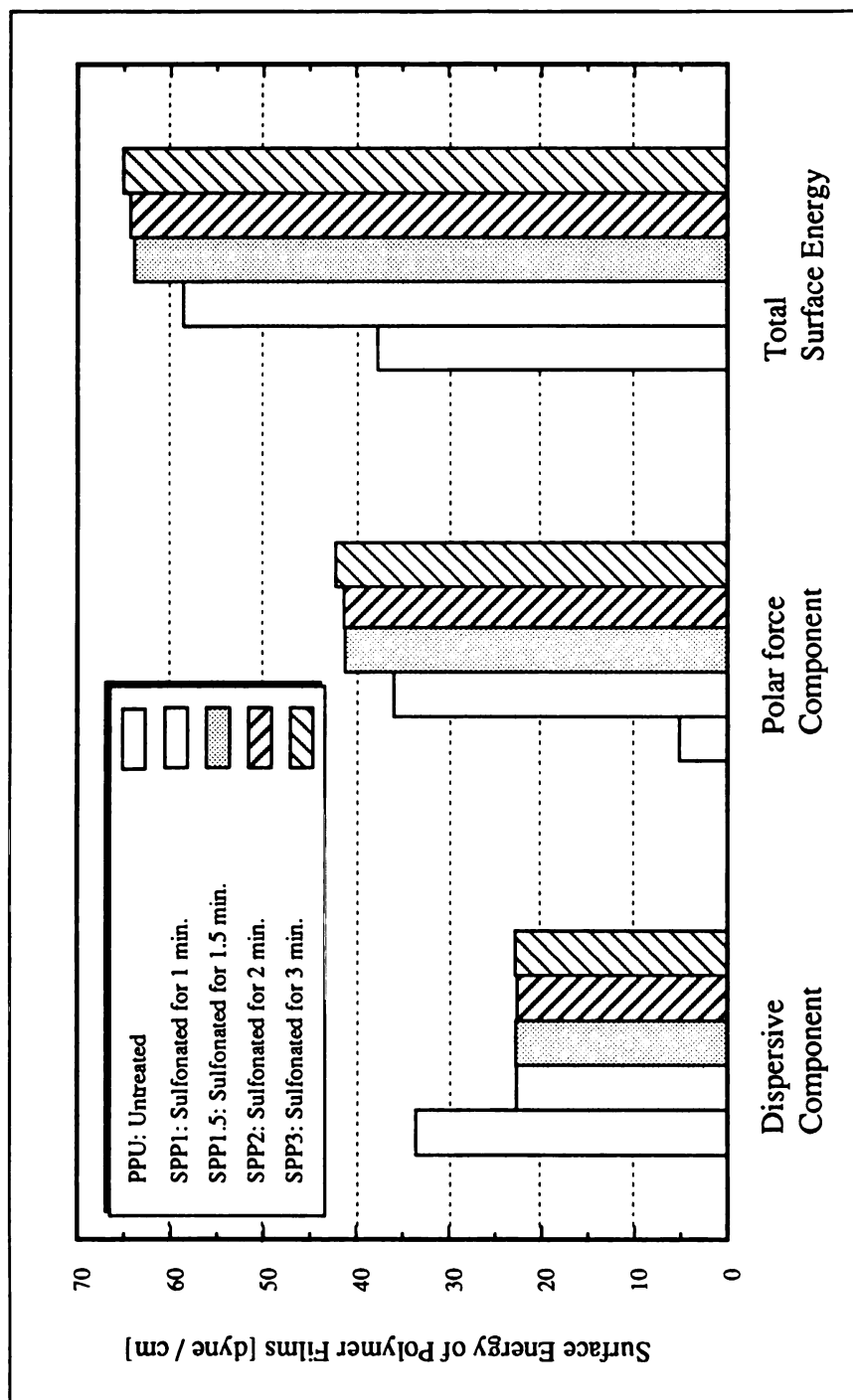


**Figure 21 (a)** Variation of solid surface energy, dispersive and polar energy components for untreated and sulfonated PP films

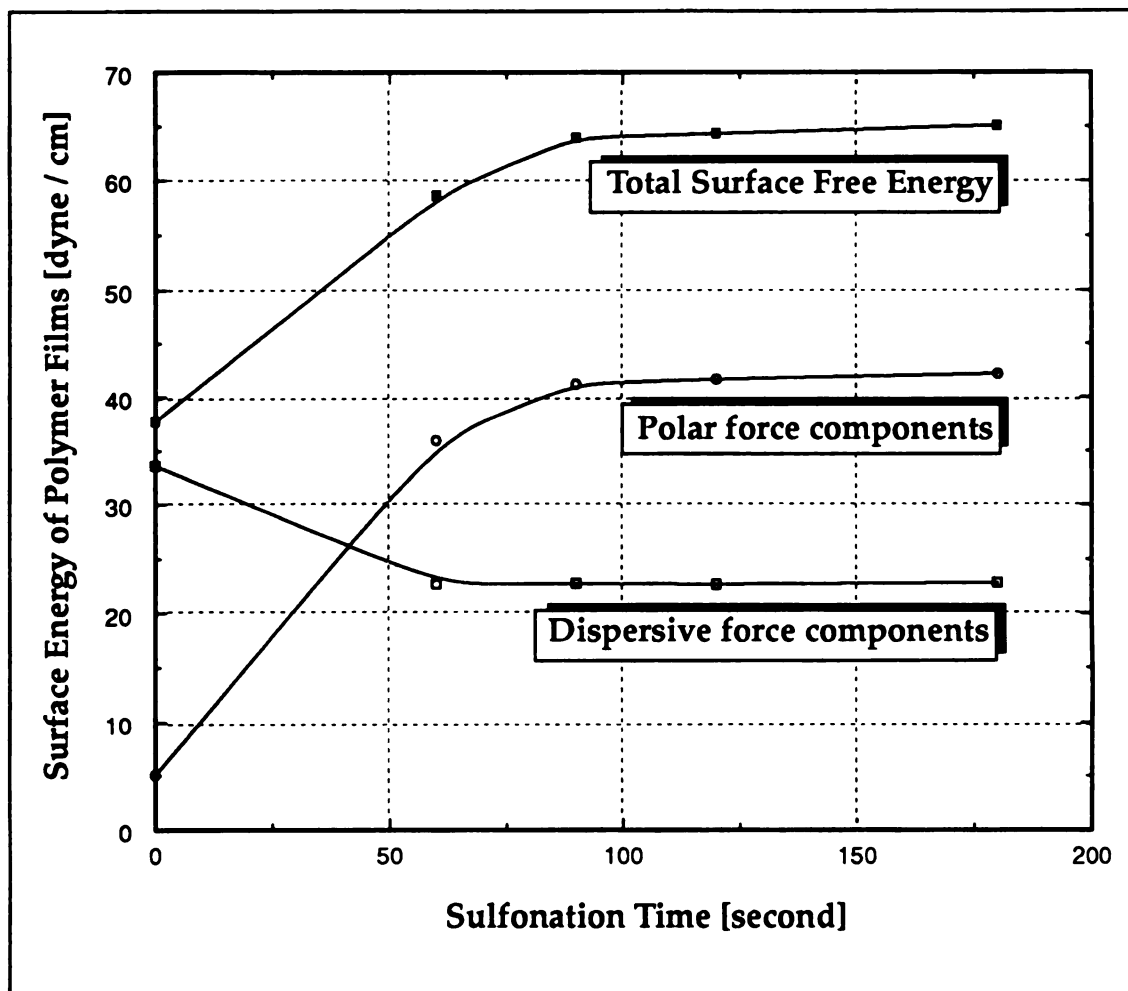
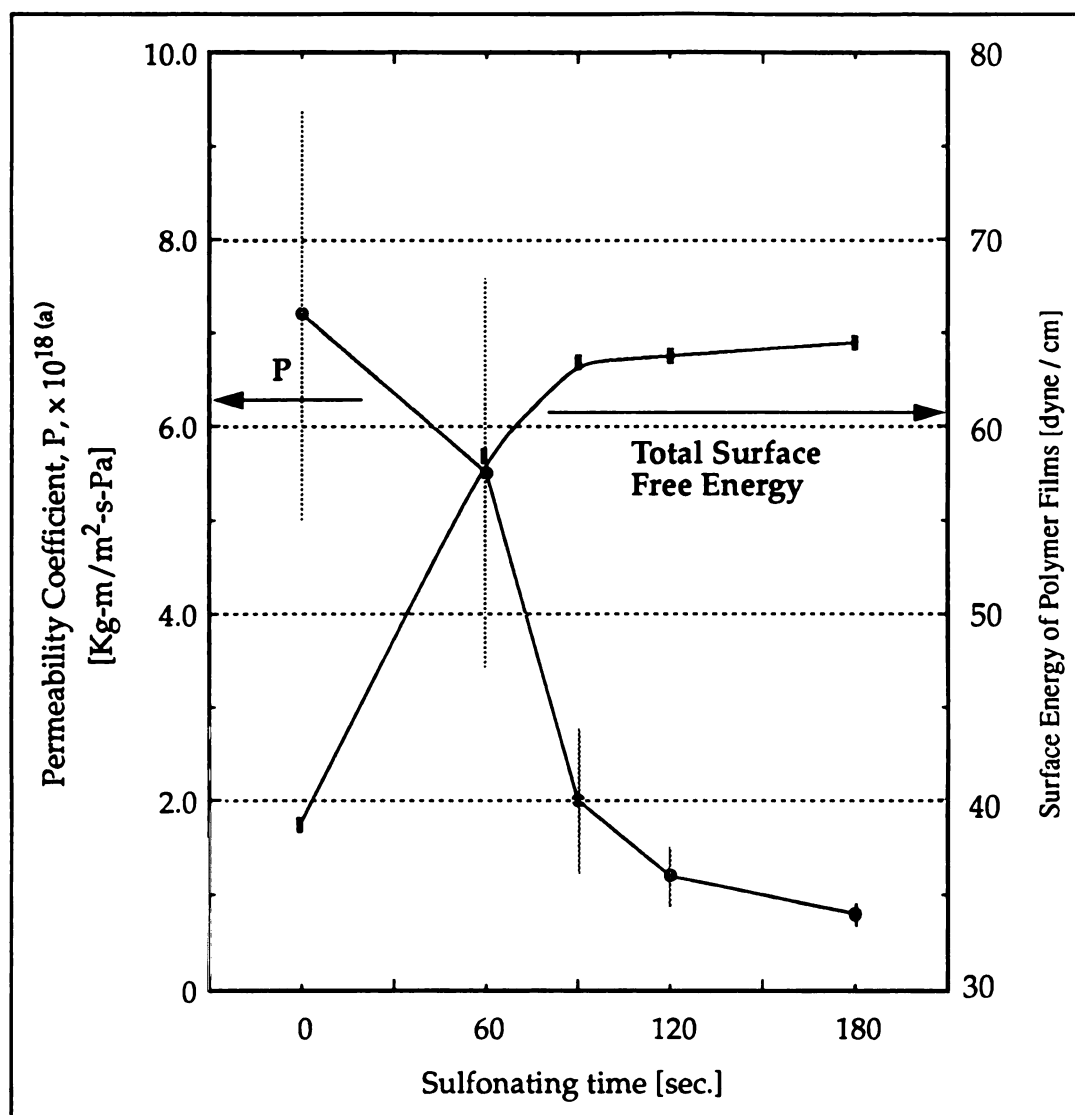


**Figure 21 (b)** Variation of surface free energies, corresponding to the dispersive and polar force components for untreated and sulfonated PP films as function of sulfonation time. Note the visible changes in polar force component of surface free energies of solid appeared within the one minute of sulfonation time.





(a) Shade line shows the deviation errors.

**Figure 22** Relationship between *Permeability Coefficient* of Ethyl Acetate in Polypropylene films and *Total Surface Free Energy* as a function of sulfonation time. Note the apparent changes occurred in the 90 sec., while the surface free energy changed within one minute of sulfonating time.

#### 7.4. Results and discussions of peel adhesion test

The results of ESCA and contact angle analysis of various liquids on the respective film sample clearly indicate that surface treatment using sulfonation on the OPP film changes the surface chemistry, resulting in an increase of surface polarity, and of polar components contributing to the surface energies of the respective film samples. The changes of surface chemistry and surface energies due to the sulfonation have been discussed in the previous chapter.

**Table 11** Peel adhesion strength for sulfonated film samples with the data of surface free energies

	Surface free energies of solid [Dyne/cm]		Peel Adhesion Strength [Gram/0.5 inch]	Adhesion-interaction term, $A_{pt}$
	Dispersive Component	Polar Component		
PSA tape	18.66	2.8	-	-
UPP	32.61	5.11	63.36 $\pm$ 3.02	28.45
PPS1	22.69	35.94	165.97 $\pm$ 7.4	30.61
PPS1.5	22.75	41.22	178.44 $\pm$ 11.74	31.35
PPS2	22.66	41.67	184.12 $\pm$ 6.7	31.36
PPS3	22.86	42.22	184.11 $\pm$ 11	31.2

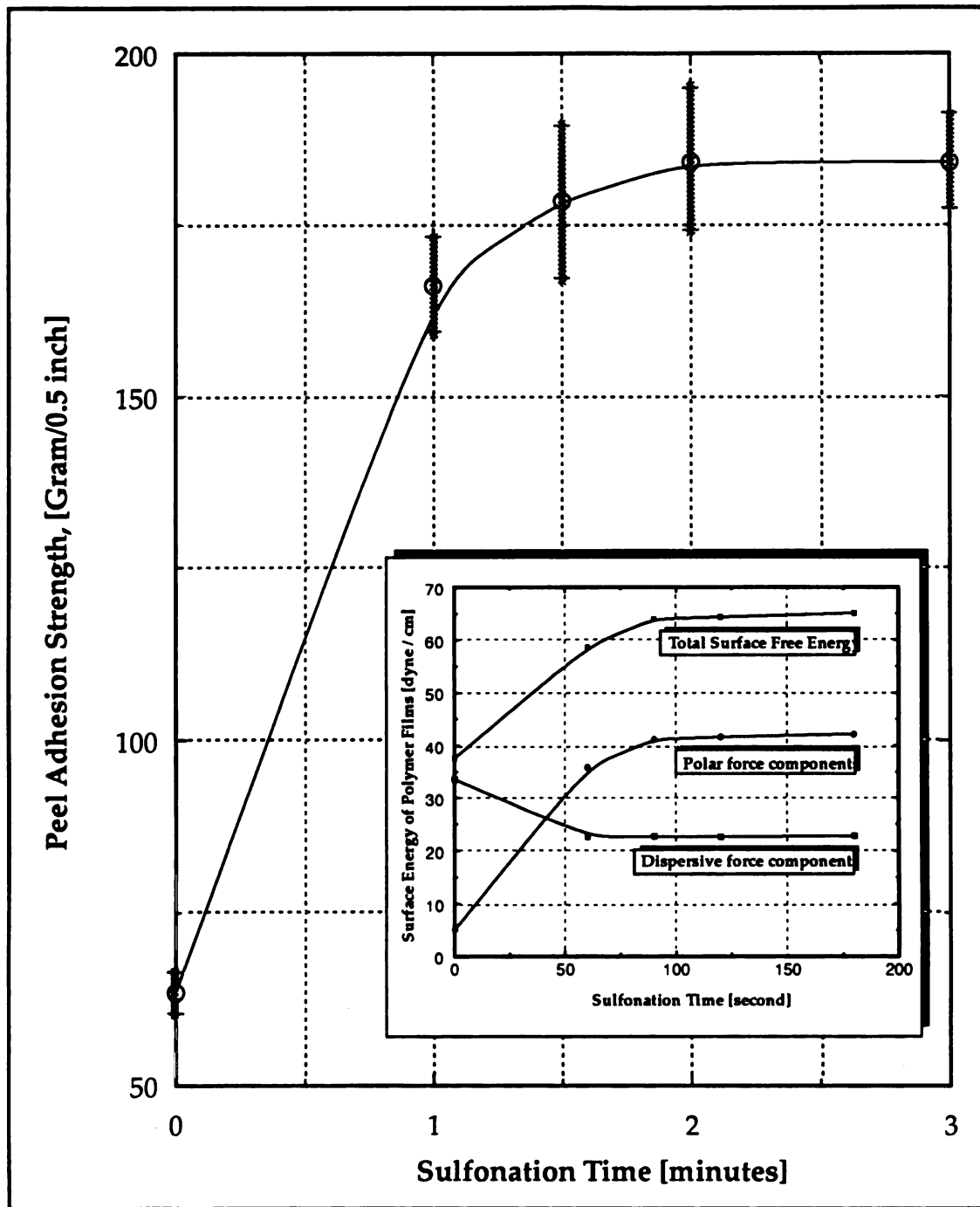
The peel adhesion test was then carried out to determine whether changes in surface chemistry and surface free energy would result in increased adhesion strength of the surface treated OPP films. Peel adhesion strength values reported in the present study are the average of the three replicates for each respective film sample. The results are summarized in *Table 11*. Also summa-

Table 11 are the corresponding surface free energy and adhesion-interaction values. The results are also presented graphically in Figure 23 (on page 79), where the peel adhesion strength as a function of sulfonation time is plotted. The trend in the observed increase in the adhesion strength with increased sulfonation time follows the increase in polar components contribution to the total surface energies of film, as shown in the insert box in Figure 23. This suggests that, up to a certain level of surface treatment, the adhesion strength will increase at a high rate, due to the increase in the polar components of the surface free energy of the respective film samples.

The adhesion-interaction terms,  $A_{pt}$ , are calculated by using equation [6.2] (on page 61) to correlate the surface energy changes due to the sulfonation and adhesion properties. The relationship of the peel adhesion strength to the adhesion-interaction term is nearly linear in the range studied, as shown in Figure 24 (page 80). These results indicate that the increased surface free energy following sulfonation treatment is primarily responsible for the increase in the adhesion strength between the treated film surface and the applied PSA tape.

rized *Table 11* are the corresponding surface free energy and adhesion-interaction values. The results are also presented graphically in *Figure 23* (on page 79), where the peel adhesion strength as a function of sulfonation time is plotted. The trend in the observed increase in the adhesion strength with increased sulfonation time follows the increase in polar components contribution to the total surface energies of film, as shown in the insert box in *Figure 23*. This suggest that, up to a certain level of surface treatment, the adhesion strength will increase at a high rate, due to the increase in the polar components of the surface free energy of the respective film samples.

The adhesion-interaction terms,  $A_{pt}$ , are calculated by using equation [6.2] (on page 61) to correlate the surface energy changes due to the sulfonation and adhesion properties. The relationship of the peel adhesion strength to the adhesion-interaction term is nearly linear in the range studied, as shown in *Figure 24* (page 80). These results indicate that the increased surface free energy following sulfonation treatment is primarily responsible for the increase in the adhesion strength between the treated film surface and the applied PSA tape.



**Figure 23** Peel adhesion strength of OPP films tested as a function of sulfonation time. In insert box, surface energies of the respective film samples vs. sulfonation time are presented for comparison with the increasing trend of the peel

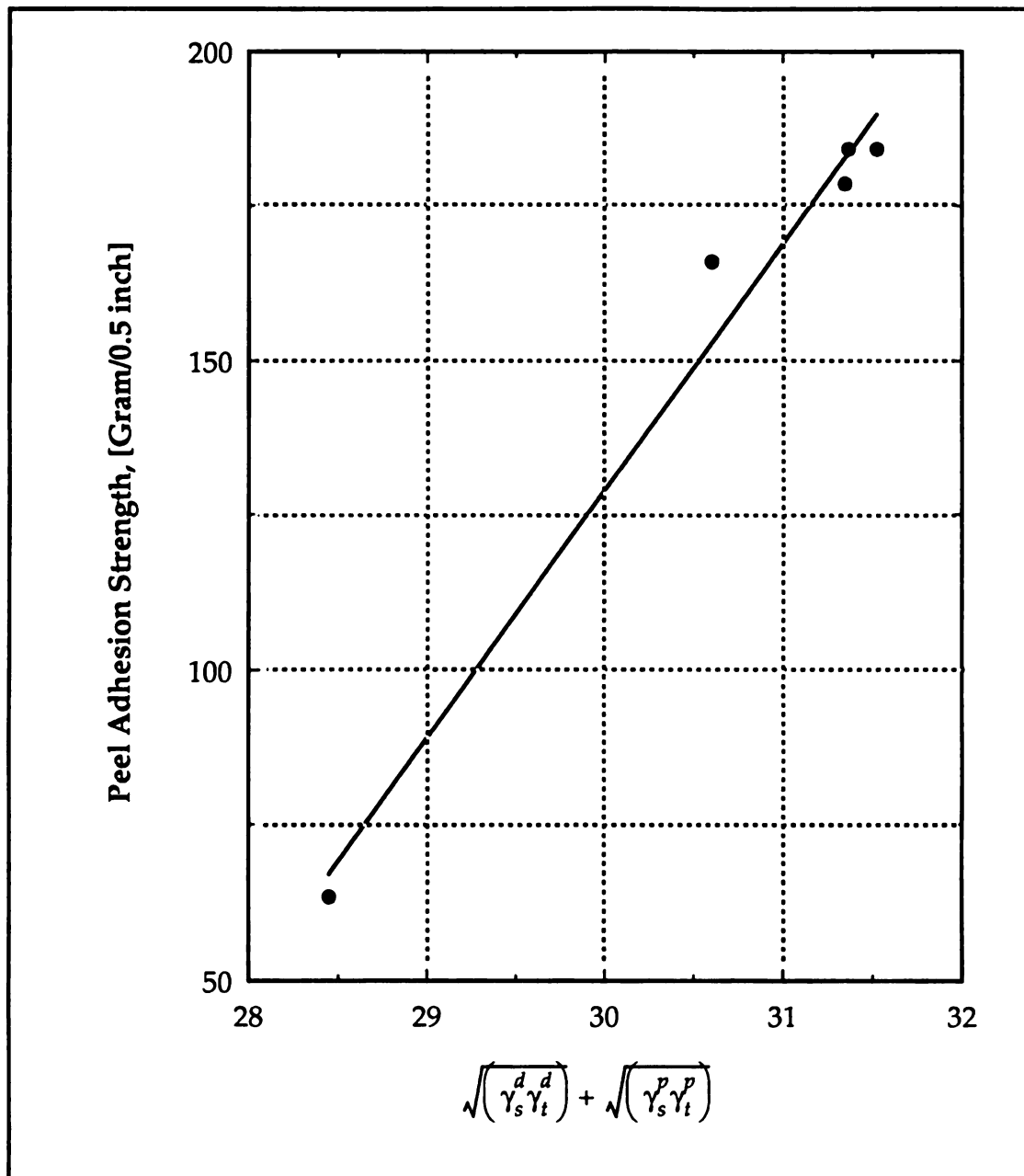


**Figure 24** The relationship of peel adhesion strength vs. adhesion-interaction term.

## 7.5. Conclusions

The above results show that sulfonation of PP film surface is a suitable method to progressively increase the polar components of the surface free energy, while results in an increase in the adhesion strength of the film surface. A treatment time of 1 minute, for the given sulfonating conditions and parameters, results in a reproducible surface state, exhibiting dramatically increased values for the polar components of the surface energy and the polarity of the surface. This increase in surface free energy is due to the insertion of polar, sulfonic acid groups, on the film surface. However, further reaction time with gaseous  $\text{SO}_3$ , though effective in enhancing the barrier properties of the film by interdiffusion of the sulfonic group through the bulk phase<sup>[21]</sup>, results in minimal changes in surface properties, but lead to color changes from light brown to dark brown.

Adhesion depends fundamentally on forces of attraction across an interface, which is directly related to the surface energy properties of sample film. Results of peel adhesion studies show that surface modification of OPP films, using sulfonation is undoubtedly an effective method. Comparing polar and dispersion components at the interface between the tape and the treated polymer surface, and peel adhesion strength, a good correlation was found. This is mostly attributed to the increase in the polar component of the surface free energy, which results in an increase in the adhesion strength between the treated film surface and the applied PSA tape.

## ***Chapter 8. Sulfonation of Polyethylene***

### **8.1. Introduction**

Polyethylene (PE) film is known to be readily sulfonated by reaction with gaseous  $\text{SO}_3$ , with fuming sulfuric acid, or with  $\text{SO}_3$  in chlorinated hydrocarbons, resulting in changes in its surface properties, and increasing commercial applications and uses. Ihata<sup>[26]</sup> evaluated the structure of the PE film sulfonated by using gaseous  $\text{SO}_3$  and found that sulfonation resulted in the formation of alkanesulfonic acid,  $\text{C-SO}_3\text{H}$  groups, with highly conjugated  $\text{C}=\text{C}$  unsaturated bonds on the PE surface. Fonseca et. al. also<sup>[11]</sup> observed that fuming sulfuric acid etching of PE film results in the formation of sulfonic acid groups in the polyethylene chain.

Among the packaging applications of PE film, a main consideration is the enhancement of its adhesion properties. For the present study, ESCA analysis was carried out to determine the extent of PE sulfonation under the experimental conditions used. Thus, the aim of the present study was to determine the effect of sulfonation on the adhesion properties of HDPE film by means of estimating the surface energies of the film, since the adhesion properties are directly related to changes in the films surface energy values. Specifically, peel adhesion strength values have been determined to correlate the changes in surface free energies of sulfonated polyethylene film with film adhesion properties.



## 8.2. Sulfonation degree determined by the ESCA

The surface composition of an untreated HDPE film, corona treated HDPE film, and sulfonated HDPE samples were determined by the ESCA technique. The results are summarized in *Table 12*, and presented graphically in *Figure 25*, where the increase of the atomic percent of sulfur on the surface of sample films as a function of reaction time is plotted. The extent of sulfonation for each film given in *Table 12* was estimated by an S/C value based on the results of ESCA analysis, although degree of the sulfonation on the surface layer may be different from that of the inner layer.

All the experiments in the present study were run with a constant  $\text{SO}_3$  gas concentration of approximately 1% at room temperature. The S/C ratio value of 0.3% for HDPE film sulfonated for 1.5 minutes suggests that the sulfonation conditions in the present test were not adequate to graft sufficient level of sulfonic groups onto the HDPE film surface. Little or no changes in the sulfur content of PE film surface following extended reaction times, under our sulfonation condition, makes it evident that reaction time is not the only variable for introducing the sulfonic groups onto the surface of PE film. For example, Ihata<sup>[25]</sup> observed progressively increased sulfur content from 1.26% to 11.55% in the PE film after 1 minute, and 5 minute treatment, respectively, and the color changes of samples from pale green to dark brown.

**Table 12** Surface composition of HDPE film samples before and after sulfonation treatments at a various exposure time over SO<sub>3</sub> gas, determined by ESCA<sup>a</sup>

Sample	Reaction time [sec]	Percentage Atomic Concentration			Atomic ratio (S/C x 10 <sup>2</sup> )
		C (%)	O (%)	S (%)	
UPE	0	98.51	1.49	0	0
PE1.5	90	98.23	1.47	0.3	0.3
PE3	180	95.3	4.09	0.61	0.64
PE5	300	92.78	6.59	0.63	0.69
PEC	-	91.3	8.7	0	-

a. UPE: Untreated polyethylene film

PE1.5: Sulfonated PE film for 90 seconds

PE3: Sulfonated PE film for 180 seconds

PE5: Sulfonated PE film for 300 seconds

PEC: Corona treated PE film

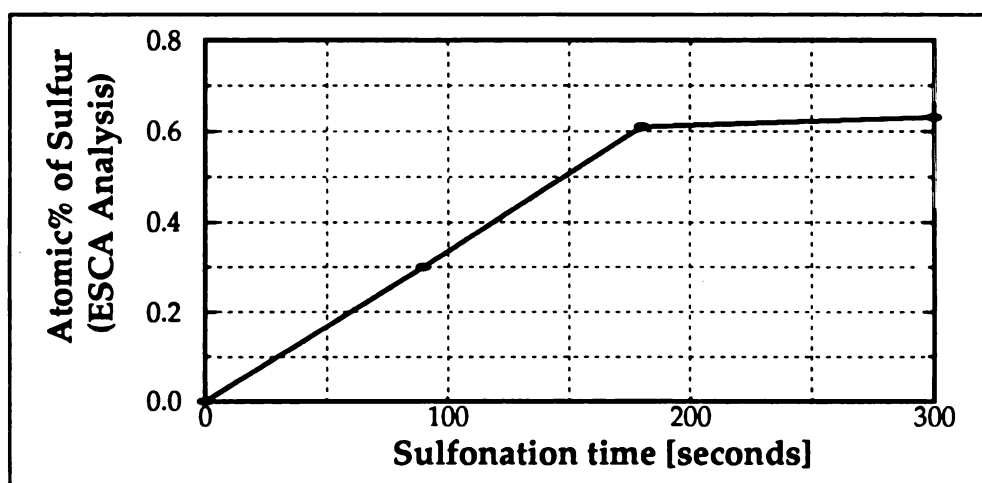


**Figure 25** Atomic% of sulfur measured by ESCA as a function of sulfonation time.

### 8.3. Results and discussions of contact angle measurements

#### 8.3.1. Contact angles of probe liquids on PE films tested

The contact angle measurements were made on the untreated, sulfonated and corona treated HDPE films with liquids having strong polar properties, such as distilled water, and formamide, and with liquids having weak polar properties like di-iodomethane, and tricresyl phosphate as the probe liquids. The results are summarized in *Table 13* and a histogram of the contact angles measured on the HDPE film samples is given in *Figure 26*.

**Table 13** Contact angle obtained on sulfonated polypropylene using various liquids.

Sample	Contact Angle Measured, mean $\theta$ [degrees] <sup>a</sup>			
	Distilled Water	Formamide	Di-iodomethane	Tricresyl phosphate
UPE	90.6 2.6	69.6 2.4	48.4 2.8	31.9 2.4
PE1.5	85.2 2.0	69. 2.29	45.7 1.8	32.3 1.9
PE3	80.4 2.9	67.4 1.7	43.2 2.2	35.7 1.9
PE5	83.7 2.1	67.1 1.8	41.1 2.2	31.3 2.0
PEC	64.7 2.6	46.3 1.9	34.5 2.1	10.7 2.0

a. Averaged value over at least 10 different measurements, performed in different positions of the sample surface. The typical standard error was within  $\pm 3^\circ$ .

As shown, no significant changes of the contact angle for the liquids used were observed for the HDPE film following sulfonation. This implies that the sulfonic groups are rarely introduced onto the surface of HDPE, under the



present sulfonation conditions.

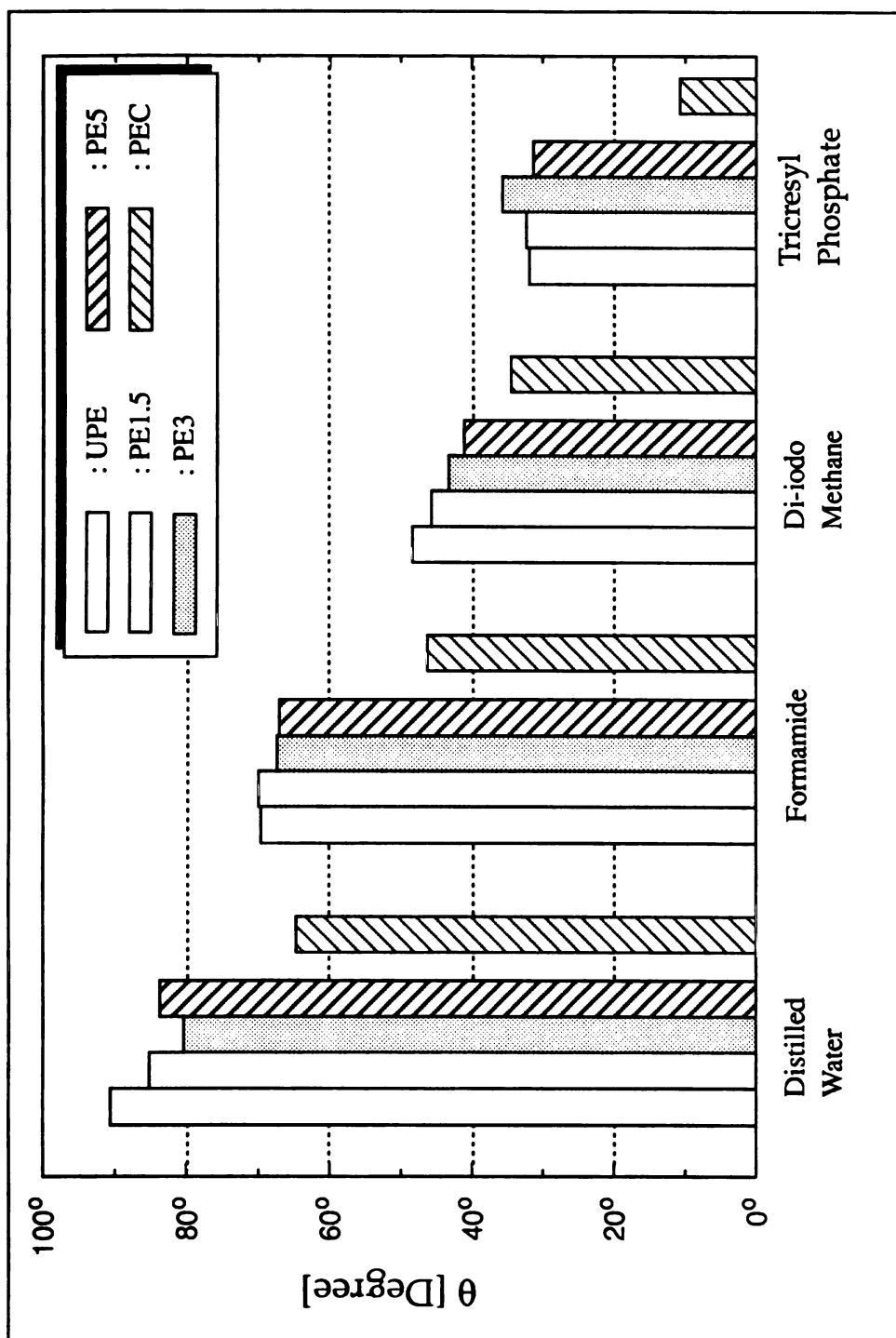


**Figure 26** The changes in contact angle of 4 liquids on polyethylene with increasing time of sulfonation based on the untreated PE film as reference.

### 8.3.2. Determination of surface free energies of films

The surface free energies, and corresponding polar and dispersive components, were calculated using the computer program SFE in accordance with the method described in *Chapter 3.3.1(a) "The least square method" on page 23*. The surface free energy values obtained from the contact angle of various liquids are summarized in *Table 14*. The polarity, atomic% of sulfur for the sulfonated film sample and atomic% of oxygen for the corona treated film sample are also presented in *Table 14*. The variation of surface energy, dispersive and polar energy components, for untreated, sulfonated HDPE films as a function of reaction time, and corona treated HDPE film is shown in *Figure 27*.

**Table 14** Surface Free Energy of PE films, Polarity, and Atomic% of Sulfur by ESCA for PEU (untreated), PE1.5 (Sulfonated for 1.5 minute), PE3 (Sulfonated for 3 min.), PE5 (Sulfonated for 5 min.), and PEC (Corona treated)

Sample film	Surface free energies of solid [dyne/cm]			Polarity	Atomic% of Sulfur
	Dispersive Component	Polar Component	Total		
PEU	33.69	1.58	35.27	0.045	0 (1.49) <sup>a</sup>
PE1.5	32.97	2.43	35.4	0.069	0.3 (1.47)
PE3	31.48	3.96	35.44	0.112	0.61(4.09)
PE5	32.7	3.78	36.5	0.104	0.63 (6.59)
PEC	32.37	11.7	44.07	0.265	0 (8.7)

a. The atomic% of oxygen is presented to compare the with result of the corona treated HDPE film samples.

*Table 14* and a graphical presentation (*Figure 27*) show that sulfonation of HDPE film under the experimental conditions used is much less efficient than corona treatment in modifying the surface free energy of the HDPE film. No significant changes of surface energy, of the corresponding polar and dispersion components, were found between untreated and sulfonated HDPE film samples. This is due to the limited sulfonic acid functional group content on the film surface achieved, resulting in no increase in surface polarity following sulfonation.

Apparent changes in the surface free energy of the PEC film were the result of an increase in the polar components of the surface free energy, due to the introduction of oxygen onto the film surface as a result of corona treatment. From this result, it is apparent that increased polarity by introduction of functional groups contributes to the surface energy and consequently enhances adhesion strength.

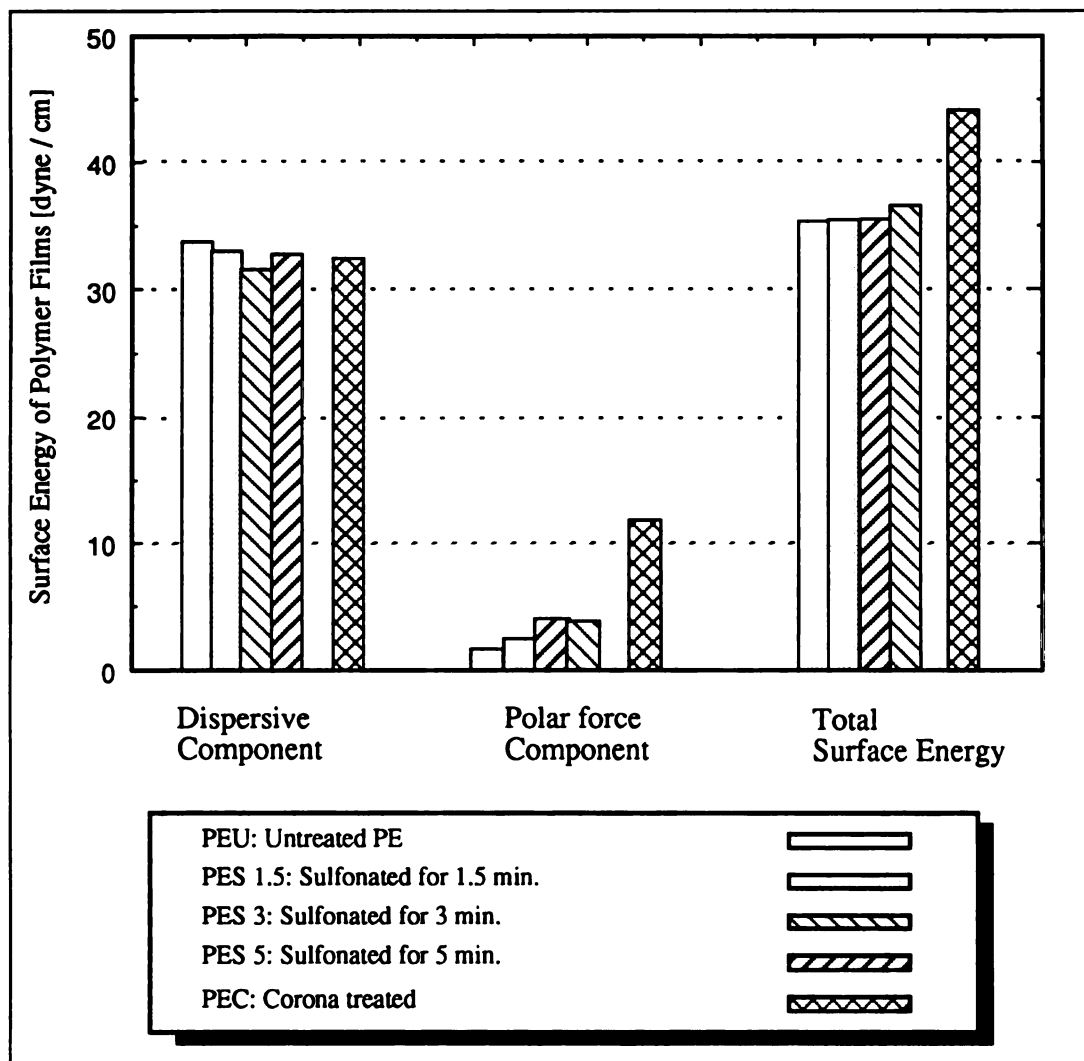


**Figure 27** The effect of sulfonation time on the change in total surface free energy and the respective energy components for untreated, sulfonated HDPE films as a function of reaction time, and corona treated HDPE film.



#### 8.4. Results and discussions of the peel adhesion test

The peel adhesion test results for the sulfonated and corona treated HDPE film samples are shown in *Table 15* with surface free energies, and graphically presented in the *Figure 27 (a)* (*page 91*), where peel adhesion strength as a function of sulfonation time is plotted. In *Figure 27 (b)* (*page 92*), the histogram of the peel adhesion strength of untreated, sulfonated HDPE film samples, and corona treated HDPE film sample is presented to evaluate the effect of sulfonation on the HDPE film.

**Table 15** Peel adhesion strength for sulfonated film samples with the result of surface free energies in polar dispersion and polar components

Sample	Surface free energies of solid [Dyne/cm]		Peel Adhesion Strength <sup>a</sup>
	Dispersion Component	Polar Component	[Gram/0.5 inch]
PEU	33.69	1.58	15.08 $\pm$ 1.94
PE1.5	32.97	2.43	43.86 $\pm$ 3.21
PE3	31.48	3.96	43.5 $\pm$ 2.97
PE5	32.7	3.78	44.9 $\pm$ 1.23
PEC	32.7	11.7	107.54 $\pm$ 6.87

a. Averaged value over three test results of each respective film samples.

As expected from the results of the surface free energy values determined, an improvement of peel adhesion strength was found between untreated and sul-

fonated film samples. However, the peel adhesion strength for the sulfonated PE films was approximately 50% lower than that of the corona treated film. This suggests that the peel adhesion strength is directly associated with the polar component of the surface free energy, and implies that an increased polar contributions to the surface energy of the polymer film results in an enhanced peel adhesion strength between treated film surfaces and applied PSA tape.

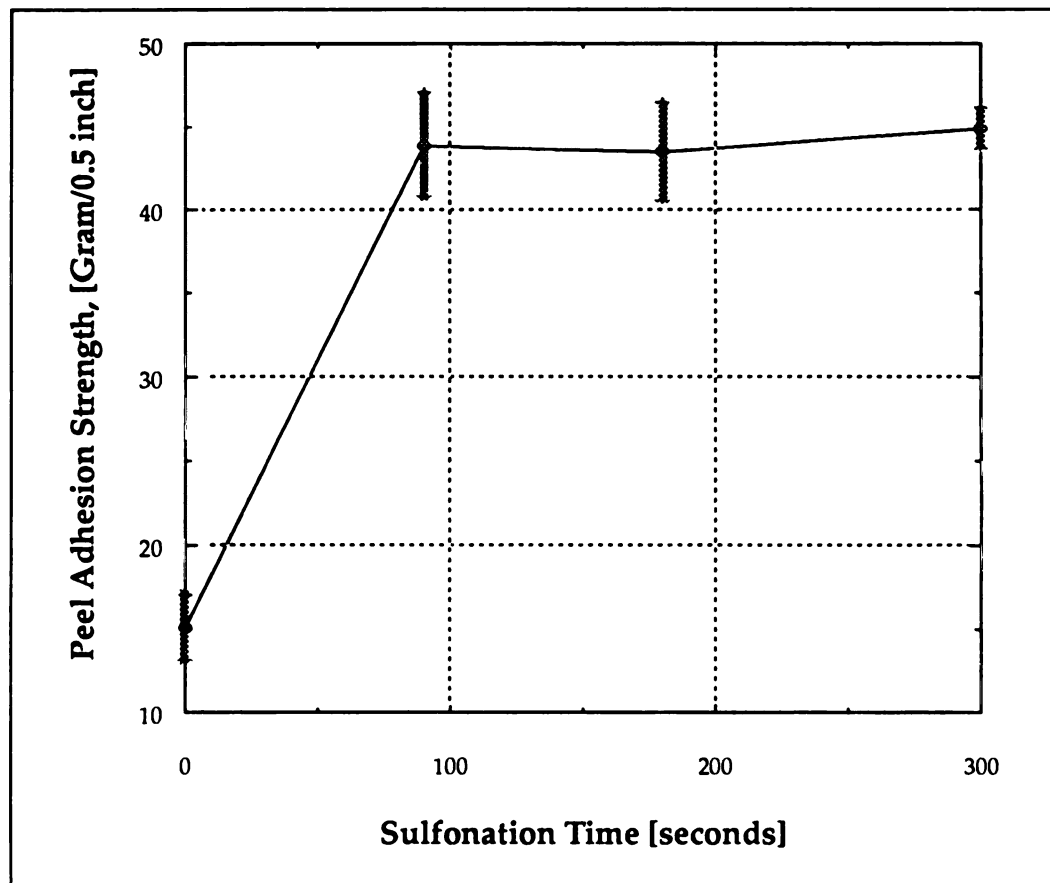


**Figure 27 (a)** Peel adhesion strength of HDPE film samples as a function of sulfonation time.

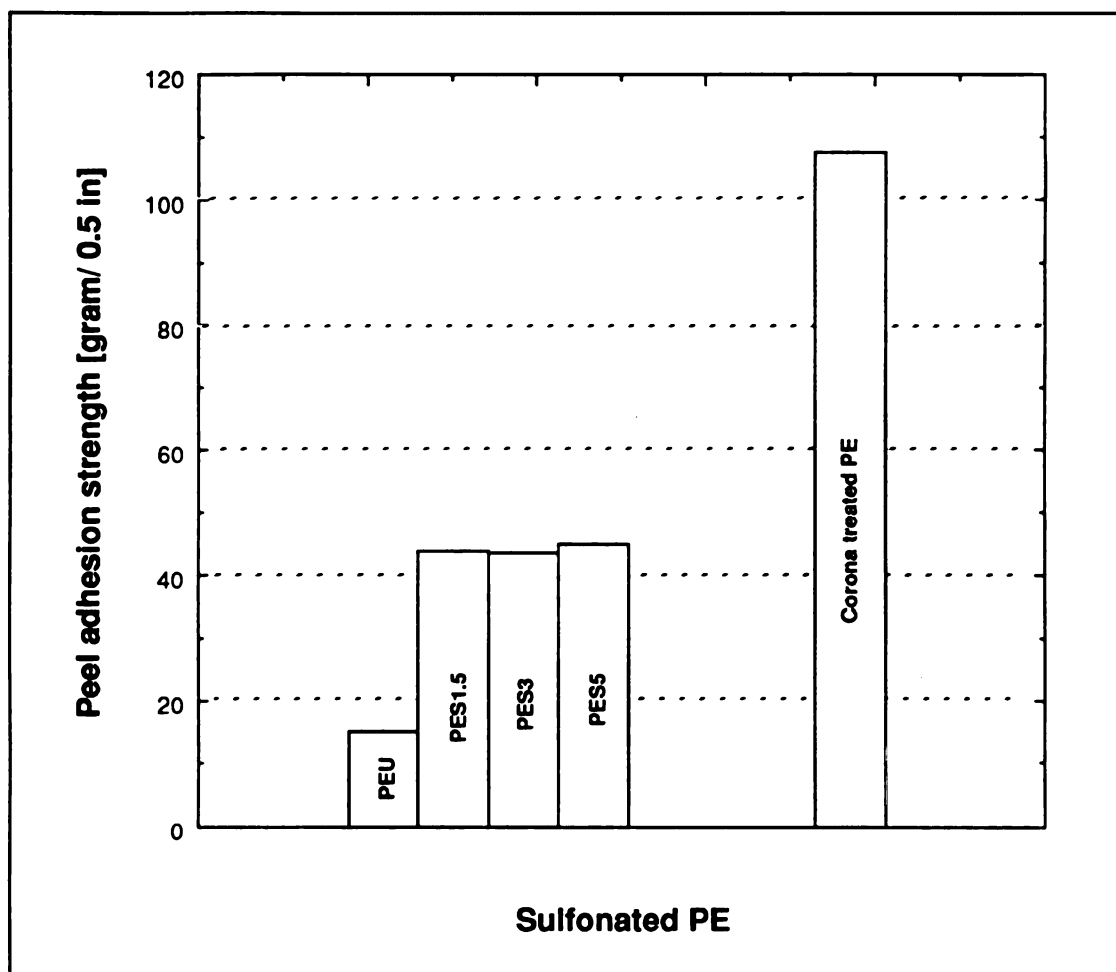


**Figure 27 (b)** Histogram of peel adhesion strength of untreated, sulfonated HDPE film samples and corona treated HDPE film samples.



## 8.5. Conclusion

The above results show that sulfonation of polyethylene film under the test conditions employed does not provide an alternative method to increase the surface free energy and the surface properties, such as the peel adhesion strength. For HDPE film under the treatment conditions used, a limited number of sulfonic acid groups were substituted onto the film surface, as a result of the sulfonation of reaction.

## ***Chapter 9. Sulfonation of Polyethylene terephthalate (PET) film***

### **9.1. Introduction**

In the present study, the sulfonation of polyethylene terephthalate (PET) was investigate to determine the effect of sulfonation treatment on the surface free energy of the polymer. Surface characteristics were based on contact angle analysis and ESCA analysis. ESCA analysis of the PET surface suggests that sulfonation was minimal on the PET film surface under the conditions used.

### **9.2. Results and Discussions**

The atomic composition of the polymer surface of the untreated and sulfonated PET film samples was determined by ESCA analysis. The results are summarized in *Table 16*. The atomic composition of the PET surface is 69.6% and 30.4% for carbon and oxygen, respectively. For PET film samples subjected to sulfonation treatment, no increase in the sulfur concentration on the surface of the sulfonated polymer samples was observed with increased treatment time. This implies that only a limited number of sulfonic groups can be grafted onto the film surface. For PET, the site for the substitution of sulfonic groups would be on the aromatic ring position.<sup>[23]</sup> Since the aromatic ring is already stable, the hydrogen extraction is not easily achieved during treatment of the polymer.

**Table 16** <sup>a</sup>Surface composition of PET film samples before and after sulfonation treatments at a various exposure time over SO<sub>3</sub> gas, determined by ESCA

		Percentage Atomic Concentration			
Sample	Reaction time [minutes]	C (%)	O (%)	N (%)	S (%)
PET	0	69.6	30.4	0	0
PET3	3	78.1	21.1	0	0.4
PET5	5	70.2	29.4	0	0.4

---

a. PET: Untreated polyethylene terephthalate film

PET1: Sulfonated polyethylene terephthalate film for 1 minute

PET3: Sulfonated polyethylene terephthalate film for 3 minutes

---

Contact angles of liquids (distilled water, formamide, and di-iodomethane) were measured on the untreated PET samples and film samples sulfonated for 1 minute and 3 minutes, respectively. The values obtained for the corresponding samples are summarized in *Table 17*, and presented by a histogram in *Figure 28*. *Table 17* shows that most of the contact angle changes following the sulfonation of PET film occurred with distilled water, and formamide (both have high polar properties). This suggests that sulfonation of the PET film is mostly associated with changes in the polar properties of the polymer surface. Different reaction timed, under the conditions used, had little effect on the surface properties. This finding was in agreement with the ESCA analysis.

**Table 17** Contact angle of liquids on the untreated PET film and sulfonated PET samples for 1 min. and 3 min. reaction time.

Sample	Contact Angle Measured, mean $\theta$ [degrees] <sup>a</sup>		
	Distilled Water	Formamide	Di-iodomethane
UPET	66.9 1.5	50.6 2.4	20.9 2.4
PET1	55.0 1.9	30.1 2.1	18.7 2.4
PET3	56.6 2.7	24.9 2.0	24.8 2.6

a. Averaged value over at least 10 different measurements, performed in different positions of the sample surface. The typical standard error was within  $\pm 3^\circ$ .

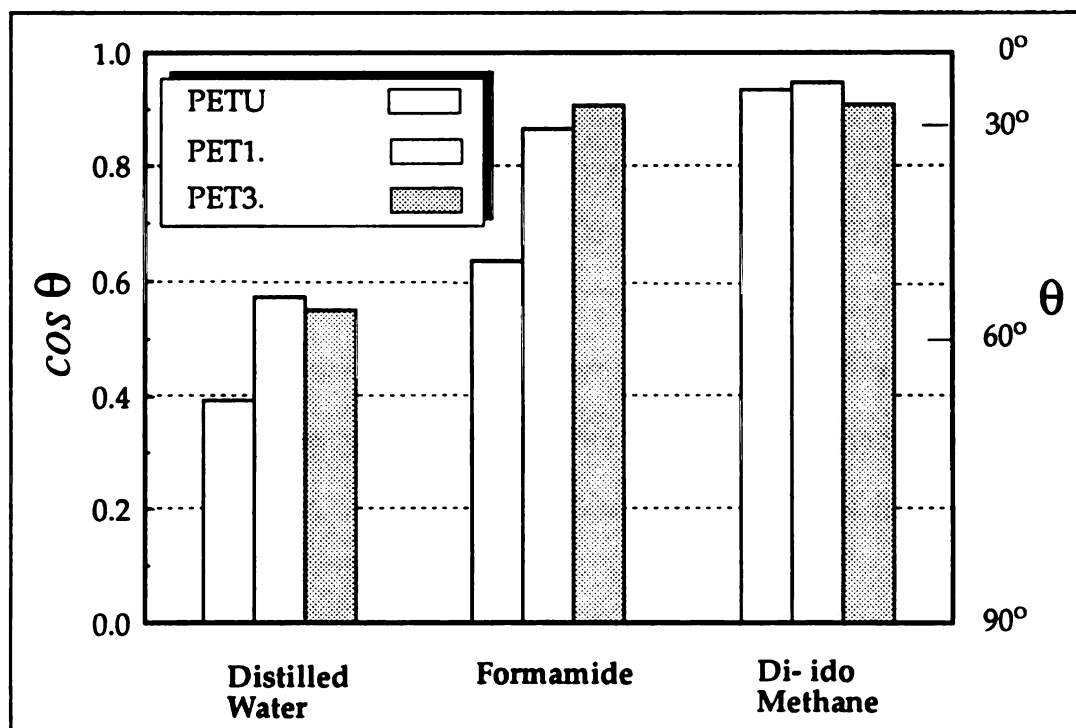


**Figure 28** Contact angle change of liquids for sulfonated PET samples with increasing time of sulfonation. Based on the untreated PET film as reference.



The surface energy,  $\gamma_s$ , of a solid is the sum of the dispersion component,  $\gamma_s^d$ , and the polar component,  $\gamma_s^p$ . These values are obtained by measuring the contact angle of the strong polar liquid (distilled water, formamide, etc.), and weak polar liquids (di-iodomethane). Similar surface free energy values have been reported by Cuff, et. al.<sup>[54]</sup> for PET films, 40 dyne/cm and 3 dyne/cm respectively, for the dispersion component and the polar component (typically from the 39 to 47 dyne/cm for total surface energy of PET film).

The results given in *Table 18* show the surface free energy and the corresponding dispersion and polar components. For PET samples with different reaction times of treatment, the atomic% of sulfur on the sample surface from ESCA analysis and film polarity values are summarized in *Table 18*. The effect of sulfonation time on the change in total surface free energy, and the respective free energy components, of PET samples is shown in *Figure 29*. From *Table 18*, and the graphical analysis of the surface energy parameters, the surface treatment of PET film by sulfonation did not change, significantly, the dispersion component of the surface free energy of the PET. On the other hand, sulfonation appeared to increase the polar component contribution. The content of sulfur (i.e. sulfonic acid groups) on the surface following sulfonation seems to be the predominant factor in changing surface properties of PET film.

**Table 18** Surface Free Energy of PET films, Polarity, and Atomic% of Sulfur by ESCA for PETU (untreated), PET1 (Sulfonated for 1.5 minute), PET3 (Sulfonated for 3 min.)

Sample film	Surface free energies of solid [dyne/cm]			Polarity	Atomic% of Sulfur
	Dispersive Component	Polar Component	Total		
PETU	40.85	6.94	47.79	0.15	0
PET1	38.84	14.83	53.67	0.28	0.4
PET3	37.38	15.86	53.24	0.3	0.4

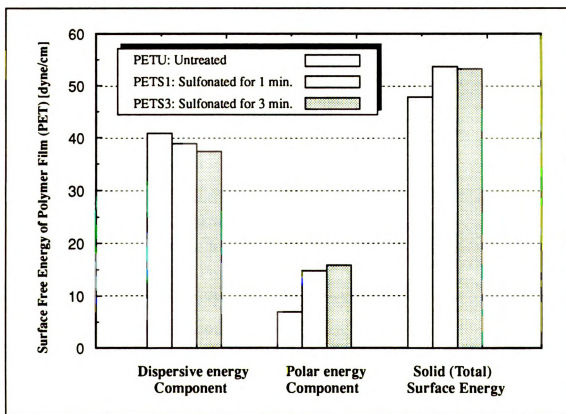


**Figure 29** Variation of solid surface energy corresponding dispersion and polar components for untreated and sulfonated PET samples.

## *Chapter 10. Conclusions*

1. Surface sulfonation of OPP film, using gaseous  $\text{SO}_3$ , was found to be a very effective method of enhancing the surface free energy of the film, which results in an increase in peel adhesion strength. For polypropylene, the tertiary carbons in the molecule were found to be the site for the insertion of sulfonic acid groups onto the polymer backbone.
2. It was found that surface sulfonation exhibited varying levels of effectiveness for polymers studied, depending on their molecular structure. The reason for this behavior can be attributed to the steric hinderance to substitution of sulfonic acid groups onto the polymer backbone. As large functional groups such as the sulfonic acid group are introduced onto the polymer surface beyond a limit, the spatial restrictions will not allow the substitution of additional sulfonic acid group. Further, the number of active sites for substitution are limited.
3. An additional reason for a limited sulfonation can be attributed to the repulsion of adjacent sulfonic acid groups. The inserted sulfonic acid group, which is considered to exhibit a negative charge, may require a distance limit for the insertion of additional sulfonic acid groups onto the polymer surface. For polypropylene the limit was reached in about 1 minute of reaction time, and was equivalent to one sulfonic acid group per three repeating monomer units.
4. Sulfonation of OPP film increased by almost one order of magnitude of the polar component contribution to the surface free energy within the first minute of reaction time, as compared to the untreated OPP film.

Further sulfonation of OPP film showed little or no changes on the surface properties, as a result of the spacial restrictions for additional sulfonic acid group insertion to tertiary carbon bonds.

5. Sulfonating OPP film significantly increased the films peel adhesion strength, as compared to the untreated OPP film.
6. Surface free energy and adhesion strength results indicated that sulfonation of OPP film is a suitable and alternative method to other techniques currently employed to modify the surface properties of polymer film.
7. Under the sulfonation conditions employed, ESCA showed that sulfonation of was ineffective in modifying the PE film surface properties, of PE film. Sulfonation of PE film was ineffective in increasing the surface free energy and peel adhesion strength of treated film, as compared to the untreated PE film.
8. Sulfonation was found to be less effective than corona treatment in increasing the surface free energy and peel adhesion strength of PE. The polar component of the surface free energy of the corona treated PE film was about three times the observed values for the sulfonated PE film. The peel adhesion strength of the corona treated PE film was twice that of the sulfonated PE film.
9. Sulfonation of PET was found to have little or no effect on the surface free energy of treated PET film. This can be attributed to spatial restrictions for sulfonic acid group substitution into the ortho positions of the terephthalate group.

## ***Chapter 11. Possible Future Studies***

### **11.1. Sulfonation method**

In this study, sulfonating HDPE and PET film was not successful in significantly changing the surface properties of these film. It would be interesting to investigate different sulfonating method on those films to increase the extent of sulfonic acid group substitution onto the polymer surface. Under the same conditions, the sulfonating LDPE and/or LLDPE would be useful to investigate the problem of the sulfonating conditions on HDPE film.

### **11.2. Surface free energy**

In performing contact angle analyses, different types of testing liquids can be selected for determining the effect of surface sulfonation of the surface free energy of the treated film. It may be considered important to evaluate related variables of the test procedure, such as temperature, since the viscosity of the is the function of temperature.

Furthermore the application of a related method, such as the IGC analysis, would be useful to investigate the effect of the surface sulfonation on the surface properties of treated film.

### **11.3. Ink printability**

In this present study, sulfonating OPP film increased the surface free energy and peel adhesion strength. It would be useful to study the effect of sulfonation on ink printability. It Oxidation following sulfonation may be possible to

investigate the aging effect on the surface free energy and ink printability that may be changing due to oxidation following sulfonation.

## Bibliography

- [1] Wu, S, Polymer Interfaces and Adhesion, Dekker Inc., New York, 1982
- [2] Sapieha, S., Cerny, J., Klemberg-Sapieha, J.E. and Martinu, L., *"Corona Versus Low Pressure Plasma Treatment: Effect on Surface Properties and Adhesion of Polymer"*, J. of Adhesion, Vol. 42, 91-102, 1993 [
- [3] Liston, E.M., Martinu, L., and Wertheimer, M.R., "Plasma surface modification of polymers for improved adhesion: a critical review", J. of Adhesion Science and Technology, Vol. 7, No. 10, 1091-1127, 1993
- [4] Foerch, C.H. Kill, G, and Walzak, M.J., "Plasma surface modification of PE: short-term vs. long-term plasma treatment", J. of Adhesion Science and Technology, Vol. 7, No. 10, 1993
- [5] Occiello, E., Morra, M., Morini, G., Garbassi, F., and Humphrey, P., "Oxygen-plasma-treated PP interfaces with air, water, and epoxy resins: Part I. Air and water", J. of Applied Polymer Science, Vol. 42, 551-559, 1991
- [6] Wittenbeck, P., and Wokaun, A., Plasma treatment on PP surfaces: Characterization by contact-angle measurements", J. of Applied Polymer Science, Vol. 50, 187-200, 1993
- [7] Hollander, A., Behnisch, J., and Zimmermann, H., "Surface modification of PE in an *rf* downstream remote plasma reactor", J. of Applied

Polymer Science, Vol. 49, 1857-1863, 1993

- [8] Forch, R., McIntyer, N.S., and Sodhi, R.N.S., "Nitrogen plasma treatment of PE, and PS in a remote plasma reactor, J. of Applied Polymer Science, Vol. 40, 1903-1915, 1990
- [9] Forch, R., Izawa, J., and Spears, G., "A comparative study of the effects of remote nitrogen plasma, remote oxygen plasma, and corona discharge treatments of the surface properties of PE". J. of Adhesion Science and Technology, Vol. 5, No. 7, 549-564, 1991
- [10] Papierer, E., Wu, D.Y., and Schultz, J., "Adhesion of flame-treated polyolefins to styrene butadiene rubber", J. of Adhesion Science and Technology, Vol. 7, No. 4, 343-362, 1993
- [11] Fonseca, C., Perena, J.M., and Fatou, J.G., "Sulphuric acid etching of PE surfaces" J. of Material Science, Vol. 20, 3283-3288, 1985
- [12] Carley J.F., and Kitze P.T., "*Corona-Discharge Treatment of PE Films. I. Experimental Work and Physical Effects*", J. Polymer Engineering and Science, Vol. 18, No 4, 326 ~ 33, 1978
- [13] Strobel, M., Lyons, C.S., Strobel, J.M., and Kapaun, R.S., "Analysis of air-corona-treated PP and PET films by contact-angle measurements and ESCA", J. of Adhesion Science and Technology, Vol. 6, No. 4. 429-443, 1992
- [14] Vandermei, H.C., Stokroos, I., Schakenraad, J.M., and Busscher, H.J., "Aging effects of repeatedly glow-discharged PE: influence on con-



tact angle, infrared absorption, elemental surface composition, and surface topography", J. of Adhesion Science and Technology, Vol. 5, No. 9, 757-769, 1991

- [15] Gatenholm, P., Bonnerup, C., and Wallstrom, E., "Wetting and adhesion of water-borne printing inks on surface-modified polyolefins", J. of Adhesion Science and Technology, Vol. 4, No. 10, 817-827, 1990
- [16] Malpass B.W., and Bright, K., in: Aspects of Adhesion, Vol. 5, p.214, Alner D.J. (Ed.), CRC Press, Cleveland, Oh, 1969
- [17] Delescluse, P., Schultz J., and Shanahan, M.E.R., in: Adhesion, Vol. 8, p. 79, Allen, K.W. (ed.), Elsevier Applied Sci. 1983
- [18] Balta Calleja, F.J., Fonseca, C., Perena, J.M., and Fatou, J.G., "Surface hardening of PE through sulfuric acid exposure" J. of Material Science Letters, Vol. 3, 509-511, 1984
- [19] Erickson, B.L., "On the enhancement of adhesive bonding to polymer and composite surfaces through gas phase sulfonation" Master Thesis, Department of Chemical Engineering, Michigan State University, East Lansing, Mi., 1991
- [20] Amini, M. A., "Surface and Hydrocarbon-barrier modification", The Wiley Encyclopedia of packaging Tech., 620-622, 1986
- [21] Wangwiwatsilp, K., "The effect of surface sulfonation on barrier properties of polymer films", Master Thesis, School of Packaging, Michigan State University, East Lansing, Mi., 1993

- [22] Walles, W.E, "Barrier properties added to plastics via sulfonation and reductive metallization", American Chemical Society
- [23] Asthana, H., "Chemical modification of polymer surfaces using sulfonation to improve adhesion properties", Master Thesis, Department of Chemical Engineering, Michigan State University, East Lansing, Mi., 1993
- [24] Ihata J. "Formation and reaction of polyenesulfonic acid I. Reaction of PE films with  $\text{SO}_3$ ", J. Polymer Sci.: Part A: Polymer Chemistry, Vol. 26, 167-176, 1988
- [25] Ihata J. "Formation and reaction of polyenesulfonic acid II. Photoreaction of Polyenesulfonic Acids", J. Polymer Sci.: Part A: Polymer Chemistry, Vol. 26, 177-185, 1988
- [26] Ihata J. "Formation and reaction of polyenesulfonic acid III. Preparation and Photoreaction of 1,3,5-Hexatriene-1,6-disulfonic Acid", J. Polymer Sci.: Part A: Polymer Chemistry, Vol. 26, 187-194, 1988
- [27] Watts, J.F., "X-ray Photoelectron Spectroscopy investigations of acid-base interactions in adhesion", J. of Adhesion, Vol. 41, 81-91, 1993
- [28] Clark, D.T., Feast, W.J., Musgrave, W.K.R, and Ritchie, I. "Applications of ESCA to polymer chemistry. Part VI. Surface fluorination of PE. Application of ESCA to the examination of structure as a function of depth", J. of Polymer Science: Polymer Chemistry Ed., Vol. 13, 858-890, 1975

- [29] Creuzet, F., Ryschenkow, G. and Arribart, H., "A new tool for adhesion science: The atomic force microscope", *J. of Adhesion*, Vol. 40, 15-25, 1992
- [30] Schreiber, H.P., "Specific interactions and contact angle measurements on polymer solids", *J. Adhesion*, Vol. 37, 51-61, 1992
- [31] Klubek, J., and Schreiber, H.P., "Note: Further comments on contact angle measurements on polymer solids", *J. Adhesion*, Vol. 42, 87-90, 1993
- [32] Zisman, W.A., "Relation of the equilibrium contact angle liquid and solid constitution", Kendall Award Address, in *Contact Angle, Wettability and Adhesion*", *Advances in Chemistry Series*, Amer. Chem. Soc., Washington, D.C. 43, 1, 1964
- [33] Riedl, B., and Kamdem, P.D., "Estimation of the dispersive component of surface energy of polymer-grafted lignocellulosic fibers with inverse gas chromatography", *J. of Adhesion Science Technology*, Vol. 6, No.9, 1052-1067, 1992
- [34] Borch, J. "Thermodynamics of polymer-paper adhesion: a review", *J. of Adhesion Science Technology*, Vol. 6, No.5, No. 7, 523, 541, 1991
- [35] Papier, E., and Balard, H., "Influence of surface chemistry and surface morphology on the acid-base interaction capacities of glass fibers and silicas", *J. of Adhesion Science Technology*, Vol. 4, No.5, 357-371, 1990

- [36] Kinloch, A.J., and Kodokian, G.K.A., "On the calculation of dispersion and polar force components of the surface free energy", J. of Adhesion, Vol. 34, 41-44, 1991
- [37] ASTM Bull., D 2578-67 (Reapproved 1979), American Society for Testing Materials, Philadelphia, PA., 494
- [38] Voyutskii S.S. "Aautohesion and Adhesion of High Polymers", Wiley Inter science, New York, 1963
- [39] Kinloch, A.J., "Adhesion and Adhesives: Science and Technology", Chapman and Hall, New York, 1987
- [40] Satas, Donatas, "Plastics, finishing and decoration", Vsn Nostrand Reinhold Company, New York, 70~100, 1986
- [41] Allen, K.W., "A review of contemporary views of theories of adhesion", in Adhesion Society Meeting (10th, 1987, Willamsburg, Va.), Sharpe, L.H. (Ed.), Gordon and Breach Science Publishers, New York, 1987
- [42] Hsieh, Y.L., Timm, D.A., and Wu, M, J. appl. Polym. Sci 38, 1719-37 (1989)
- [43] Duprè, A. "Theoric mechanique de la chaleur, Gauthiervillars, Paris, 1869
- [44] Deryagin, B.V., and Smilga, V.P., "Adhesion Fundamentals and Practice", McLaren, London, 1969

- [45] Hata, T., Kitazaki, Y. and Saito, T., "Estimation of the surface energy of polymer solids", in Adhesion Society Meeting (10th, 1987, Williamsburg, Va.), Sharpe, L.H. (Ed.), Gordon and Breach Science Publishers, New York, 1987
- [46] Good, R.J. "Theory for the estimation of surface and interfacial energies. Contact angle, wettability and adhesion", Am. Chem., Soc. Series, No. 43, 74, 1964
- [47] Good, R.J., and Girifalco, J., "A theory for estimation of surface and interfacial energies. III. Estimation of surface energies of solid from contact angle data", J. of Physical Chemistry, 64, 561, 1960
- [48] Fokwes, F.M., in Contact Angle, Wettability and Adhesion", Advances in Chemistry Series, Amer. Chem. Soc., Washington, D.C. 43, p. 99, 1964
- [49] Young, T., "An essay on the cohesion of fluids", Phil. Trans. Roy. Soc. 95:65, London, 1805
- [50] Dann, J.R. "Forces involved in the adhesive process I. Critical tensions of polymeric solids as determined with polar liquids", J. of colloid and Interface Sci., Vol. 32, No. 2, 302-320, 1970
- [51] Dann, J.R. "Forces involved in the adhesive process I. Nondispersion forces at solid-liquid interfaces", J. of colloid and Interface Sci., Vol. 32, No. 2, 321-338, 1970
- [52] Owens and Wendt, J. of Applied Polymer Science, 13, 1741, 1969

- [53] Kaelble, D.H. and Cirlin, E.H., "Dispersion and Polar contributions to surface tension of poly (methylene oxide) and Na-treated polytetrafluoroethylene", J. of Polymer Science: PArt A-2, Vol. 9, 363-368, 1971
- [54] Cueff, R., Baud, G., Besse, J.P., and Jacquet, M. "Surface Free Energy modification of PET by Plasma treatment- influence on Adhesion", J. of Adhesion, Vol.42, 249-254, 1993
- [55] Manual, Rame-hart, inc. "Surface Science Instrumentation" for Research and Quality Control.
- [56] Sullivan, M.J., and Weiss, R.A., "Characterization of Blends of an amorphous polyamide with lightly sulfonated PS ionomers", J. of Polymer engineering and Science, Vol. 32, No. 8, 517-523, 1992

MICHIGAN STATE UNIV. LIBRARIES



31293010205015